U.S. Department of Energy, Office of Fossil Energy

DOE Award: DE-FE0031524
November 16, 2017 – November 15, 2019

At-source Recovery of Rare Earth Elements from Coal Mine Drainage

Project Summary Report

Principal Investigator:
Paul Ziemkiewicz, PhD
Director, WV Water Research Institute
Paul.ziemkiewicz@mail.wvu.edu
304-293-6958

Submitted by:
Christopher Vass, Ph.D., P.E.
Facility Manager, WV Water Research Institute
crvass@mail.wvu.edu
304-293-7083

Submission Date:
February 14, 2020

West Virginia University Research Corporation
DUNS Number: 191510239
886 Chestnut Ridge Road, PO Box 6845
Morgantown, WV 26506-6845

WVU Team Members
Virginia Polytechnic Institute and State University
Shonk Investment Partners, LLC

Acknowledgment: "This material is based upon work supported by the Department of Energy National Energy Technology Laboratory under Award Number DE-FE0031524."

Contents

Executive Summary

Conventional acid mine drainage (AMD) treatment consists of pH adjustment, oxidation, and separation of solid precipitates from discharge quality water. Alkaline addition increases the pH to the range 7 to 9 to precipitate the regulated metals Al and Mn ions as hydroxides. Mechanical or chemical oxidation then converts the reduced iron species Fe^{2+} to Fe^{3+} which precipitates at a low pH value as ferric hydroxide ($Fe(OH)_3$). Co-precipitation of Rare Earth Elements (REEs) with hydroxides creates a gangue-rich matrix from which REEs must be separated. $Fe(OH)_3$ is generally the most abundant gangue-forming metal.

Current research by the project team has shown raw, untreated AMD has an average total rare earth element content (TREE) of about 287 µg/L (0.287 ppm). Operators of AMD-producing facilities are obliged to treat it to neutralize acidity and remove regulated metals (e.g., iron (Fe), aluminum (Al), and manganese (Mn)) prior to discharge. Ongoing research indicates conventional AMD treatment concentrates TREE in resulting precipitates (AMD sludge) by an average factor of 2,635x to an average dry weight, elemental concentration of 708 g/t (ppm). While the economics of recovering REEs from AMD sludge are appealing, much of the cost of REE recovery would be incurred during separation of REEs from the gangue metals: Fe, Al, and Mn. Significant gains can be made by precipitating REEs when most of these gangue metals are still in solution.

Significant improvements in REE extraction efficiency can be obtained through separation of REEs from the aqueous phase AMD, upstream of conventional AMD treatment by: 1) creating an enriched REE feedstock, 2) producing a more consistent feedstock, 3) reducing transportation costs to an REE refinery, 4) reducing acid consumption in the acid leaching step, and 5) reducing the volume of waste produced at the ALSX plant.

This project is exploring two novel approaches for extracting REEs upstream of the conventional AMD treatment plants to create a purified REE feedstock while leaving the bulk of the Fe, Al, and Mn in solution for subsequent treatment. While the average TREE concentration of raw AMD is low and individual sites range between 10 and 2,200 µg/L, successful at-source REE separation will generate a superior feedstock to a conventional ALSX process and significantly improve the economics and environmental performance of REE extraction from AMD. AMD can be classified into two types: type A is net acid and iron is partly oxidized while type B is net alkaline, and iron occurs in the reduced, ferrous state.

In Case A, the pH is raised slightly, which will precipitate $Fe^{3+}$and Al^{3+} but not REEs. The other important type of AMD is net alkaline water found in flooded, anoxic deep mines. These generally have a pH > 6.0 and are net alkaline. REE concentrations are also much lower than those found in acidic AMD while the volumes and flux are much higher. Most of these are pumped discharges with almost no Al.

Case B AMD is strongly reduced and, like Case A water, Fe and Mn ions are similarly reduced and therefore soluble at pH <9.0. REEs and an array of transition ions will be the only trivalent cations in this type of AMD. In Case B, both upward pH adjustment under reducing conditions and application of an electrochemically stimulated supported liquid membrane strategy to separate REEs from ferrous ion will be explored.

Project Objectives: Develop and test a process to extract an enriched REE feedstock from AMD at the site of production, upstream of conventional AMD treatment. Prior knowledge of AMD chemistry yields two distinct AMD cases: net acid and net alkaline, (Cases A and B, respectively), which will be explored. The resulting products will be processed through our acid leaching/solvent extraction facility to compare performance with ongoing SX trials using AMD sludge as the feedstock.

Sub-objective 1. Extraction strategy Case A, low pH AMD: Maintain reducing conditions in feed water. Determine the effect of titrating pH from 3.0 to 4.5. Collect precipitate for analysis.

Sub-objective 2. Extraction strategy Case B, net alkaline AMD: Maintain reducing conditions in feed water, explore electro-membrane extraction methods to separate REEs from matrix.

Sub-objective 3. Process resulting precipitates through our Solvent Extraction facility to a target REE oxide purity in excess of 90% and evaluate performance versus the AMD sludge feedstock pathway.

Sub-objective 4. Evaluate technical and economic advantages over at-source REE recovery versus the AMD sludge feedstock pathway.

Accomplishments

Task 1.0 – Project Management and Planning

Overview

Project management functions were preformed to ensure that the project team executed all tasks and subtasks to completion and maintained consistent communications while working towards project objectives. WVU managed and directed the project in accordance with a Project Management Plan to meet all technical, schedule, and budget objectives and requirements. WVU coordinated activities in order to effectively accomplish the work, ensuring that project plans, results, and decisions were appropriately documented, and that project reporting and briefing requirements were satisfied. Additionally, bi-weekly meetings were held throughout the course of the project to monitor researcher progress and allow for collaborative understanding.

Approach

This task included all work elements required to maintain and revise the Project Management Plan, and to manage and report on activities in accordance with the plan. It also included the necessary activities to ensure coordination and planning of the project with DOE/NETL and other project participants. These included, but are not limited to, the submission and approval of required National Environmental Policy Act (NEPA) documentation.

Results and Discussion

Presentations/Publications:

1. Ziemkiewicz, P.F., Finklea, H.O., Lin, L-S. At-source Recovery of Rare Earth Elements from Coal Mine Drainage. Kickoff meeting. 16 Feb 2018, USDOE/NETL Pittsburgh PA.
2. WVU's REE research program: North American Coalbed Methane Forum, Cannonsburg PA, 18 Apr 18. Ziemkiewicz
3. WVU's REE research program: Briefings for WV Congressional Delegation, Washington DC, April 2018. Ziemkiewicz
4. Ziemkiewicz, Paul. (2019). West Virginia Mine Drainage Task Force Symposium. Morgantown, WV, March 26, 2019.
5. Ziemkiewicz, Paul. (2019). Briefings for West Virginia Congressional Delegation. Washington, DC, April 23, 2019.
6. Ziemkiewicz, Paul. (2019). Reporter from WOWK Charleston at Omega site REE. Morgantown, WV, July 7, 2019.
7. Ziemkiewicz, Paul. (2019). Pittsburgh Coal Conference. Pittsburgh, PA, September 5, 2019.
8. Ziemkiewicz, Paul. (2019). Briefings for USEPA Region III Administrator Cosmo Servidio. September 11, 2019.
9. Ziemkiewicz, Paul. (2019). Council of Government Mining Attorneys. September 24, 2019.

Task Completion Status
100% complete.

Task 2.0 – Case A. Low pH Mine Drainage Extraction Strategy

Subtask 2.1. Characterization of REE Load Variations in AMD Waters

Overview
The short-term and long-term variability of acid mine drainage (AMD) feedstock was determined through ongoing sampling and analytical analysis. The preferred site chosen for long term sampling was AQ-2. This site was selected over other previously sampled sites due to the consistency of flow over the project period. Other previously monitored sites had flows altered due to construction of treatment plants (AQ-3) or were otherwise not feasible to monitor due to irregular flows from varying sources across the mine properties. The AQ-2 site was analyzed for specific conductance, pH, redox potential, gangue metal concentrations, and rare earth element (REE) concentrations for approximately one year.

In addition to the change in AMD quality over time, a comparison was conducted to evaluate the amenability of seven different low pH mine waters using a precipitation method developed with AQ-2 raw water. This comparison not only characterized multiple feedstocks, but also, showed that the precipitation procedures developed by the researchers are applicable across many different AMD discharges. While the scope if this research exceeds that of the defined task, it was essential to validate the technology across different AMD feedstocks given the difficulty encountered with acquiring raw water from the AQ-3 and AQ-1000 sites.

Approach
Evaluate the results of previous sampling (DE-F 0026927) to determine the short- and long- term variability of Case A feedstock: raw AMD from the AQ-2, AQ-3, and AQ-1000 treatment sites. Specifically, included redox potential and iron speciation to the analytical suite.

Results and Discussion
Characterization analysis is shown below in Table 1, Table 2, and Table 3. The evaluated parameters varied in pH, redox potential, iron concentration, and TREE concentration throughout the reporting periods. Of particular importance is the delineation in Table 1 showing different flow characteristics of the influent at AQ-2.

The AQ-2 site has two primary flows that feed the AMD plant. During the latter part of testing, one of the flows reduced dry drought-like conditions. The effect of the reduced flows is observed in the specific conductance and ORP values shown in Table 1.

The raw water characteristics are shown below in Tables 4 - 6. The grades of the precipitates ranged from 1.1 to 4.8% REE. There were no water quality parameters which correlated well with REE grade or recovery. However, raw water concentrations of Mn, Ni, and Zn were well correlated with REE concentration in the raw water as well as REE precipitate mass.

Table 1. Raw water specific conductance, pH, and ORP of site AQ-2 from February 2018 through January 2019.

Collection Date	Specific Conductance uS/cm	pH	ORP mV
2/12/18	3270	2.31	462.60
2/24/18	3670	2.25	498.90
4/12/18	3200	2.30	480.80
5/9/18	2945	2.39	474.20
5/10/18	2962	2.36	475.70
5/14/18	3036	2.39	461.50
5/21/18	2850	2.40	483.20
6/4/18	2901	2.42	469.30
6/11/18	2943	2.47	473.20
6/26/18	2627	2.59	457.10
7/16/18	1139	2.76	546.00
7/23/18	1995	2.81	550.30
8/20/18	1031	2.73	522.80
11/16/18	1195	3.05	506.10
12/17/18	1323	3.20	517.30
1/14/19	1901	2.72	523.50

AQ-2 Flow Pattern Change

Table 2. Dissolved metal concentrations (mg/L) for the raw AMD collected from site AQ-2 from June 2018 through January 2019.

		Collection Date						
Parameter	**Units**	**6/26/18**	**7/16/18**	**7/23/18**	**8/20/18**	**11/16/18**	**12/17/18**	**1/14/19**
Al	mg/L	94.26	89.78	92.21	70.05	64.39	72.18	64.34
Ca	mg/L	83.72	92.38	121.70	90.01	88.16	106.45	111.66
Cd	mg/L	0.02	0.02	0.01	0.01	0.01	0.01	0.01
Co	mg/L	0.34	0.33	0.32	0.24	0.21	0.26	0.23
Cr	mg/L	0.07	0.06	0.05	0.04	0.04	0.05	0.04
Cu	mg/L	0.25	0.21	0.07	0.30	0.31	0.08	0.20
Fe	mg/L	224.89	224.15	174.67	97.02	110.09	162.04	163.59
Mg	mg/L	34.89	36.06	39.19	30.08	27.97	32.71	30.47
Mn	mg/L	1.26	1.40	1.62	1.17	1.15	1.32	1.22
Ni	mg/L	0.76	0.74	0.73	0.55	0.51	0.60	0.52
Zn	mg/L	1.89	1.95	2.01	1.70	1.50	1.65	1.50

Table 3. Rare earth element concentrations (mg/L) for the raw AMD collected from site AQ-2 from June 2018 through January 2019.

		Collection Date						
Parameter	**Units**	**6/26/18**	**7/16/18**	**7/23/18**	**8/20/18**	**11/16/18**	**12/17/18**	**1/14/19**
Sc	ug/L	60.01	50.72	51.89	38.75	30.72	37.44	31.58
Y	ug/L	86.35	88.20	102.71	72.81	62.60	78.08	64.23
La	ug/L	12.67	16.74	17.64	11.89	11.66	13.37	11.78
Ce	ug/L	47.28	61.61	66.83	43.96	39.64	49.95	42.28
Pr	ug/L	7.11	10.37	11.11	7.24	6.68	8.39	6.95
Nd	ug/L	33.96	50.64	56.55	36.88	33.83	40.74	33.61
Sm	ug/L	13.81	14.73	18.22	11.17	10.18	12.64	9.87
Eu	ug/L	3.96	3.83	4.86	2.85	2.68	3.30	2.52
Gd	ug/L	21.94	20.94	29.13	16.77	15.80	19.43	14.48
Tb	ug/L	3.92	3.73	5.19	2.95	2.92	3.55	2.77
Dy	ug/L	24.85	22.74	33.13	18.71	17.52	21.91	15.75
Ho	ug/L	4.75	4.31	6.21	3.48	3.40	4.21	3.04
Er	ug/L	13.88	12.44	17.93	10.07	9.44	11.69	8.35
Tm	ug/L	1.80	1.86	2.53	1.37	1.27	1.59	1.16
Yb	ug/L	10.11	9.97	14.39	7.93	7.47	9.33	6.55
Lu	ug/L	1.53	1.57	2.18	1.18	1.12	1.37	1.00
TREE	**ug/L**	**347.93**	**374.40**	**440.50**	**288.00**	**256.94**	**317.00**	**255.92**

Seven-Site Comparison

This study was preformed to determine if water quality parameters in raw AMD could predict the grade of REE precipitates using the standard three-step sequential precipitation procedure. Both the recovery of the rare earth elements as well as the grade of the precipitate are important factors to consider when scaling up the precipitation procedures. It is undesirable to have low recovery because it is a loss of a potential salable product. Grade must be considered because it may affect downstream purification procedures, as well as increasing transportation costs. A lower grade would result in a larger mass of precipitate required for productions and transportation to achieve the same mass of REE when compared to a feedstock with higher grade.

The first question to consider in large scale application of the precipitation procedure is the location of the treatment facility. While the sources of AMD are plentiful, each varies greatly in terms of physicochemical characteristics. Determining if raw water characteristics can predict REE precipitate grades would be beneficial when determining possible treatment sites, as it would be unfortunate to construct a site which yields low REE grade and recovery. The data collected from the seven sites was used to assess relationships between raw water characteristics and REE grade, recovered mass, and overall recovery.

Site Characterization

Seven acid mine drainage sites were chosen across northern West Virginia with a variety of water quality characteristics. Figure 1 is a map displaying the AMD collection sites. All raw AMD samples were collected upstream of any treatment. The specific conductance, pH, and ORP were measured at the time of collection (Table 4). The metal concentrations for each site are found in Table 5, and the rare earth element concentrations are shown in Table 6.

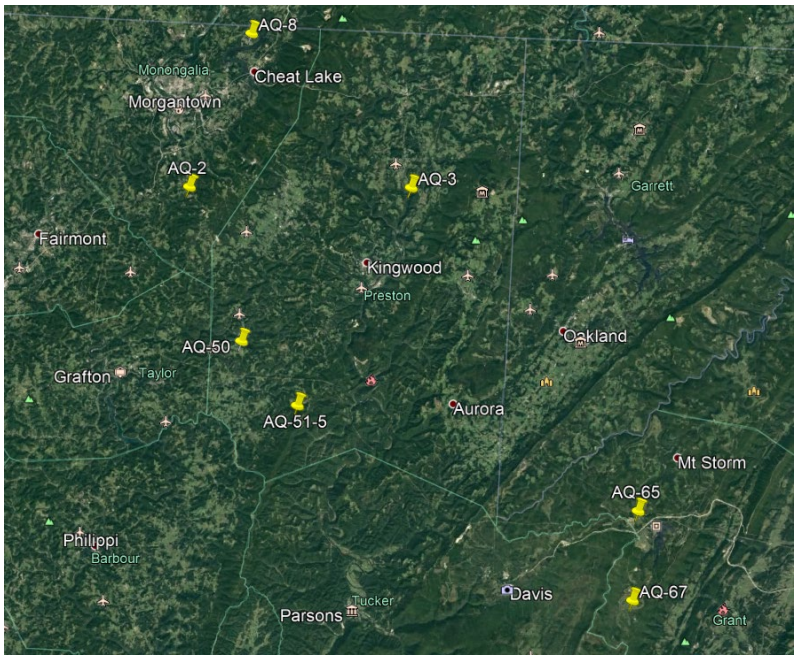

Figure 1. Locations across northern West Virginia of the seven AMD collection sites: AQ-2, AQ-8, AQ-50, AQ-51-5, AQ-3, AQ-65, and AQ-67.

Table 4. Raw water specific conductance, pH, and ORP during collection at the seven sites.

Site	Specific Conductance uS/cm	pH	ORP mV
AQ-2	1031	2.73	552.80
AQ-8	2360	3.11	502.90
AQ-50	2032	2.87	448.90
AQ-51-5	1074	2.96	-
AQ-3	1591	2.82	-
AQ-65	2019	3.03	460.50
AQ-67	991	3.23	417.60

Table 5. Dissolved metal concentrations (mg/L) for the raw AMD collected at the seven sites.

		AMD Site						
Parameter	**Units**	**AQ-2**	**AQ-8**	**AQ-50**	**AQ-51-5**	**AQ-3**	**AQ-65**	**AQ-67**
Al	mg/L	68.6	72.2	39.8	28.6	27.2	66.3	45.3
Ca	mg/L	90.2	208.6	132.2	53.7	160.8	172.5	62.8
Co	mg/L	0.2	0.9	1.1	0.2	0.1	0.9	0.4
Cu	mg/L	0.3	0.0	0.1	0.0	0.1	-	-
Fe	mg/L	95.5	34.5	354.9	2.7	27.1	3.3	5.3
Mg	mg/L	30.0	129.8	84.0	40.8	33.9	108.8	26.6
Mn	mg/L	1.2	44.5	38.9	15.1	1.2	27.3	14.9
Ni	mg/L	0.6	1.1	1.0	0.3	0.2	1.0	0.5
Si	mg/L	-	-	-	-	-	17.6	18.3
Zn	mg/L	1.7	3.5	3.1	0.7	0.7	2.8	1.4
SO4	mg/L	-	-	-	-	-	1,385.0	541.0

Table 6. Rare earth element concentrations (ug/L) of the raw AMD collected at all seven sites.

		AMD Site						
Parameter	**Units**	**AQ-2**	**AQ-8**	**AQ-50**	**AQ-51-5**	**AQ-3**	**AQ-65**	**AQ-67**
Sc	ug/L	37.6	6.6	4.6	4.3	3.6	17.2	1.7
Y	ug/L	75.5	388.4	367.1	96.4	36.0	389.6	196.8
La	ug/L	11.6	91.9	134.5	29.4	8.5	80.0	41.0
Ce	ug/L	43.3	260.8	296.8	77.7	27.5	221.6	136.6
Pr	ug/L	7.1	40.6	37.1	10.8	4.7	42.6	21.4
Nd	ug/L	35.6	204.5	130.8	49.8	23.9	218.0	110.0
Sm	ug/L	10.9	61.4	38.0	14.5	7.0	64.0	31.5
Eu	ug/L	2.8	17.4	10.6	4.1	1.7	16.6	7.9
Gd	ug/L	16.3	96.3	60.4	21.5	9.2	95.4	45.7
Tb	ug/L	2.8	14.6	9.9	3.3	1.4	13.8	7.0
Dy	ug/L	18.1	80.4	58.8	18.4	8.1	75.3	38.0
Ho	ug/L	3.4	14.6	11.7	3.4	1.5	13.8	7.2
Er	ug/L	9.8	38.2	32.0	9.2	4.1	36.2	18.8
Tm	ug/L	1.3	5.0	4.2	1.2	0.6	4.8	2.5
Yb	ug/L	7.5	28.7	24.4	7.2	3.1	25.9	12.3
Lu	ug/L	1.1	4.3	3.5	1.0	0.4	3.8	5.0
TREE	**ug/L**	**284.5**	**1,353.7**	**1,254.5**	**352.2**	**141.3**	**1,318.6**	**683.5**

Results

Composition of the precipitates containing most of the REEs varied between sites (Table 7). The percentage of Fe was greatly reduced from the raw water and ranged from 0.2 to 2.5%. The percentage of aluminum ranged from 3.6 to 10.7%. Other major metals in the precipitate were Zn, (1.7- 11%), Ca (0.5-4.6%), and Mg (0.3 to 3.3%).

Table 7. Composition of the precipitates for all seven AMD sites. The concentrations of the precipitates are given in mg/kg, as well as the weight percentage of each element.

		AMD Site						
Parameter	**Units**	**AQ-2**	**AQ-8**	**AQ-50**	**AQ-51-5**	**AQ-3**	**AQ-65**	**AQ-67**
Al	mg/kg	10,668	77,109	59,381	86,880	55,300	35,704	69,829
Ca	mg/kg	12,419	45,955	4,779	18,251	16,568	9,930	13,543
Co	mg/kg	240	2,296	583	4,060	1,160	8,025	43,445
Fe	mg/kg	11,149	2,213	6,310	5,116	25,298	7,053	4,760
Mg	mg/kg	3,019	30,858	2,355	22,859	15,139	32,540	22,747
Mn	mg/kg	972	50,522	9,576	74,638	6,194	63,521	64,162
Ni	mg/kg	475	2,468	629	3,081	1,365	5,710	3,665
SO4	mg/kg	-	-	-	-	-	7,107	4,753
Si	mg/kg	-	-	-	-	-	98,068	110,201
Zn	mg/kg	17,516	95,805	16,882	28,305	38,115	110,268	68,018
HREE	mg/kg	11,380	13,151	11,991	4,965	8,060	21,675	15,598
LREE	mg/kg	6,100	13,698	13,105	6,090	10,429	26,322	18,311
Sc	mg/kg	176	7	19	20	23	18	7

The overall recovery of rare earth elements for each of the seven sites was determined by comparing concentrations from the raw water to the filtrate. The overall recovery of rare earth elements ranged from 46.2% to 98.8% (Table 8). The site with the lowest REE recovery was AQ-67, which only recovered

46% of the REE from the raw water. AQ-2 recovered 75% of the REE, AQ-50 recovered 94%, AQ-65 recovered 95%, AQ-8 recovered 97%, and AQ-3 recovered 97% REE. AQ-51-5 had the highest REE recovery at 99%. In all sites the recovery of LREEs was not as high as the HREEs with lanthanum having the lowest recovery.

Table 8. Recovery of each of the REE from each of the seven sites.

		AMD Site						
Element	**Units**	**AQ-2**	**AQ-8**	**AQ-50**	**AQ-51-5**	**AQ-3**	**AQ-65**	**AQ-67**
Sc	**%**	99	98	99	100	99	99	93
Y	**%**	77	97	97	99	97	95	46
La	%	26	83	79	98	86	92	37
Ce	**%**	51	98	96	99	96	95	45
Pr	**%**	62	96	96	99	96	94	43
Nd	**%**	66	96	97	99	96	95	44
Sm	**%**	81	99	99	99	98	95	47
Eu	**%**	84	99	99	99	99	96	47
Gd	**%**	80	98	98	99	99	95	47
Tb	**%**	87	99	99	99	99	96	49
Dy	**%**	90	99	99	99	99	96	50
Ho	**%**	89	99	99	99	99	96	50
Er	**%**	91	99	99	99	99	97	53
Tm	**%**	95	99	100	100	100	97	56
Yb	**%**	97	100	100	99	100	97	55
Lu	**%**	96	100	100	100	100	97	83
HREE	**%**	82	98	98	99	98	96	48
LREE	**%**	58	95	93	99	95	94	44
TREE	**%**	**75**	**97**	**95**	**99**	**97**	**95**	**46**

Discussion

This study demonstrated that the multi-step precipitation procedure developed for the AQ-2 site worked equally well with sites that had differing water quality. The first step was effective at iron removal while the second step removed the majority of the aluminum. Most of the rare earth elements were recovered in the final precipitate. The compositions of the final precipitates were more varied than the previous precipitates. All final precipitates contained residual aluminum and contained various metals which precipitate out at a higher pH range, such as magnesium, manganese, nickel, and zinc. The variable concentrations of these metals in the final precipitates were likely due to differences in raw water concentrations. However, regardless of the metals which contributed to the final precipitates, the precipitates were enriched in REE, with grades above 1.0%. The smaller concentration of metals in the precipitate helped to improve the REE grade by reducing the dilution effect seen in the midstream precipitates. The REE grade of the precipitates ranged from 1.1% at AQ-51-5 to 4.8% at AQ-65.

The REE recoveries of the seven sites ranged 46% to 99%. Recovery was greater than 90% for all sites except AQ-67 and AQ-2. None of the raw water parameters correlated well with recovery. Additionally, none of the raw water characteristics correlated well with grade of the final precipitates. However, there were significant correlations with mass of the final precipitates. Total REE, Zn, Mn, and Ni concentrations were all good predictors of REE mass in the final precipitate. Zn, Mn and Ni are all parameters that are commonly measured and relatively inexpensive allowing for the screening of many sites to determine which should be investigated further.

Subtask 2.2. REE Precipitation Under Reducing Conditions

Overview

The ability to separate REEs from gangue metals such as Fe, Al, and Mn was investigated under varying redox conditions between pH 6 to 8.

Approach

AMD collected from the AQ-2 site was precipitated under oxidizing, reducing, and fully oxidized conditions. It was found that fully oxidized conditions improved REE separation from gangue metals. The partially reduced samples displayed overlap of iron removal with the REE recovery pH range. A multi-step sequential precipitation on fully oxidized AQ-2 AMD determined that iron and aluminum precipitated from solution. Scandium precipitation dynamics were very similar to aluminum. The remainder of the REEs, along with Ni and Zn, precipitated in the upper pH setpoints.

Results and Discussion

Oxidizing and Reducing Conditions

Fully oxidized

In the fully oxidized sample, there was substantial removal of Iron, chromium, and cadmium. 100% of iron was removed, 94% of chromium was removed, and 80% of cadmium was removed. It is likely that chromium experienced greater removal, but our calculations stopped at 94% due to the concentration reaching below the detection limit. Cadmium was expected to have the same trend, however it showed increased removal at elevated pH setpoints. The final cadmium removal was 90%. The bulk of aluminum (97%) was also removed during the testing and ultimately reached 100% removal. Copper was removed across the entire pH range of the experiment.

Removal was limited between lower pH setpoints, with only 19% removed. Removal increased to 32% y , 55%, 81% , and finally 94% for the upper range of the pH adjustments. Manganese began precipitating midway through the precipitation but did not show significant precipitation until the upper limits were obtained, where removal reached 99%. Nickel and cobalt removal also occurred at the higher pH setpoints and reached 94% and 100%. Neither calcium nor magnesium were removed during pH adjustment.

The recovery of the rare earth elements during the fully oxidized precipitation procedure varied greatly between the HREEs, LREEs, and scandium. The scandium was recovered in a similar trend to aluminum, with the bulk of scandium was recovered between near the mid-point of the pH ranges used in testing. However, 100% scandium recovery was not achieved until elevated pH values were observed. The HREEs and LREEs had a wider gap between recoveries across the pH range, but both showed 100% recovery at upper pH limits.

Partially Reduced

In the partially reduced sample iron removal occurred over a wide range of pHs and was not completed until the upper pH setpoint was reached. Cadmium also showed delayed precipitation similar to the iron and was not fully removed until past mid-way in the pH testing range. Cadmium only displayed 88% recovery due to the concentration in the filtrate being below detection limits. Chromium did not appear to be as impacted by being in a partially reduced sample. The recovery of chromium was 93% at a mid-level pH setpoint. Higher recovery was not observed for chromium due to the concentrations being at or below detection. Aluminum removal was similar to that observed in the fully oxidized testing results. Copper also precipitated out near the mid-level pH range. The bulk of zinc removal occurred between at upper pH setpoints. 99% of zinc was removed by the final testing setpoint.

Nickel and cobalt had similar precipitation trends, and reached 54% removal and 50% removal, respectively at the upper end of the pH testing range. Manganese had three reductions in removal during the pH adjustments. At the mid-point, the removal of manganese had reached 8%, but decreased to 1% at the next whole pH increment. At the following whole increment, the removal had increased to 18%. The second decrease in recovery occurred in the upper pH range with 12% removal. The removal of manganese increased at the penultimate pH setpoint to 28%, but then decreased the third time at the final setpoint to 22%. By the uppermost set-point, calcium removal was 0% and magnesium removal was 2%. However, calcium removal peaked at 7% at and magnesium removal peaked at 10% at the middle pH ranges.

Scandium recovery was not significantly altered with the partially reduced conditions. The bulk of scandium recovery occurred between at the mid-range pH (91%), with 99% recovery at one full pH unit above the midpoint. The recoveries of HREEs and LREEs did not significantly differ across the pH range of the experiment, with both groups reaching 100% recovery at the upper pH values.

Reducing conditions

The removal of iron and cadmium was similar to the partially reduced sample, but the complete removal of cadmium did not occur, while removal of iron did not occur until the upper pH limit with 88% and 100% removal, respectively. The removal of aluminum and chromium was also similar to the partially reduced sample. The bulk of aluminum was removed by the pH mid-point (96%), with 100% of removal occurring by the uppermost pH setpoint. Most of the chromium was removed between the lower quarter pH setpoints (75%), and 93% removal was achieved by the pH midpoint Copper began precipitating out just below the midpoint and finally reached 97% removal at the uppermost pH setpoint. Zinc was removed between at the upper pH ranges and100% removal was achieved.

The bulk of nickel and cobalt removal occurred between the upper pH limits, with 80% removal of nickel and 83% removal of cobalt. Nickel removal peaked at 93% at the uppermost setpoint, while cobalt removal reached 97%. Manganese did not begin precipitating out until past the middle setpoint, and only achieved 52% removal by the uppermost pH. Removal of both calcium and magnesium was minimal over the entire pH range of the experiment.

The bulk of scandium was removed below the midpoint pH, with continuing recovery until in the upper pH levels. There was a slight differentiation between recovery efficiency for HREEs and LREEs, but full recovery was reached at the uppermost setpoint for both HREEs and LREEs. A slight decrease in HREE and LREE recovery was observed. HREE recovery decreased from 29% to 25%, and LREE recovery decreased from 16% to 12% below the pH midpoint. Recovery continually increased after this pH step.

Effects of Redox Conditions on Metal and REE Removal

Not all sources of acid mine drainage are completely oxidized. Many sources are either partially oxidized or heavily reduced. The effects of redox conditions were observed during the pH adjustments of fully oxidized, oxidizing, and reduced AMD samples. As expected, the removal of metals and rare earth elements changed depending on redox conditions. The major difference between the fully oxidized, partially reduced, and reduced conditions was the precipitation range of iron.

Iron is one of the major constituents in AMD and is considered a contaminant in REE sludge products due to its issues in downstream refinement processes. Comparing the oxidized and reduced samples, the iron precipitated out at a lower pH when the sample was more oxidized. The iron was completely removed by the second pH setpoint in the fully oxidized sample. However, both the partially reduced and reduced samples showed delayed removal of the iron. The partially reduced sample had complete iron removal by the sixth setpoint, and the reduced sample had removal by the eighth setpoint.

The differences in iron removal are most likely due to the differences in precipitation pH between ferric

iron and ferrous iron. Ferric iron precipitates out of solution at lower pH values, while ferrous iron precipitates much later at higher pH values. The fully oxidized sample contains only ferric iron, which is completely removed at the second pH setpoint. The partially reduced sample contains both ferric and ferrous iron. The first sharp peak between the lower pH values for the reduced sample is the precipitation of ferric iron. The removal of iron plateaus until the pH midpoint, and then significant removal is observed at the upper pH setpoints. At this range, the ferrous iron was removed as a blue-green precipitate. Iron removal from the partially reduced sample was more gradual due to the oxidation of ferrous iron to ferric during the pH adjustments. Iron removal in the reduced sample occurred over an even more extended range as the iron was maintained in the ferrous form. The prolonged removal of iron of the partially reduced samples is not ideal for the precipitation procedure.

The removal of aluminum did not appear to be impacted by the redox conditions of the pH adjustment. In all three samples, the aluminum precipitated beginning at the lowest pH value, with bulk removal by the midpoint. The only difference in removal appeared to be that slightly more aluminum was removed in the more oxidized samples. The fully oxidized sample had 12% of the aluminum removed by the second pH setpoint, while the partially reduced and reduced samples had 6% and 1% removal, respectively. The general trend of removal was the same for all three samples.

The scandium recovery was minimally impacted by the redox conditions of the pH adjustments. The bulk of recovery occurred in the same range as aluminum. The recovery of scandium from both the partially reduced and reduced samples were almost identical, varying by only a few percentages. The fully oxidized sample showed the greatest deviation, with a larger percentage of scandium being removed by the second setpoint (24%), as well as a higher pH for complete removal. Considering the precipitation procedure, the behavior of the scandium in the partially reduced samples is preferable due to the near complete removal between setpoints two and four.

There was more variation in removal of both the HREEs and LREEs due to the redox conditions. For HREE, both the partially reduced and reduced samples had similar recovery at like pH setpoints. The fully oxidized sample had a more gradual recovery and did not show complete recovery until the penultimate setpoint. The LREEs displayed a similar pattern, with the partially reduced and reduced samples having the bulk of recovery by the sixth setpoint and recovery by the penultimate setpoint for the fully oxidized sample.

The change in the recovery of rare earth elements in the partially reduced samples is likely due to the incomplete removal of iron at a lower pH. Both iron and aluminum-based compounds have previously been used in REE sorption experiments and proven effective. The impact of the presence of both iron and aluminum was determined to be significant during the seeding experiment discussed in a later section. The removal of REEs in the partially reduced samples increased when in the presence of increased iron precipitates relative to the fully oxidized sample. For both LREE and HREE recovery, the recovery of REE at a later pH is preferred for the precipitation procedure. Just as it is ideal to remove the iron as early as possible, the later removal of REEs helps to separate the REE precipitation from the precipitation of the bulk of the metals. The partially reduced and reduced samples showed partial HREE and LREE by pH setpoint four. The fully oxidized sample did display some recovery in HREEs by setpoint four, but LREE recovery did not occur until pH setpoint six.

Considering the precipitation procedure discussed previously, having a fully oxidized sample is preferential to a partially reduced sample. The iron is completely removed from the fully oxidized sample at a much lower pH than the partially reduced sample. This creates a clear separation between iron removal and REE recovery. Both the partially reduced samples had significant iron removal between pH setpoints four and seven, which is the range of the REE enriched sludge. This would both dilute the sludge and decrease the REE grade, as well as create issues in downstream refinement processes. The

fully oxidized sample also showed increased HREE and LREE recovery.

The recovery of HREE and LREE was delayed compared to the partially reduced and reduced samples. As with the explanation for iron removal, the delayed REE recovery is beneficial because it further separates the recovery of REEs from the precipitation of waste metals. Although the removal of scandium is slightly more efficient with the partially reduced samples, the early removal of iron and late removal of HREE/LREE of the fully oxidized sample is more significant to the three-step precipitation procedure. As such, following precipitation procedures were conducted in fully oxidized conditions.

Multi-Step Precipitation

Methods

Fully oxidized raw AMD collected from AQ-2 was adjusted to thirteen pH increments. 16 L raw AMD was adjusted to each target pH using a caustic material. Filtrate and precipitate samples were collected for each target pH and analyzed using inductively coupled plasma optical emission spectrometry (ICP-OES) and inductively coupled plasma mass spectrometry (ICP-MS) for metal and REE concentrations.

Results

The major metals in the raw AMD were iron (40.4%), calcium (28.1%), aluminum (21.3%), and magnesium (9.1%). Zinc (0.5%), manganese (0.4%), and nickel (0.2%) were present as were cobalt (0.1%), copper (0.02%), chromium (0.1%) and cadmium (0.003%). Total REE were 0.001% of the concentration of the major metals.

Metals were removed over a broad pH range. Iron, the most prevalent metal in AMD was removed by pH setpoint three with 100 % recovery. Aluminum was removed between setpoints three and six with 98% of the aluminum removed by the fifth and the remaining 2% removed by the sixth. Zinc precipitation occurred around middle pH setpoint and reached 100% removal by the penultimate setpoint. Approximately 97% of zinc removal was completed by the ninth pH setpoint. Nickel and cobalt had bulk precipitation between mid and upper pH setpoints. By the uppermost setpoint, 99% of nickel and 100% of cobalt was removed. Manganese began precipitation around the fourth setpoint, however the bulk of removal began at the ninth setpoint. By the last setpoint, only 85% of the manganese was removed. It is likely that if the pH range was expanded, to higher pH values, that 100% of the manganese would be removed. Neither calcium nor magnesium were removed efficiently by the uppermost setpoint. Only 8% of the calcium was removed, while 12% of the magnesium was removed. Chromium, cadmium and copper were present in small quantities (<0.1 mg/L) in the raw water which made determining when complete removal was achieved difficult. Chromium and cadmium were removed at the lower range of setpoints; however, recovery was 92% and 86%, respectively. At these lower pH values, concentrations were below detection but the total mass precipitated was less than what was present in the raw water yielding less than 100 % recovery. Removal of copper began at pH setpoint four with 92% removal by the seventh setpoint with a concentration that was below detection limits

The REEs were separated into HREEs (Gd - Lu, Y), LREEs (La - Eu), and scandium. Scandium was removed at pH values below the middle setpoint with 99% recovery. Removal dynamics were very similar to aluminum. Removal of LREEs and HREEs followed slightly different patterns. Both the HREE and LREE showed similar recoveries at lower pH values, but the HREEs had more efficient recovery for the middle pH range. At this middle range, the HREEs were 20%, 47%, 85%, and 98% recovered, respectively. However, the LREE recoveries were much lower at 13%, 23%, 53%, and 88%, respectively. The LREEs did not show 98% recovery until pH setpoint ten.

Discussion

The recovery of the rare earth elements occurred across a broad pH range. The HREEs, LREEs, and

scandium were recovered at different stages of the pH adjustment. Scandium was recovered at pH values below the midpoint with considerable overlap with the removal of aluminum. The HREEs were recovered between setpoints four and nine, while the LREE were recovered between setpoints four and eleven. However, the majority of HREE and LREE recovery did not occur until the fifth setpoint.

The pH range of precipitation for most of the metals was not in agreement with those predicted by published Pourbaix diagrams (Takeno, 2005). Aluminum, iron, and scandium precipitated close to the predicted precipitation ranges. Cadmium, cobalt, chromium, copper, manganese, zinc, and the remaining REEs began precipitating at a much lower pH and generally were completely removed before or around the predicted pH. The Pourbaix diagrams referenced were determined considering pure metal solutions while AMD may contain a variety of metals as well as high concentrations of sulfates, carbonates or silicates. Interactions between all the ions may have caused changes in expected precipitation patterns. It is possible that the earlier recovery of REEs is due to the presence of other metals which precipitated out during the same range. Zinc, manganese, cobalt, and nickel all precipitated out during the same pH range as the REEs, and likely promoted coprecipitation

Both the recovery pH ranges as well as the market value of the separate REEs were considered when determining the stages of the sequential precipitation procedure for REE recovery. Based on the metal and REE removal data, an optimal precipitation procedure was developed.

Subtask 2.3. REEs Extraction Optimization

Overview

The optimization of the precipitation procedure was assessed based on the data collected from the fully oxidized precipitation procedure previously discussed. From this data, two precipitation procedures were developed. Both procedures produced a precipitate that was enriched in REEs with grades greater than 1%. The use of a flocculent during either precipitation procedure improved REE recovery but reduced the grade as more gangue metals were also precipitated. Flocculants are needed to reduce settling time, increase precipitate floc size and improve retention floc within a geotextile bag. Thoughtful application within the treatment process may reduce the undesirable effects. Seeding the supernatant with either precipitated iron or aluminum, but not raw AMD, improved recovery of the REEs.

Approach

Assess stability, selectivity, and enrichment parameters and adjust the design to enhance these parameters. It is expected that both Eh and pH conditions would affect stability, selectivity, and enrichment of REEs. Given the kinetics of Fe^{2+} oxidation at low pH values, it will be determined if this REE strategy can be operated under ambient condition by quantifying Fe^{2+} oxidation rate in untreated AMD samples and develop a guideline for treatment time. The final pH endpoint for optimal separation of REEs and the gangue metals will be determined for the three selected AMD sources and compared for variability.

Results and Discussion

Seeding Test for Improved REE Recovery

Methods

A seeding test was performed to determine whether the addition of iron or aluminum precipitates would facilitate REE recovery and sorption. Three samples of filtrate were seeded separately with lower pH precipitate one (0.615 mg iron dry weight), precipitate two (0.615 mg aluminum dry weight), and a volume of raw AMD calculated to contain 0.615 mg iron by dry weight. Each sample was rapid mixed for 1 minute, and slow mixed for each 15 minutes. After mixing, the samples settled for 30 minutes and

were then filtered. The samples were maintained at a constant pH value during the seeding test. The total REE concentration of the precipitate was approximately 1% of the original concentration of the raw AMD.

Results

The aqueous samples collected from the seeding test were analyzed for REEs. The additional removal of REEs due to seeding was calculated by comparing concentrations of the pre- and post-seeding filtrates. The recovery of REEs due to the iron precipitate, aluminum precipitate, and raw water is shown below in Figure 2. The HREE showed greater recovery than the LREE for the iron precipitate, aluminum precipitate, and raw water. The LREEs averaged at 77% recovery, while HREEs averaged at 87% recovery after seeding. For all lanthanides except lanthanum, cerium, praseodymium, and neodymium, the aluminum precipitate had an equal or higher percentage of recovery. The raw water had significantly less recovery when compared to both the iron and aluminum precipitate. The aluminum precipitate averaged 85% recovery across all REEs, iron precipitate averaged 83% recovery, and the raw water averaged 69%.

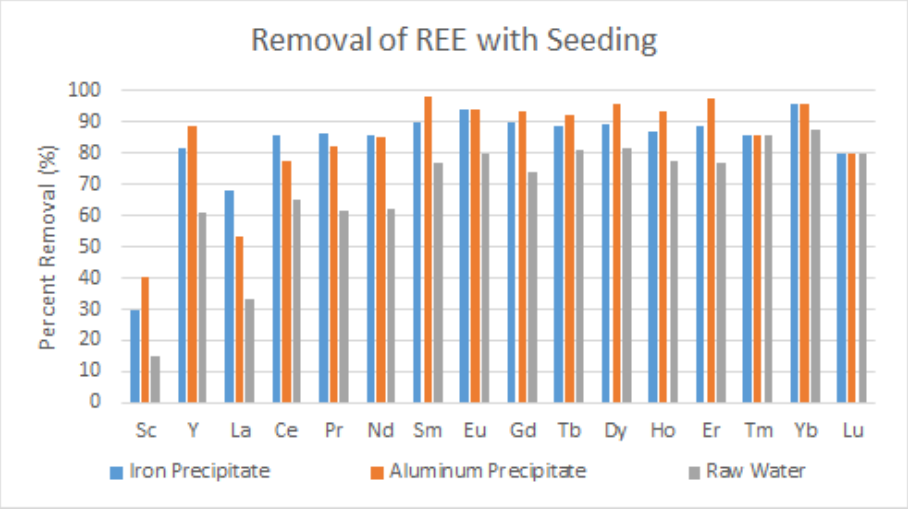

Figure 2. Recovery of residual REEs from filtrate after seeding with iron precipitate, aluminum precipitate, and raw AMD.

Task Completion Status

100% complete.

Subtask 2.4. Cost Effectiveness Assessment

Overview

Task 2.0 was successful at generating a high grade REE product with the assistance of Solvent Extraction (SX). Furthermore, the process developed during this task is considered supplemental to other ongoing research conducted on award DE-FE0026927. As a result, comparing economics between projects is unreasonable given the dependency between the two processes. For a complete economic analysis, please refer to Task 5.0.

Approach

At the end of the first year, we assessed the economic viability of the low pH AMD extraction technology. Economic parameters for this extraction strategy were compared to those of our ongoing REE extraction from AMD sludge. This is a Go/No Go decision point for this extraction strategy.

Results and Discussion

Based on the progress of the research, this task is redundant.

Subtask 2.5. Treatment Protocol Development

Overview

A novel approach was required to produce a sufficient quantity of material to feed the ALSX system. As discussed below, the treatment of a very large volume of AMD is required to produce a sufficient quantity of feedstock. As a result, a mobile plant was constructed that could be operated at the AQ-2 treatment site. In all, over 160kg of mobile plant product (MPP) was produced to feed the ALSX system.

Approach

Produced sufficient enriched product to feed into the ALSX facility (Task 4.0). If this extraction strategy compares favorably with REE extraction from AMD sludge, this subtask will determine a treatment protocol to produce sufficient REE precipitates for following ALSX treatment.

Results and Discussion

Task 4 requires that the precipitate from the net-acidic AMD route will be processed through the WVU ALSX system. As such, a considerable mass of precipitate is required to generate the feedstock for the 150 ml/min SX system. Unfortunately, multiple experiments from Task 2 have shown that only a small amount of the concentrated REE product is produced from a given amount of AMD, as seen below in Table 9. This shows that egregious amounts of water must be processed at the WVU facility to produce enough precipitate feedstock. As a result, a mobile plant was constructed to apply the staged precipitation technology at an operating AMD site.

Table 9. Mass of the REE precipitate from Task 2 experiments.

Site	Units	AQ-2	AQ-8	AQ-50	AQ-51-5	AQ-3
Emperical Data						
Treated Volume	(l)	32	75	75	75	75
Precip. Mass	(mg)	177	2,136	2,827	1,371	251
Precip. Production Rate	(mg/l)	6	28	38	18	3
SX Mass Calculations						
Precip Mass Required	(kg)	5	5	5	5	5
AMD Required	(l)	905,490	175,572	132,633	273,499	1,495,949
AMD Required	(gal)	239,547	46,448	35,088	72,354	395,754

After construction of the mobile plant was completed, it was delivered to the AQ-2 AMD site. Once located on site, the plant was plumbed into the AQ-2 treatment system, allowing for a split of the clarified water to be pulled from the clarifier before discharge to the settling ponds. Supplemental chemical treatment was also installed so that the AQ-2 clarifier could operate at lower pH levels, while still maintaining compliance at the National Pollutant Discharge Elimination System (NPDES) outlet at the end of the finishing pond.

After installation, shakedown testing was started to train the pH controllers to maintain a constant level in the two tanks. Operating schemes for parallel and series operation were developed to maximize flexibility of the plant. Initial testing has produced several kg of product.

The mobile plant was operated continuously for approximately ten days. During this time the precipitate was collected in 5-gallon buckets for transport to the NRCCE laboratory. Table 10 below shows a comparison between the typical AQ-2 AMD precipitate and the mobile plant product (MPP). Overall, the

REEs in the MPP were enriched by a factor greater than 5. Additionally, a significant reduction in the amount of Fe present in the MPP is shown when compared to the typical AQ-2 AMDp. This is significant as the Fe results in a considerably higher acid consumption rate during leaching and can cause third phase formation in the SX circuit.

Table 10. Comparison between AQ-2 Precipitate and MPP.

Parameter	Units	AQ-2 AMD Precipitate	Mobile Plant Product (MPP)	Enrichment Factor
Major Metal				
Al	(mg/kg)	57,356.47	120,742.38	2.11
Ca	(mg/kg)	11,591.48	28,897.76	2.49
Co	(mg/kg)	219.68	991.73	4.51
Fe	(mg/kg)	202,047.72	37,434.89	0.19
Mg	(mg/kg)	5,749.14	5,490.40	0.95
Mn	(mg/kg)	1,116.92	3,334.25	2.99
Na	(mg/kg)	198.29	824.11	4.16
Si	(mg/kg)	17,736.40	73,965.97	4.17
Cl	(mg/kg)	17.28	14.08	0.82
Moisture	(%)	78.25	80.54	1.03
REE				
Sc	(mg/kg)	31.97	44.22	1.38
Y	(mg/kg)	63.23	475.14	7.51
La	(mg/kg)	14.34	109.61	7.64
Ce	(mg/kg)	51.02	316.42	6.20
Pr	(mg/kg)	8.52	46.54	5.46
Nd	(mg/kg)	42.03	224.21	5.33
Sm	(mg/kg)	13.06	59.29	4.54
Eu	(mg/kg)	3.41	15.43	4.53
Gd	(mg/kg)	20.05	97.81	4.88
Tb	(mg/kg)	3.80	17.88	4.70
Dy	(mg/kg)	23.17	99.26	4.28
Ho	(mg/kg)	4.46	20.61	4.62
Er	(mg/kg)	12.30	52.23	4.25
Tm	(mg/kg)	1.65	7.00	4.23
Yb	(mg/kg)	9.55	36.66	3.84
Lu	(mg/kg)	1.47	5.61	3.81
Actinides				
Th	(mg/kg)	8.52	2.53	0.30
U	(mg/kg)	4.99	8.01	1.61
TOTALS				
TREE	(mg/kg)	304.02	1,627.91	5.35
LREE	(mg/kg)	132.37	771.49	5.83
HREE	(mg/kg)	171.65	856.42	4.99
CREE	(mg/kg)	152.27	914.31	6.00

While the grade of the MPP was significantly enriched over the typical AMDp, it still did not exceed 1% as seen in laboratory-scale testing. While unfortunate, it was not entirely unexpected. The scale of the mobile plant did not provide a sufficient residence time in the mixing chamber to allow for full separation of the metals and REEs. On a pilot or full-scale plant using clarifiers verses tanks with plate and frame filters a longer residence time would allow for production of a higher-grade product. In all, 164.32 kg (wet basis) if MPP was collected during the testing run. This material was split into two aliquots, one for exploratory testing and one for end-to-end testing used to complete the Task 4.4 objective.

Task Completion Status

100% complete.

Task 3.0 – Case B. Net Alkaline Mine Drainage Extraction Strategy

Subtask 3.1. Characterization of AMD Source Compositions, Design of the Electro-Membrane Extraction System

Overview

A supported liquid membrane was constructed and tested using a synthetic solution. Results from these experiments indicated that while the membrane was able to separate REEs, the size of the membrane in relation to the flux required was not feasible. Additionally, issues relating to the stability of the membrane were encountered that did not allow for testing of large volumes of water. As a result, the Task 3 path was deemed irrelevant and research efforts were focused on Task 2 research.

Approach

Evaluate the results of ongoing sampling (DE-SOL-0009607) to determine the short- and long- term variability of Case B feedstock: Steele Shaft AMD. Specifically, included redox potential and iron speciation to the analytical suite. Acquire parts and assembled the electro-membrane extraction system. The initial design work is based on the sub-liter scale.

Results and Discussion

The feedstock for Task 3 is net-alkaline AMD, which typically originates in flooded underground mines. The water chemistry of these flooded AMD outflows differs significantly from above-drainage mines. Typically, the pH of AMD discharged from these mines has a higher pH value since the oxidizing conditions that produce AMD are not present. Table 11 shows the composite of 13 AMD samples from the flooded underground mine feedstock used in Task 3. Given the technical difficulties observed using this technology, further characterization of the feedstock was deemed irrelevant.

Table 11. Typical REE concentration for a net-alkaline flooded underground mine.

Site	SS
Mine Type	Underground
Horizon	Delow Brainage
Seam (s)	Pittsburgh
AMD Samples	13
pH	6.71
REEs (µg/L)	
Sc	3.82
Y	13.27
La	0.32
Ce	1.49
Pr	0.35
Nd	2.55
Sm	0.92
Eu	0.29
Gd	1.83
Tb	0.28
Dy	1.78
Ho	0.42
Er	1.21
Tm	0.15
Yb	0.81
Lu	0.13
TREE	30
HREE	24
LREE	6
CREE	18

A cell with a Supported Liquid Membrane, a dimensionally stabilized anode, a stainless-steel cathode and 2 Ag/AgCl reference electrodes was constructed. The effective area of the membrane was 6 cm^2. The SLM was a porous polypropylene film, 25 microns thick, saturated with a 6:1 mixture of dodecane and di-(2-ethylhexyl) phosphoric acid (DEHP). Solutions containing dilute NaCl (0.05 M) and mixtures of La(III) and Fe(III) showed that La(III) was selectively transported across the membrane. A diagram of the constructed membrane is shown in Figure 3.

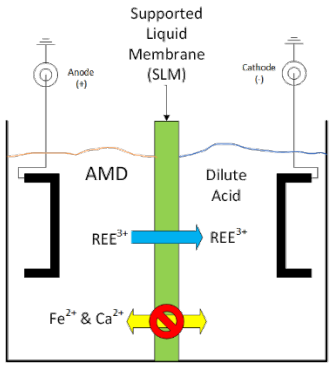

Figure 3. Diagram of electro-membrane separation.

Subtask 3.2. Evaluation of the Electro-Membrane Extraction System on Synthetic AMD Samples

Overview

The original goal was to investigate the viability of using a supported liquid membrane in an electrochemical cell to transport REEs selectively from AMD to an acidic strip solution. The method worked, but the rate of transport with and without an electric field was judged to be insufficient for practical extraction. In addition, the supported liquid membrane was unstable.

Approach

Tested the electro-membrane extraction system on synthetic samples ranging from simple aqueous solutions containing just the REEs to solutions mimicking the AMD. Focused on those elements with greater economic benefit: scandium (Sc), yttrium (Y), neodymium (Nd), and dysprosium (Dy). Tested neutral and acidic ligands for extraction. Evaluated liquid membrane stability and any type of fouling of the membrane by precipitates; adjusted conditions to enhance stability and inhibit fouling. Measured fluxes and acceptor solution concentrations of REEs and gangue metals (e.g., Fe, Mn, Al, Mg, and Ca).

Results and Discussion

The base experiment consisted of a solution containing 0.05 M NaCl, 1 mM La(III) (140 ppm), on the anode side, and a 0.1 M HCl solution on the cathode side. Samples of the catholyte were collected and analyzed for La(III) concentration using the Arsenazo colorimetric reagent. With no current flow, the flux of La across the membrane was $1.4x10^{-8}$ mol/s/cm^2 of membrane (equivalent to 70 g/hr/m^2). With a current flow of 16 uA/cm^2 (70 mV across the membrane, with the strip solution negative relative to the source solution), the flux did not increase significantly.

Extrapolating this result to AMD with REE concentrations more than 100-fold lower predicts that fluxes of REEs would be proportionally lower. Another problem is a slow thinning of the supported liquid membrane as indicated by the resistance and capacitance of the electro-membrane cell (measured by electrochemical impedance spectroscopy). Based on these observations, the electro-membrane approach to extracting REEs from AMD was judged to be uneconomic. This approach was abandoned, and Subtask 3.3 (Evaluation of the electro-membrane extraction system on real AMD samples) was not performed.

Typical AMD solutions contain relatively high concentrations of Fe in its reduced form. The new strategy

consisted of oxidizing the Fe(II) to Fe(III) and then collecting REEs by co-precipitation with $Fe(OH)_3$. Experiments with solutions containing Fe(II) and selected REEs showed that quantitative oxidation of the Fe(II) to Fe(III) using H_2O_2 and titration resulted in quantitative co-precipitation of the REEs with the $Fe(OH)_3$. This method achieved a 10-fold concentration enhancement of the REEs, but there was still a problem of separating the REEs from the iron. Partial oxidation of Fe(II) to Fe(III) and titration again achieved near quantitative collection of the REEs while reducing the total amount of $Fe(OH)_3$. Attempt to precipitate REEs as the hydroxides in the absence of Fe were not successful. Attempts to maintain reducing conditions by removing dissolved oxygen while raising the pH were not successful because $Fe(OH)_2$ precipitated and collected the REEs. Addition of coagulants (AQ200 and AQ590, Aquamark) to collect and settle $Fe(OH)_3$ floc was successful in removing most of the Fe at low pHs, but floc coagulation was not successful at higher pH values, the pH range at which REEs were co-precipitated. In general, basic pH values used in the presence of $Fe(OH)_3$ was needed to quantitatively collect REEs from the simulated AMD. The best strategy was to oxidize all of the Fe(II) to Fe(III), carefully titrate to a pH at which most, but not all of the Fe formed $Fe(OH)_3$ floc, remove the floc, then titrate, and collect the mixture of residual $Fe(OH)_3$ and REEs.

A simulated alkaline AMD solution with bicarbonate and REEs was treated with H_2O_2 to oxidize Fe. The pH did not drop. Removal of the resulting $Fe(OH)_3$ precipitate resulted in 90% of the Fe and more than 90% of the REEs collected in the precipitate. Since partial separation of Fe from alkaline AMD was the goal, this experiment demonstrated that alkaline AMD would have to be converted to acidic AMD in order to achieve maximum collection of REEs with minimal collection of REEs. This approach was abandoned.

The project goals were then changed to isolation of REEs from the acidic strip solution obtained from solvent extraction of acid treated AMD sludge. The goal was a solid containing more than 90% REE oxides by weight.

Subtask 3.3. Evaluation of the Electro-Membrane Extraction System on Real AMD Samples

Overview

Task 3.0 was unsuccessful in producing REEs from net alkaline mine water. As a result, this task did not warrant an economic evaluation.

Approach

Tested the electro-membrane extraction system on the selected alkaline AMD sample. Assessed stability, selectivity and enrichment parameters and adjusted the design to enhance these parameters.

Results and Discussion

N/A

Subtask 3.4. Cost-Effectiveness Assessment

Overview

Task 3.0 was unsuccessful in producing REEs from net alkaline mine water. As a result, this task did not warrant an economic evaluation.

Approach

At the end of the first year, assessed the economic viability of the electro-membrane extraction technology. Factors included the suitability of the acceptor solution for ALSX treatment and the projected cost of treating large volumes of alkaline AMD. If this method shows promise, proceed with scale up from milliliters to liters of alkaline AMD donor solutions.

Results and Discussion
This approach was deemed technically infeasible; therefore, no economic evaluation was conducted.

Subtask 3.5. Treatment Protocol Development
Overview
Task 3.0 was unsuccessful in producing REEs from net alkaline mine water. As a result, this task did not warrant development of a treatment protocol.

Approach
Produced sufficient enriched product to feed into the ALSX facility (Task 4.0).

Results and Discussion
N/A

Task Completion Status
100% complete.

Task 4.0 – Solvent Extraction of Resulting Precipitates
Subtask 4.1. Model System Evaluation, Gangue Separations
Overview
In this subtask, solvent extraction (SX) was used to separate REEs from major gangue elements. The objective of this testing was to raise the REE concentrate from a nominal grade of 0.5% to over 90% while optimizing various SX operating conditions. Tests were conducted at the laboratory scale, and simplified synthetic solutions were used to simulate the pregnant leach solution produced from full dissolution of pre-concentrate. The specific recipe for this synthetic solution was determined from the mobile plant product generated from field testing at the AQ-2 Mine site. Five surrogate REEs (Sc, Y, Ce, Nd, Dy) and nine surrogate gangue elements (Al, Ca, Mg, Zn, Fe, Cu, Co, Ni, and Mn) were used in the solution. SX tests evaluated the influence of pH, phase ratio, and reductant dosage on the process efficiency in the extraction, scrubbing, and stripping stages. The results show that through proper optimization of the process parameters, mixed REE oxides exceeding 90% purity can be produced via solvent extraction.

Approach
In this subtask, “model” systems were used to determine the optimal solvent extraction chemical conditions and flowsheet that separates REEs from common gangue metals, such as Fe, Al, Mn, Mg, Ca, and/or Si. Initially, a bulk quantity of solution was generated using standard metal solutions with concentrations commensurate with the pre-treatment products produced from Tasks 2.0 and 3.0. Next, batch-wise, laboratory-scale solvent extraction tests were conducted using 500 to 1,000 mL separatory funnels that were hand shaken. Parametric testing evaluated the influence of solution pH, reagent type, reagent concentration, aqueous to organic (A:O) ratio, solution feed concentration, gangue metal concentration, contact time, and other influential parameters as appropriate. Experimental measurements included the pH before and after contact as well as the REE and gangue metal concentrations before and after contact. Calculated output factors included the distribution coefficient, the selectivity index, the final product purity, and the final grade. All factors were evaluated for statistical significance with respect to the input parameters, and once an optimal condition is determined, an additional test suite was conducted to construct the McCabe-Thiele diagram that can be later used for process scale up and design. Overall, the objective of this task was to determine the appropriate solvent extraction scheme that can successfully remove gangue metals while enriching the REE product.

Results and Discussion

Materials – Synthetic Simulated Leachate

The desired concentration of the synthetic leachate was determined by assuming full dissolution of 136 grams of pre-concentrate in a 1L acid solution. By calculation, this dissolution procedure will produce a total concentration of the five surrogate REEs (i.e. Sc, Ce, Nd, Dy, and Y) of approximately 100 mg/L. The target concentration of the five REEs as well as the surrogate gangue metals in the leachate has been calculated and is listed in Table 12. Using these guidelines, the simulated leachate was prepared by dissolving calcium hydroxide ($Ca(OH)_2$) and metallic nitrates ($Al(NO_3)_3$, $Cu(NO_3)_2$, $Fe(NO_3)_3$, $Mg(NO_3)_2$, $Mn(NO_3)_2$, $Ni(NO_3)_2$ and $Zn(NO_3)_2$) in deionized water. The resultant solution was then mixed with standard solutions of Co(III), Sc(III), Y(III), Nd(III), Dy(III) and Ce(IV). The actual concentration of the synthetic solution was verified via ICP-MS. This data is shown in Table 12.

Table 12. Target Concentration and Actual Concentrations of Elements in Simulated Leachate.

	Major Gangue Metals			Minor Gangue Metals						REEs				
mg/L	Al	Ca	Zn	Mg	Ni	Mn	Fe	Co	Cu	Sc	Ce	Nd	Dy	Y
Target	20883.4	861.2	507.1	173.0	146.9	114.6	80.4	52.7	17.4	20.0	24.0	20.2	0.1	41.0
Actual	19177.0	837.2	486.9	178.5	144.4	105.6	81.7	51.0	17.2	20.0	23.1	19.3	0.1	40.5

During the tests with the simulated leachate, notable precipitation occurred. As a result, the initial solvent extraction experiments were conducted at pH 0.7, which was the original pH of the simulated leachate after preparation.

Experimental Procedures

Solvent extraction experiments were performed in a 1000 ml separatory funnel at room temperature, using a mechanical shaker (Yamato, SA320). After extraction, the aqueous phase was separated from the organic phase and diluted to rational multiples to analyze the concentrations of metals via ICP-MS. The organic phase was collected for the stripping tests.

As the organic phase cannot be directly analyzed with ICP-MS, HNO_3 was used to digest the organics before analysis. After digestion, the concentrations of metals in the loaded organic were determined with ICP-MS. Stripping experiments were conducted in a 125 ml separatory funnel. In each test, the loaded organic was mixed with HCl solution at different concentrations and agitated by a shaker. After stripping, the organic phase was digested with HNO_3 and diluted prior to the ICP-MS analysis of metal concentrations.

In tests where the organic phase was not digested and analyzed, the metal content in the organic phase was determined by the mass balance. The extraction efficiency *(%Extraction)* and stripping efficiency (*%Stripping)* were calculated to evaluate the extraction and stripping stages, respectively, which is given by:

$$\%Extraction = \frac{C_O V_O}{C_O V_O + C_A V_A} \times 100 \quad \text{Eq. 1}$$

$$\%Stripping = \frac{C_A V_A}{C_O V_O + C_A V_A} \times 100 \quad \text{Eq. 2}$$

where C_A and C_O represent the concentration of metal ions in the aqueous and organic phase, respectively. V_A and V_O are the volumes of the aqueous phase and organic phase, respectively.

Numerous studies have shown that the extraction efficiency of Fe(III) is much higher than that of Fe(II) when using D2EHPA is the extractant (e.g. Li et al., 2011). As a result, reducing agents are needed to reduce Fe(III) to Fe(II) prior to solvent extraction to decrease the amount of Fe entering the organic phase. To optimize this processing step, reduction experiments were carried out at room temperature. In each test, simulated leachate was mixed with different amount of reductant for a fixed time. The concentrations of total Fe and ferrous Fe in the simulated leachate were determined by ICPMS and a Hach spectrophotometer, respectively.

Results –Extraction Efficiency

The extraction behavior of REEs and major metals were studied using 0.2 M D2EHPA as the extractant and different concentrations of TBPO as the modifier, e.g., 0, 2.5 and 5 vol. % at a range of phase ratios (V_O/V_A) from 1:3 to 3:1.

TBPO helps the extraction of Al(III) and its extraction efficiency increases with the increase of TBPO concentration. In addition, the extraction efficiency of Al(III) increases with the increase of phase ratio (V_O/V_A) in the presence of TBPO; however, the extraction efficiency is not sensitive to phase ratio in solutions without TBPO. Likewise, the extraction efficiency of Zn increases with the increase of phase ratio (V_O/V_A); however, the TBPO has only little effect on its extraction. More than 30% extraction of Al(III) and Zn(II) is observed at the phase ratio (V_O/V_A) of 3:1 with TBPO concentration of 5 vol.%, which is detrimental to the REEs/Gangue metals separation. Since the total amount of Al(III) and Zn(II) is about 200 times higher than that of the REEs, a slight increase in the extraction efficiency of Al(III) and Zn(II) will lead to large amount of Al(III) and Zn(II) entering organic phase with REEs. In addition, there is a slight increase in the extraction efficiency of Ca(II) with the increase of phase ratio and TBPO concentration.

Similar to Al(III), TBPO facilitates the extraction of Cu(II) greatly and its extraction efficiency increases with the increase of TBPO concentration. In addition, with 2.5 and 5 vol. % TBPO, a high phase ratio (V_O/V_A), also causes a sharp increase in the extraction efficiency of Cu(II), which can reach to 80% ~ 90%. The extraction efficiency of Fe(III) is more than 90% for all test conditions, confirming the hypothesis above that Fe(III) cannot be separated from REEs by solvent extraction.

The total extraction efficiency of the five REEs increase with the increase of phase ratio (V_O/V_A). In addition, TBPO also significantly facilitates REE extraction. The results are consistent with the discussion in the foregoing part as well as the results obtained in Subtask 4.2.

Overall, TBPO not only helps REE extraction, but it also enables greater extraction of Al(III) and Cu(III). This result is not conducive for the separation of REEs and gangue metals, particularly for Al(III) removal. Fortunately, the data shows that this problem can be corrected by conducting solvent extraction at low phase ratio (V_O/V_A), since this condition produces a much lower extraction efficiency for most gangue metals (except Fe(III).

As shown in Table 13, when the TBPO concentration is 2.5 vol.% and the phase ratio (V_O/V_A) is 1:3, the extraction efficiencies of Al(III) and Cu(II) are less than 5% and the extraction efficiencies of Ca(II), Zn(II), Mg(II), Ni(II) and Co(II) are 0%. At the same time, the extraction efficiency is more than 83.9% for TREEs. Although a large amount of gangue metals still enters the organic phase, the gangue metals except for Fe(III) can be removed by multi-staged solvent extraction due to the high selectivity of REEs over these metals (Table 13). In this case, the separation factor was calculated by the distribution coefficient of TREEs over that of the gangue metal, which is given by,

$$\alpha_{TREE/Gangue} = \frac{C_{org\_TREE} \times C_{Aqu\_gangue}}{C_{Aqu\_TREE} \times C_{org\_gangue}} \quad \text{Eq. 3}$$

where C_{org_TREE} and C_{org_gangue} represent the concentration of TREEs and gangue metal in organic phase, respectively. C_{Aqu_TREE} and C_{Aqu_gangue} represent the concentration of TREEs and gangue metal in aqueous phase, respectively.

Table 13. The results of solvent extraction test with 2.5 vol.% TBPO at phase ratio (V_O/V_A) of 1:3.

	Al	Ca	Zn	Mg	Ni	Mn	Fe	Co	Cu	TREE
Extraction %	4.7	2.0	1.3	1.9	0	0	94.6	0	4.3	83.9
Con. in organic (mg/L)	1846	49.9	19.2	10.4	0	0	232	0	2.2	259.2
Separation factor	3770	4279	1647	6456	--	--	14	--	162	/

This data suggests that an alternative approach is needed to effectively separate Fe from REEs. Numerous prior studies have shown that the ability of D2EHPA to extract Fe(II) is much poorer than that of Fe(III) (Li et al., 2011). Thus, reducing agents can be employed to reduce Fe(III) to Fe(II) before solvent extraction to decrease the amount of Fe entering the organic phase.

Results – Pretreatment via Fe Reduction

Hydroxylamine hydrochloride is one of the most effective Fe reducing agents. The reduction reaction is given by:

$$2NH_2OH + 4Fe^{3+} = 4Fe^{2+} + N_2O + 4H^+ \quad \text{Eq. 4}$$

To determine the optimal reducing conditions for the simulated leachate, various experimental parameters, including reaction time and the dosage of reductant, were investigated.

The reaction kinetics were studied using 100 ml of simulated leachate and a stoichiometric amount of reductant, i.e., 0.15 ml of 0.5 M $NH_3OH \cdot HCl$. The tests were conducted in sealed tubes to isolate the oxygen from the solution. Figure 4 shows that the reduction efficiency of Fe(III) increases with the increase of reaction time. After 20 min, the reduction efficiency is close to 100%, indicating that the reduction of Fe(III) to Fe(II) was completed.

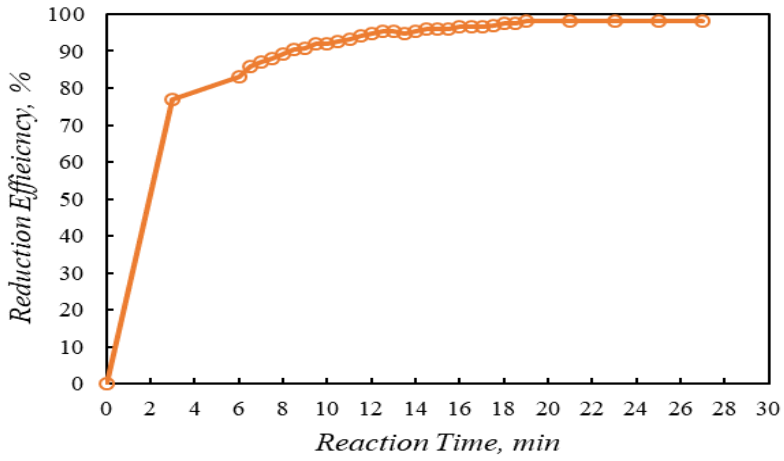

Figure 4. The effect of reaction time on the reduction efficiency. 0.15 ml of 5 M $NH_3OH \cdot HCl$ per 100 ml simulated leachate in a sealed tube.

After determining the optimal reaction time for the reducing agent, additional SX experiments were carried out to determine the optimal reductant dosage needed to minimize the extraction of iron into

the organic phase. The reducing agent was added to the synthetic leachate and mixed for 20 minutes. Next, SX as conducted using 0.2 M D2EHPA + 0.25 vol.% TBPO at a phase ratio (V_O/V_A) of 1:3. Figure 5 shows the results of this experiment. The extraction efficiency of Fe decreases considerably as the reductant dosage is increased from 1x to 40x relative to the stoichiometric requirement. Without reduction, the extraction efficiency of Fe is approximately 80%. However, as the dose is increased to 40x, the extraction of efficiency of Fe decreases to a minimum value of approximately 6%. At this condition, the presence of excess reductant help avoid the oxidation of Fe(II).

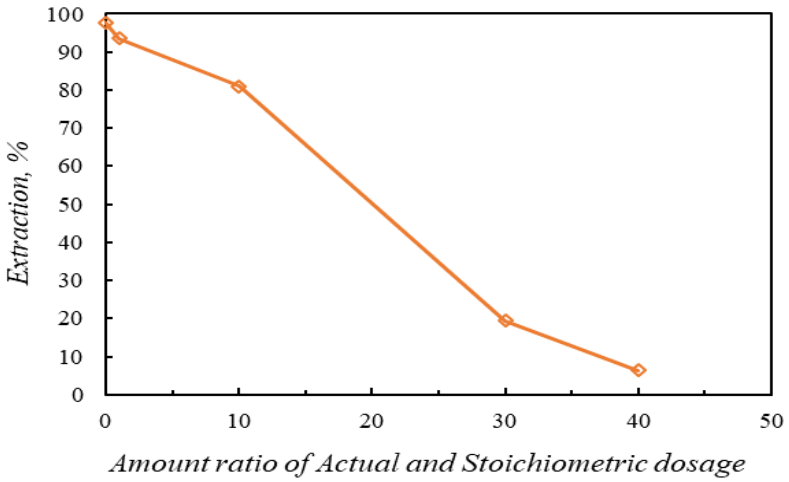

Figure 5. The effect of reductant dosage on the extraction efficiency of Fe. Reduction: T = 298 K; t = 20 min, Extraction: c(D2EHPA) = 0.2 M; c(TBPO)=2.5 vol.%; V_O/V_A=1:3; t = 10 min.

Results – Stripping Efficiency

The stripping efficiency of each element was investigated by using different concentrations of HCl (0-6 M) at a phase ratio (V_O/V_A) of 1:1. The loaded organic phase was obtained from the reduction-solvent extraction process described above. Initially, the concentration of the organic phase was determined by digesting the solution with HNO_3 and diluting the solution prior to ICP-MS. The results are listed in Table 14. Compared to the elements in simulated leachate, Ni(II), Mn(II), Co(II) and Mg(II) have been removed through solvent extraction. The REEs, especially Y(III) has been enriched significantly. Al(III) is still a major contaminant.

Table 14. ICP-MS Analysis of Loaded Organic Phase used in Stripping Optimization Tests.

	Al	Ca	Fe	Cu	Zn	Sc	Y	Ce	Nd
Conc. mg/L	647.9	54.2	85.8	22.1	23.5	59.7	122.7	15.4	17.1

Figure 6 shows the stripping behavior of gangue metals and REEs as a function of HCl concentration. The stripping efficiencies of five gangue metals increase with an increase of HCl concentrations and all REEs except for Sc(III) can be stripped with HCl, which is consistent with the data provide in Subtask 4.2. When the HCl concentration is 0, the stripping efficiencies of gangue metals and REEs are very low. This result indicates that the gangue metals cannot be efficiently removed by scrubbing with water. However, stripping with a slightly acidic 0.1M HCl solution leads to 82% removal of Zn(II) and 40% removal of the Ca(II) from the organic phase. Therefore, the removal of Zn(II) and Ca(II) may be achieved through a scrubbing stage with 0.1 M HCl. With the further increase of HCl concentration, the stripping efficiencies of REEs, especially Ce(III) and Nd(III) increase sharply and reach to nearly 100% at 6 M. At the same time, most of Fe(II), Cu(II) and Al(III) are stripped with REEs.

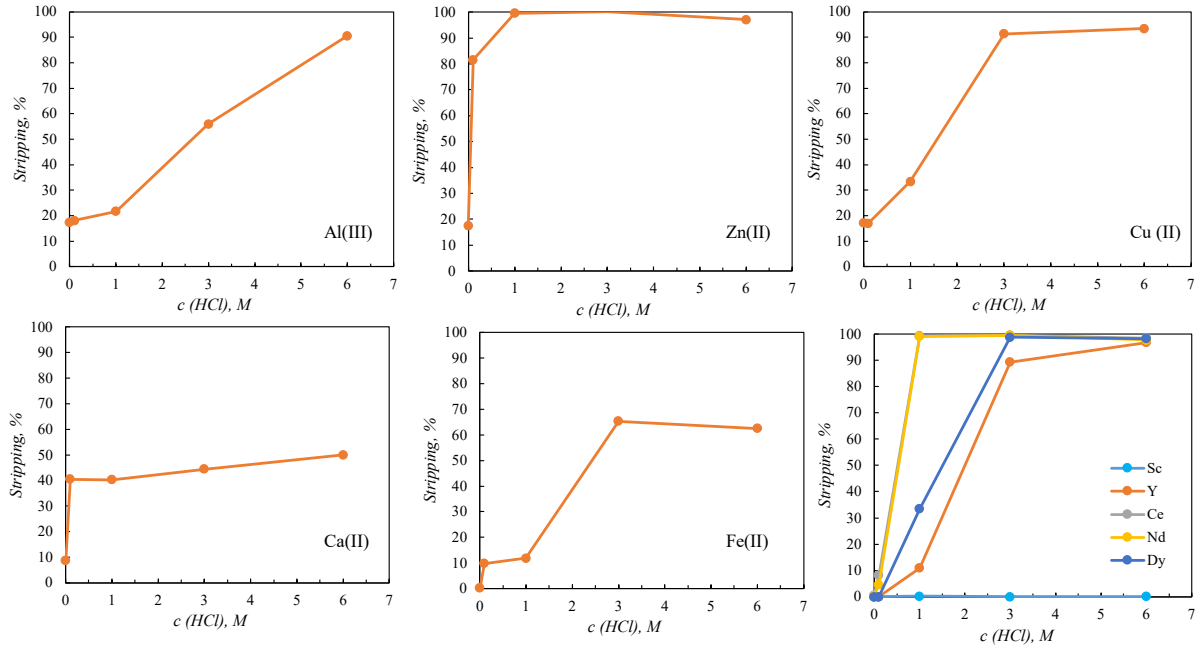

Figure 6. Stripping behavior of major elements and REEs in simulated leachate. V_O/V_A=1:1; t = 10 min.

Based on the experimental data given above, a preliminary SX process flow diagram was determined. This approach consists of the following major unit operations: (1) The reduction of Fe(III) to Fe(II); (2) Separation of REEs from gangue metals by solvent extraction with D2EHPA+TBPO; (3) Removal of Zn(II) and Ca(II) by scrubbing with 0.1 M HCl; and (4) Stripping of REEs except for Sc with 6 M HCl. The optimal conditions in reduction and solvent extraction stages have been described in the previous sections. In addition, the effect of HCl concentration on the stripping efficiency of each element has also been fully investigated.

For a single stripping stage, the fraction of the desired component that can be recovered depends on the chemical conditions as well as the aqueous to organic phase ratio. In addition, the phase ratio also affects the total concentration of REEs in strip liquor. With lower phase ratios (V_A:V_O), higher concentrations of REE in the strip liquor can be achieved; however, recovery is also reduced. Given these initial findings, additional optimization of the stripping phase ratio was warranted.

Results – Stripping Phase Ratio Optimization

The effect of phase ratio on the scrubbing of each element was investigated by using 0.1 M HCl at different phase ratios (V_A:V_O). Moreover, the previous study has indicated that Sc(III) cannot be stripped from D2EHPA with HCl at any conditions. As a result, Sc(III) results are omitted from this discussion.

Figure 7 and Figure 8 show the scrubbing efficiency as a function of phase ratio for gangue metals and REEs, respectively. Figure 7 shows that the scrubbing efficiency of Al(III) is close to 0% at all phase ratios, confirming the results presented above. Since Al accounts for nearly 80% of the total mass of gangue metals, this result suggests that dilute acid scrubbing is not an effective approach to purify the REE product. However, qualitative observations during testing showed that in tests where scrubbing was not performed, a deleterious emulsion was formed in the loaded organic after the stripping stage. Alternatively, the emulsion did not form in tests that included a dilute acid scrubbing stage, even under conditions where the metal removal was relatively low. This finding suggests that scrubbing is an essential component of the process, even if the gangue removal rate is poor.

While the Al(III) scrubbing efficiency is low, other gangue metals can be removed from the organic phase

with 0.1 M HCl, and their scrubbing efficiency increases with the phase ratio (V_A:V_O). In particular, around 80% of Zn(II) can be removed when the phase ratio is 1:1. When the phase ratio is larger than 1:1, the scrubbing efficiency of Zn(II) remains the same, and that of Ca(II) and Cu(II) increases. However, the scrubbing efficiency of Ce(IV) and Nd(III) also increases significantly, which reduces the recovery of REEs (Figure 8). Based on these findings, the optimal phase ratio (V_A:V_O) in scrubbing stage is 1:1, which represents an optimal tradeoff between gangue removal, REE recovery, and emulsion mitigation.

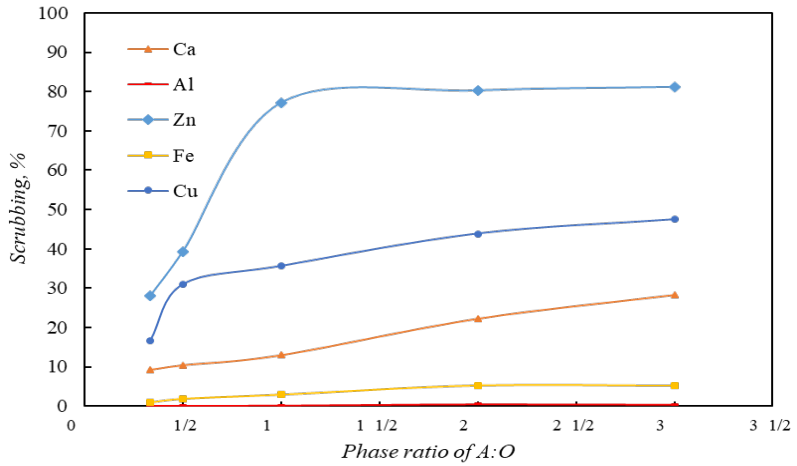

Figure 7. The effect of phase ratio on the scrubbing efficiency of gangue metals. c(HCl) = 0.1 M; t = 10 min.

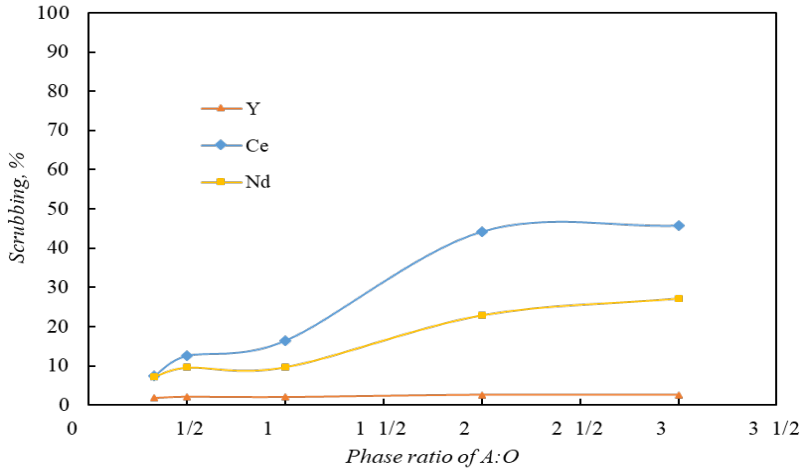

Figure 8. The effect of phase ratio on the scrubbing efficiency of REEs. c(HCl) = 0.1 M; t = 10 min.

Following the scrubbing tests, the effect of phase ratio on the stripping of each element was investigated by using 6 M HCl at different phase ratio (V_A:V_O). The loaded organic was obtained from the optimal scrubbing process. Table 15 shows the elemental composition of the organic feed for the scrubbing tests.

Table 15. ICP-MS Analysis of Loaded Organic after Scrubbing.

	Al	Ca	Fe	Cu	Zn	Sc	Y	Ce	Nd
Con. mg/L	647.1	47.2	83.3	14.2	5.4	58.3	120.1	12.8	15.5

Figure 9 shows the stripping behavior of various gangue metals and REEs at different phase ratios. The stripping efficiency of five gangue metals increases with the increase of phase ratio (V_A:V_O). In particular, the stripping efficiency of Al(III) increases from 15% to 91% when the phase ratio (V_A:V_O) was increased from 1:10 to 1:1. Since the Al(III) is the dominant contaminant, an increase in the stripping efficiency of Al(III) will lead to a large amount of Al(III) entering the strip liquor, which is detrimental to the subsequent purification of REEs. Likewise, the stripping of Fe(III) and Ca(II) is also very sensitive to the change of phase ratio. The stripping efficiency of Fe(III) and Ca(II) increased from 20.2% to 62.6% and from 10.3% to 50.0% respectively. Also, more than 90% of Cu(II) and Zn(II) were stripped from organic when the phase ratio (V_A:V_O) was larger than 1:5.

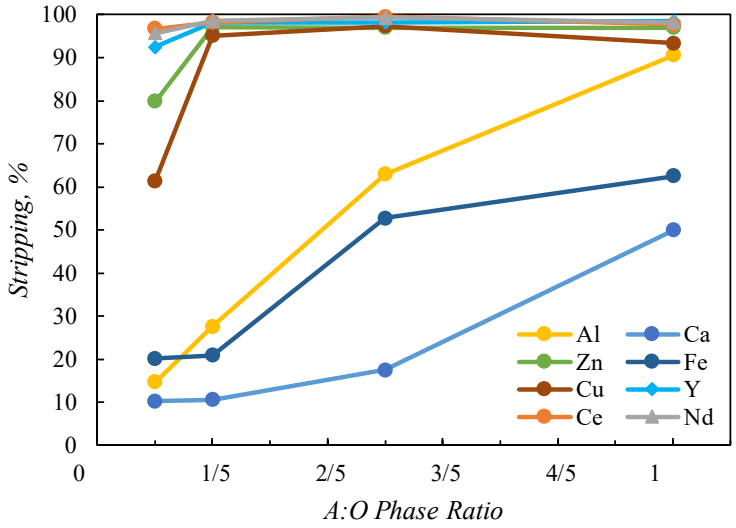

Figure 9. The effect of phase ratio on the stripping efficiency. c(HCl) = 6 M.; t = 10 min.

Concurrently, the stripping efficiency of Y(III), Ce(III) and Nd(III) remain nearly 100% at all phase ratios. Thus, stripping at low phase ratio (V_A:V_O) will achieve both high recovery of REEs and high retention of gangue metals in the organic phase. Figure 10 shows the mass percentage (i.e. solution purity) of REEs in the strip liquor obtained at different ratios. As shown, the percentage of REEs increases with the decrease of phase ratio (V_A:V_O), which is optimal for the further purification of REEs. As a result, the optimal phase ratio (A:O) of stripping was determined to be 1:10.

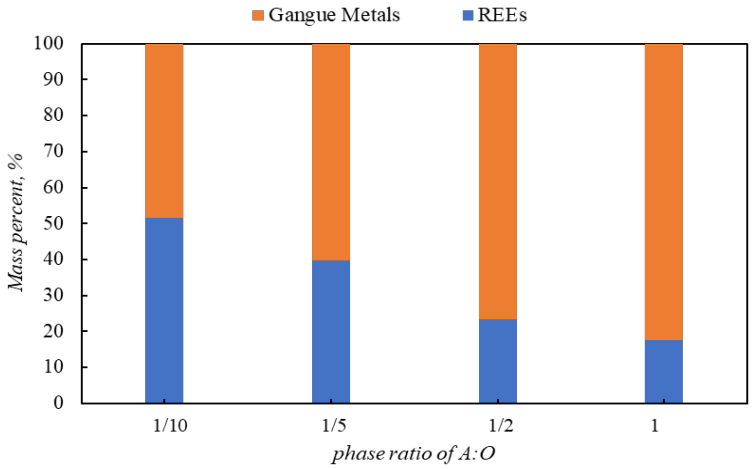

Figure 10. The effect of phase ratio on elemental composition of strip liquor. c(HCl) = 6 M; t = 10 min.

Results – Solvent Extraction Process Flowsheet

Following the detailed stripping tests, a modified SX process flowsheet was developed. The REEs except for Sc(III) are enriched throughout the process. The total amount of four REEs (Y, Ce, Nd, and Dy) accounts for only 0.37% of the total metal concentration in initial leachate and increases significantly to 50.30% in the strip liquor. Correspondingly, the amount of Al(III) decreases from 91.59% to 36.44% through the process.

Table 16 compares the element concentration in the simulated leachate and the final strip liquor. This data shows that 99.8% of the gangue metals are removed through the SX process. The removal rate of Al(III) is almost 99%; however, Al(III) is still the primary contaminant in the strip liquor because of its high concentration in the original leachate. In addition, the strip liquor also contains trace amounts of Cu(II), Fe(III), Ca(II) and Zn(II); however, the concentration of these elements is much lower than that of REEs. Furthermore, all of the Mg(II), Ni(II), Mn(II), and Co(II) are removed by the process.

Table 16. Elemental Composition of Simulated Leachate and the Final Strip Liquor following SX.

	Leachate mg/L	Strip Liquor mg/L	Removal %		Leachate mg/L	Strip Liquor mg/L	Recovery %
Al	20,840.9	952.2	99.8	Sc	20.4	0.0	0.0
Ca	756.6	48.3	99.8	Ce	23.6	124.2	17.6
Zn	485.1	42.8	99.7	Nd	20.2	147.9	24.4
Mg	169.8	0.0	100.0	Dy	0.12	0.0	0.0
Ni	138.1	0.0	100.0	Y	40.6	1,110.7	91.2
Mn	108.6	0.0	100.0	Total	104.9	1,383.0	44.0
Fe	80.0	167.9	93.0				
Co	53.7	0.0	100.0				
Cu	15.7	87.2	81.5				
Total	22,648.6	12,98.5	99.8				

In total, 44.0% of REEs are recovered to the strip liquor, and the total concentration of REEs in the strip liquor is more than ten times of that in the simulated leachate. Notably, 91.2% of Y(III) is recovered, and a high concentration of 1110.7 mg/L was produced in the strip liquor. Alternatively, Ce(IV) and Nd(III) had much lower recoveries, 17.6% and 24.4%, respectively. Ce(IV) and Nd(III) are lost in the initial extraction step given the low extraction rates of light REEs at low pH and low phase ratio (V_A:V_O) in D2EHPA. Sc(III) cannot be stripped with HCl and remains in the loaded organic.

Results –Precipitation and REO Production

Following the SX process, REE were precipitated from the strip liquor initially generated from the simulated leachate. The precipitate was then converted to oxide by calcination. Figure 11 shows the compositions of the final REE oxide produced from this end-to-end process. As shown, the total rare earth oxide content is 92.8%, of which 89.6% is Yttrium. These results confirm the feasibility of generating high grade REE oxide from simulated leachate by the optimized SX process.

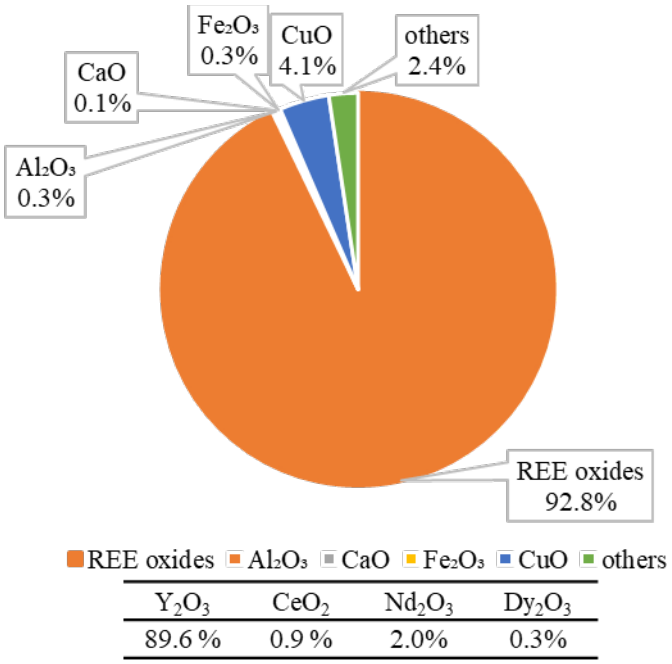

Y_2O_3	CeO_2	Nd_2O_3	Dy_2O_3
89.6 %	0.9 %	2.0%	0.3%

Figure 11. Compositions of final REO product generated from simulated leachate.

Conclusions and Discussion

This task investigated the separation of REEs from the major gangue elements including Al, Ca, Mg, Zn, Fe, Cu, Co, Ni and Mn via SX experiments using simulated leachate. An optimal SX process to recover high purity MREO from the simulated leachate was developed. Through the process, a rare earth oxide with 92.8% purity were obtained, of which 89.6% is Yttrium. Additional findings determined under this subtask include:

1. Reduction of Fe(III) to Fe(II) helps inhibit a large amount of Fe being extracted with REEs. The extraction efficiency of Fe decreases from 97.74% to 6.36% by reduction.
2. D2EHPA is able to selectively extract the REEs at low concentrations (100 mg/L) in the presence of a large amount of major elements (>20 g/L).
3. Stripping at low phase ratio (V_A:V_O) will achieve both high recovery of REEs and high retention of gangue metals in the organic phase.

Task Completion Status

100% complete.

Subtask 4.2. Model System Evaluation, REE Separation

Overview

The objective of this study was to investigate the recovery and transport of REEs in solvent extraction through controlled laboratory batch tests using artificial solutions. Rather than individually assess all 17 REEs, the experimental program was simplified to only assess five surrogate REEs, namely Yttrium (Y), Cerium (Ce), Neodymium (Nd), Dysprosium (Dy) and Scandium (Sc). These surrogate elements were carefully selected to include a mix of light REEs (Ce and Nd), heavy REEs (Nd and Dy), those that tend to be anomalously concentrated in aqueous sources (Y and Ce), and those that command the highest market value (Sc). In this study, the artificial leachate solution was accessed to study how a variety of parameters affected the extraction and stripping of these surrogate REEs in order to assess potential pathways for REE separation. The optimal solvent extraction conditions for the five REEs was

determined.

Approach

Like task 4.1, this task used model systems, derived from standard metal solutions to determine the optimal processing route needed to selectively separate individual REEs. Initial efforts prescribed two to three target elements by which the process will be optimized to recovery. The selection of target elements was based on a rigorous assessment conducted by the project PIs and consultation with the DOE Federal Project manager. Decision criteria included element criticality, importance to national defense/clean energy needs, element price/value, element abundance in AMD feedstocks, and element process amenability. Initial proposed target elements included Y, Sc, Dy, and Nd, given their fulfillment of the aforementioned criteria.

After deciding the best target elements, laboratory-scale solvent extraction tests were conducted in similar fashion as the gangue metal separations described in Task 4.1. A host of processing schemes were evaluated, particularly those in current industrial use, as described by Xie et al (2014). Once again, follow on tests were used to generate McCabe-Thiele diagrams, and a final process schematic was generated.

Results and Discussion

Materials – Aqueous Solutions

Artificial/model leachate solutions of Y(III), Nd(III), Dy(III), Sc(III), Ce(IV) were prepared by diluting the standard solutions provided by Inorganic Ventures, Inc. The target concentration of each element was 40 mg/L, and these values were confirmed by ICP-MS analysis. The results from these analyses are shown in Table 17.

Table 17. ICP-MS Analysis of REEs in the Synthetic Solution

Element	Sc(III)	Y(III)	Ce(IV)	Nd(III)	Dy(III)
Concentration, mg/L	36.18	36.78	39.04	39.09	36.95

Materials – Selection of Extractant

Prior researchers have investigated numerous extractants for the separation of REEs; however, only a small number of them are used commercially. Di-2-ethyl-hexyl-phosphoric acid (D2EHPA), 2-ethyl-hexyl-2-ethyl-hexyl-phosphonic acid (EHEHPA), Versatic acid (Versatic 10), tri-butyl phosphate, and Aliquat 336 have been widely used in rare earth industry due to their good extraction ability and low operational cost (Ismail et al, 2019; Xie et al., 2014).

Aliquat 336 is an anion extractant. The key point of the extraction lies in the coordination of metal ions with inorganic ligands (SO^{4-}, Cl^{-}, NO^{3-}) in the aqueous phase but not the affinity of metal ion for the extractant itself. The abound of metal ions like Fe^{3+}, Al^{3+}, Mg^{2+}, Mn^{2+} will compete with REE ions to coordinate with the inorganic ligands. In addition, Aliquat 336 is a relatively weak extractant for REEs compared to some cation extractants (EHEHPA and HDEHP) and high concentration of salts and acids are required to achieve a good separation (Krishnamurthy & Gupta, 2004). As a result, Aliquat 336 is not suitable for the solvent extraction of REEs from AMDp.

The same problem also lies in the extraction with tri-butyl phosphate, which is a kind of solvation extractants of which the inorganic ligands also contribute to the extraction process. The demand for a large amount of salts in extraction will increase the operation cost on scale-up process.

D2EHPA and EHEHPA are organophosphorus acids and Versatic 10 is versatic acid, which are categorized as cation extractants. One advantage of cation extraction is that the extraction and stripping of metal ions can be controlled by pH. However, Versatic 10 has a very broad pH swing between 0% extraction

and 100% extraction which make it difficult to separate different metal ions. Versatic 10 is able to form very stable complexes with Fe^{3+} (Wilson et al., 2014). Thus, Versatic 10 was not considered in this study. Among organophosphorus acids, D2EHPA has proven to be the most versatile extractant with chemical stability, good performance of extraction, loading and stripping as well as low solubility in aqueous phase. Compared to EHEHPA, D2EHPA shows a better extraction of TREEs from leach liquor bearing metals of Mn, Cu, Fe, Co and Ni (Parhi et al., 2015). Therefore, D2EHPA was selected as the main extractant in this study.

During tests, the extractant was dissolved in kerosene to obtain different concentrations. Kerosene is a non-polar diluent and has been proven to be a good choice for the solvent extraction of REEs, because it could give highest equilibrium constant when compared to other diluents like n-hexane, benzene, and chloroform (Zhang et al., 2016). In addition to kerosene, a group of commercial diluents, Elixore range solvent (supplied by Total Special Fluids, Inc., Houston, TX), were tested to seek better choice of diluent.

Tri-n-butylphosphine was used as a modifier in some SX tests. Tri-butyl phosphine is easily oxidized by air to tri-butyl phosphine oxide (TBPO) (Armarego, 2017). Solvent extraction experiments were conducted in the atmosphere and the aqueous phase contains nitric acid, which promotes a strong oxidation environment. Therefore, it is believed that Tri-butyl phosphine will be oxidized to TBPO in solvent extraction.

Experimental Procedures

Solvent extraction and stripping experiments were carried out in 125 mL separatory funnels at room temperature. The pH of the aqueous solution was adjusted to the desired value by adding sodium hydroxide (NaOH) solution or nitric acid (HNO_3). In each experiment, the aqueous feed solution and the organic phase containing extractant were added into a separatory funnel and agitated by a mechanical shaker (Yamato, SA320 shown in Figure 12) for different shaking times. After achieving equilibrium, the aqueous phase was separated from the organic phase by discharging the former from the separatory funnel.

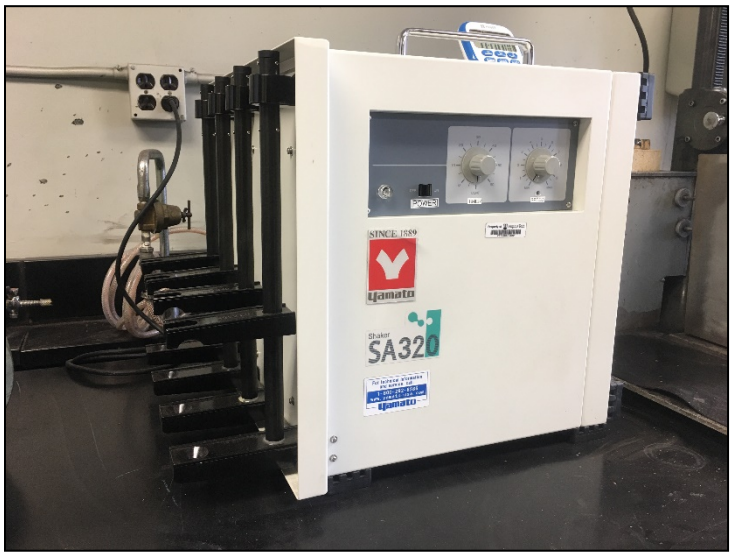

Figure 12. Yamato SA320 horizontal-vertical laboratory shaker.

Following the tests, aqueous solutions were analyzed via ICP-MS, and the metal content of the organic solutions were determined via mass balance. Further details on the analytical procedures and the subsequent calculations are given in Subtask 4.1.

Extraction Mechanism

The mechanism by which D2EHPA extracts REEs from the aqueous phase is detailed here. It is well known that D2EHPA exists as dimmers in nonpolar organic diluents. Generally, the extraction of REE in trivalent state from aqueous phase by D2EHPA can be expressed by the cation exchange reaction as below:

$$RE^{3+} + 3(HX)_2 \rightleftharpoons \overline{REX_3(HX)_3} + 3H^+ \quad \text{Eq. 5}$$

The extraction equilibrium constant K is expressed by:

$$K = \frac{[\overline{REX_3(HX)_3}][H^+]^3}{[RE^{3+}][(HX)_2]^3} \quad \text{Eq. 6}$$

As the distribution coefficient *D* is expressed by,

$$D = \frac{[\overline{REX_3(HX)_3}]}{[RE^{3+}]} \quad \text{Eq. 7}$$

The *D* can also be expressed by the *equilibrium constant K and pH,*

$$\log D = \log K + 3\log[HX] + 3pH \quad \text{Eq. 8}$$

According to the equation above, in an acidic solvent extraction system, the distribution ratio is dependent upon the solution pH, the free extractant concentration, and the solvent extraction equilibrium constant (K). The solvent extraction equilibrium constant (K) is related to many factors like metal ion species, extractant property, diluent property, *etc.* (Zhang et al., 2016).

Results – Effect of Reaction Time

To investigate the influence of reaction time, a series of solvent extraction experiments were conducted using artificial solution only containing Y(III) at varied reaction times, namely 5 min, 10 min and 15 min. Figure 13 shows the effect of reaction time on extraction efficiency of Y(III). As shown in Figure 13, the extraction efficiency does not change from 10 min to 15 min, indicating that the equilibrium of solvent extraction can be reached within 10 min. This value was thus used in all subsequent tests.

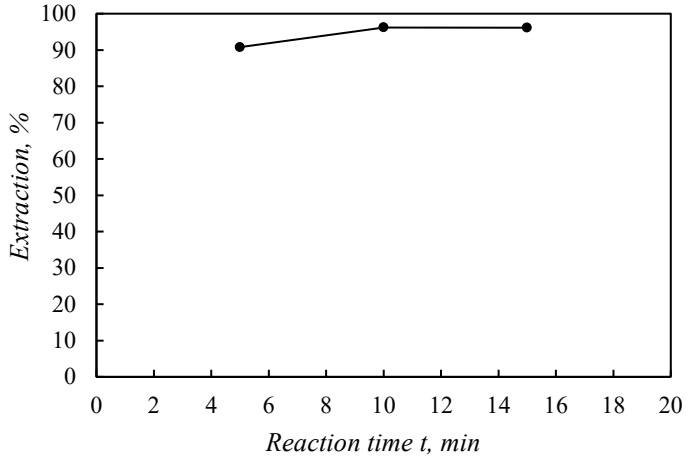

Figure 13. Effect of reaction time on the extraction efficiency of Y(III). c(D2EHPA) = 0.025 M; pH = 0.5; V_A:V_O=1:1.

Results – Effect of the REE Feed Concentration

Preliminary tests had shown that the extraction efficiency of Dy (III) was more sensitive to the experimental parameters, i.e., the concentration of extractant, than other REEs. Therefore, Dy (III) was selected to investigate the effect of feed concentration on solvent extraction. The experiments were carried out by varying Dy(III) concentration from 1 to 1000 mg/L with 0.2 M D2EHPA at an initial pH of 2. As described in prior stuides, the driving force for the mass transfer becomes stronger with the increase of the feed concentration, and as a result, higher extraction efficiencies are expected for higher feed concentrations (Chiou & Li, 2002; Huang et al., 2011). Figure 14 shows that the extraction efficiency increases with the increase of feed concentration from 1 to 200 mg/L and the extraction efficiency is essentially 100% for all concentrations greater than 200 mg/L. Therefore, the concentration of total REEs in the artificial solution used in the following parametric study was set to 200 mg/L.

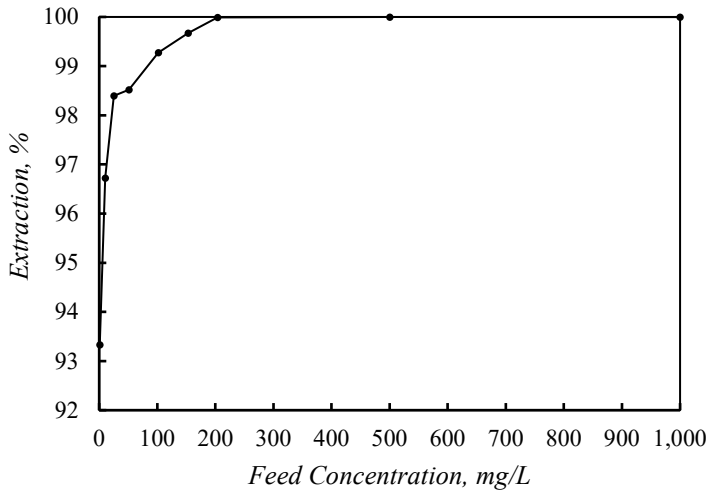

Figure 14. Effect of feed concentration on the extraction efficiency of Dy(III). pH = 2; c(D2EHPA) = 0.2 M; V_A/V_O=1:1; t = 10 min.

Results – Effect of D2EHPA Concentration

A series of tests were conducted to study the effect of D2EHPA concentration on the extraction of REEs. The selected concentrations of D2EHPA were 0.025, 0.05, 0.1, 0.2 and 0.3 M. The results showed that the extraction efficiency of Sc(III), Y(III), Dy(III), Nd(III) and Ce(IV) increased with increasing the concentration of D2EHPA (Figure 15). According to the equations above, the *D* is proportional to the third power of the free extractant concentration (H_2A_2). Thus, a higher concentration of extractant facilitated the extraction of REEs.

The extraction of the five REEs with D2EHPA from nitrate media follows the order of Ce(IV) < $\mathrm{Nd(III)} < \mathrm{Dy(III)} < \mathrm{Y(III)} < \mathrm{Sc(III)}$, which is because REEs with less basicity form more stable complexes. Therefore, REEs with less basicity can be extracted more easily. Krishnamurthy and Gupta (2004) reported the basicity order of all REEs as:

$$\mathrm{La^{3+} > Ce^{3+} > Pr^{3+} > Nd^{3+} > Pm^{3+} > Sm^{3+} > Eu^{3+} > d\ ^{3+} > Tb^{3+} > Dy^{3+} > Ho^{3+} > Y^{3+}\ Er^{3+} > Tm^{3+} > Yb^{3+} > Lu^{3+} > Sc^{3+}}$$

At pH = 0.5, the extraction efficiency of Nd(III) and Ce(IV) was very low, suggesting that Nd(III) and Ce(IV) were too difficult to extract with D2EHPA at this pH. However, this also suggests that that Nd(III) and Ce(IV) may be separated from Y(III), Sc(III) and Dy(III) by controlling pH (Figure 15). For all four REEs, no obvious increase in the extraction efficiency was observed in the range of 0.2-0.3 M. Therefore, the optimum concentration of D2EHPA was determined to be 0.2 M.

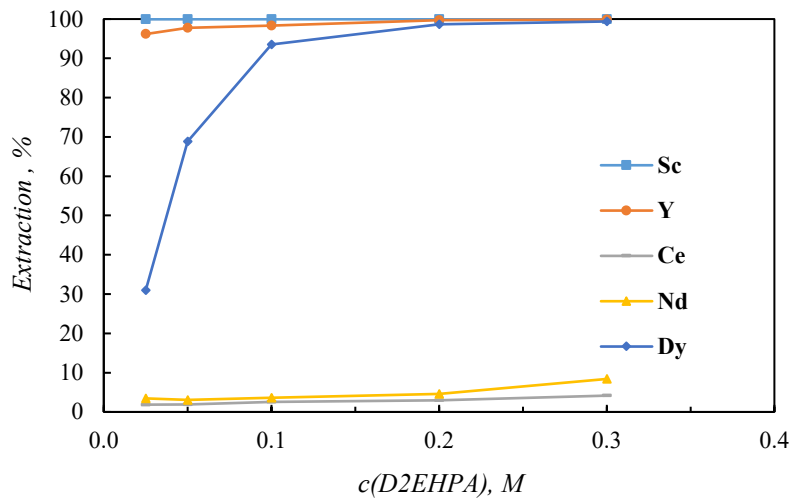

Figure 15. Effect of D2EHPA concentration on the extraction efficiency of REEs. pH = 0.5; V_A/V_O=1:1; t = 10 min.

Results – Effect of Initial pH

The second test series evaluated the influence of initial pH in aqueous phase on extraction efficiency. Solvent extraction experiments were carried out at different pH values, namely 0.5, 1.0, 1.5, 2.0, 3.0, 4.0, and the results from these experiments are shown in Figure 16. According to the equations above, the distribution coefficient is proportional to the third power of the pH value, indicating that a higher pH facilitates the extraction of REEs. All the Y(III) and Dy(III) were completely extracted when pH was larger than and equal to 1. Nd(III) and Ce(IV) were completely extracted when pH was equal to or larger than 2. Therefore, the optimum pH for full extraction was determined to be 2.0.

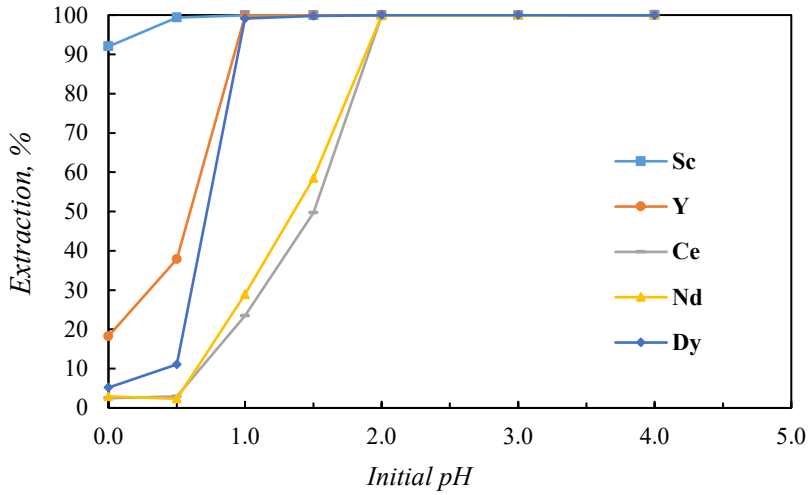

Figure 16. Effect of initial on the extraction efficiency of REEs. C(D2EHPA) = 0.2 M; V_A/V_O=1:1; t = 10 min.

Results – Effect of Diluent Type

While much of the prior testing used kerosene as a generic diluent, further testing was conducted to evaluate several specialty diluents. Technical detail on these chemicals is provided in Table 18. Like most organic solvents, kerosene is highly volatile and flammable. The moderate aromatic content also produces a foul odor and potential health effects. Altogether, an optimal diluent should not only

produce superior technical performance but should also balance any significant health, safety, and environmental concerns.

Table 18. Technical Data for Elixore Diluents (after Elixore, 2014) and Kerosene.

Parameter	Unit	Elixore 205	Elixore 230	Elixore 250	Kerosene
Flash Point PM	° C	76	103	119	37-65
Aromatic Content	--	40 ppm	40 ppm	40 ppm	<25%
Sulfur Content	ppm	<1	<1	<1	<4
Vapor Pressure at 20° C	kPa	0.016	0.002	0.0003	0.7

As an alternative to kerosene, the Elixore range is a group of aliphatic diluents designed specifically for the liquid-to-liquid extraction process[1]. Compared to the kerosene, the diluents in the Elixore range have higher flash points and lower evaporation rates. They offer a good balance between phase separation, diluent losses, and fire risk. In addition, the low aromatic content and high flash points also help enhance worker safety and meet strict environmental requirements compared to kerosene-type diluents.

In the present work, three diluents namely, Elixore 205, Elixore 230 and Elixore 250, were investigated to replace kerosene as the diluent in the extraction of REEs. As shown in Figure 17, the new diluents performed comparably with kerosene in the extraction of Y(III), Dy(III), Nd(III), Sc(III) and Ce(IV). Given these factors and availability, Elixore 205 was selected as the primary diluent for future tests.

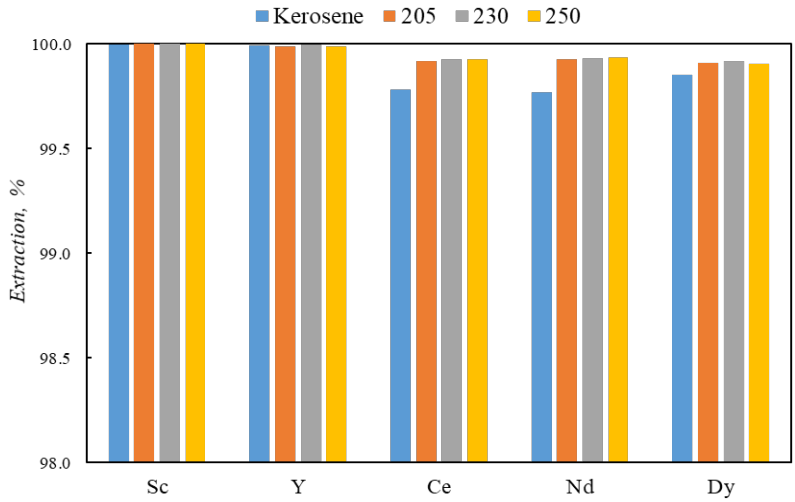

Figure 17. Comparison between Kerosene and Elixore Range of the extraction efficiency of REEs. c(D2EHPA) = 0.2 M; pH = 2; V_A/V_o =1; t = 10 min.

Results – Effect of Stripping Acid Type

Solvent stripping tests were conducted using different concentrations of HNO_3 (0.1-7 M) and HCl (0.1-7 M) at a 1:1 phase ratio. The loaded organic phase used as feed in these tests was obtained from the extraction experiments using 0.2 M D2EHPA in Elixore 205 at an initial pH 2 and a phase ratio of 1:1.

Figure 18 show that the stripping efficiency increases with increasing acid concentration, which is consistent with general expectations and previous studies (e.g. Sun et al., 2005). Using HCl as the stripping reagent, the stripping efficiency increases as the HCl concentration is increased from 0.1 M to 6 M; however, further increases above 6 M do not promote higher stripping efficiency. Likewise, HNO_3

[1] Available: < http://ressources.total.com/websites/totalspecialfluids_com/Elixore.pdf >

follows a similar trend, reaching the maximum efficiency at 5 M. When analyzing the results element-by-element, Ce(IV) and Nd(III) show no significant difference between the two acid types; however, both of these are also easily stripped in general. Alternatively, the stripping efficiencies of Y(III) and Dy(III) using HCl are higher than that using HNO_3 at the same concentration, indicating that HCl is more efficient than HNO_3 as a stripping reagent. Sc(III) was notably difficult to strip, even at the highest acid concentrations tested, 7 M.

In general, the higher the extractability of the REE is, the more difficult it is to strip the REE from the loaded organic. This behavior is also confirmed by the results shown in Figure 18. The order of stripping of REEs, namely Ce(IV) > Nd(III) > Dy(III) > Y(III) > Sc(III), is the reverse of the order of extraction. When the acid concentration was 0.5 M, it was found that most of the Sc(III), Y(III), and Dy(III) could not be stripped whereas the stripping efficiencies of Nd(III) and Ce(IV) were both more than 90%. Therefore, it may be possible to separate various REEs by controlling the acidity in the stripping system.

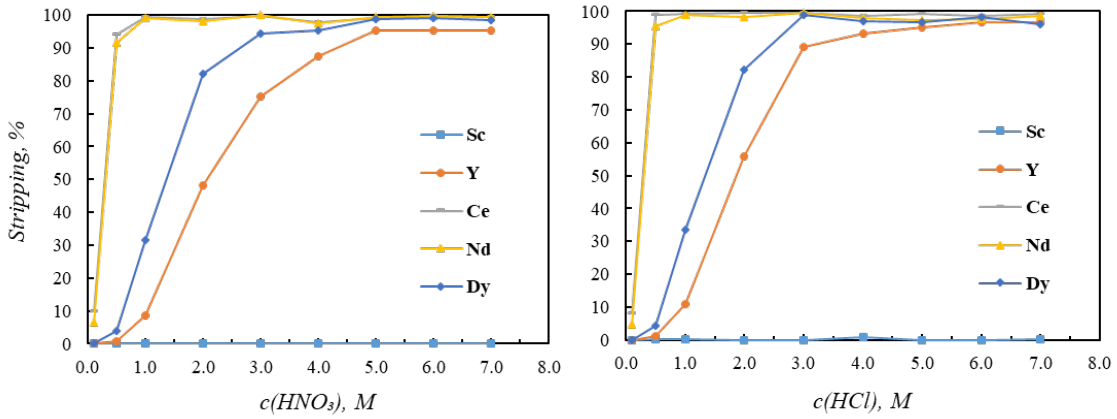

Figure 18. Effect of acid concentration on the stripping efficiency. V_A/V_O=1; t = 10 min.

Results – Effect of Modifier on Sc Stripping

Due to the strong affinity between scandium (Sc) and D2EHPA, the stripping efficiency of Sc from D2EHPA is very low, even with strong acids (Wang et al., 2013). An alternative method is to directly precipitate Sc(III) from the organic in the form of $Sc(OH)_3$. To evaluate this approach, stripping tests of Sc(III) were conducted using 2 M NaOH at phase ratio of 1:1. During these tests, an emulsion layer appeared in the stripping solution between the organic and the aqueous phases (Figure 19). After stripping, 61% of Sc(III) was recovered to the emulsion while only 24% of Sc(III) was in the aqueous strip solution (Table 19). Downstream recovery of Sc(III) from the emulsion is impractical; therefore, a phase modifier must be added to the organic solvent to help phase separation due to emulsification.

As a result, TBPO was evaluated as the modifier to help phase separation in the Sc stripping stage. The loaded organic phase used as the test feed was obtained from the extraction experiment using 0.2 M D2EHPA and 0.1 M TBPO in Elixore 205 at an initial pH 2 and a phase ratio of 1:1. As shown in Figure 19, the modifier helped the phase separation and the precipitation of $Sc(OH)_3$. The precipitated $Sc(OH)_3$ in the aqueous phase was then separated from the organic phase and disolved in acid for ICP-MS analysis. As shown in Table 19, the stripping efficiency of Sc(III) increased to 75.04% by adding TBPO. This result is considered adequate for the current stage of process development.

Table 19. The distribution of Sc(III) in the stripping process.

	Organic phase,%	Emulsion,%	Aqueous phase/Solid,%
Without Modifier	14.85	61.15	23.99
With Modifier	24.96	--	75.04

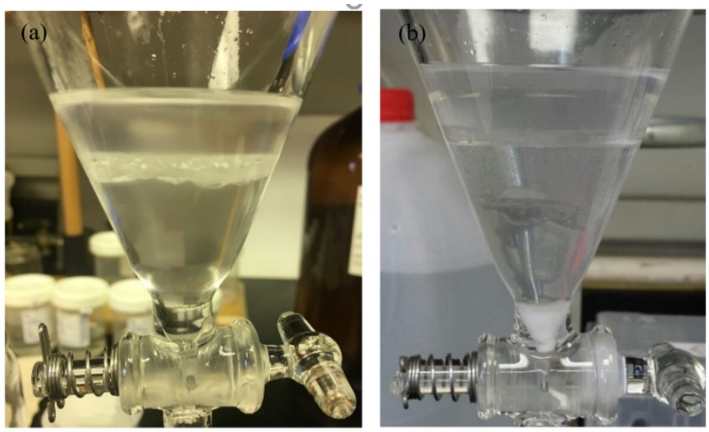

Figure 19. Stripping Solution (a) Without TBPO (b) With TBPO. c(D2EHPA) = 0.2 M. c(TBPO) = 0.1 M, c(NaOH) = 2 M, V_A/V_O=1; t = 10 min.

Results – Effect of Modifier Dose

In order to investigate the influence of the interaction between TBPO and D2EHPA on the extraction of REEs, additional experiments were conducted by using 0.2 M D2EHPA containing various TBPO concentrations, namely, 0, 2.5 and 5 vol.%. As shown in Figure 20, the extraction of the five REEs follows the order of Ce(IV) < Nd(III) < Dy(III) < Y(III) < Sc(III) under all the concentrations of TBPO. This result indicates that the addition of TBPO does not change the extraction order of the five REEs with D2EHPA.

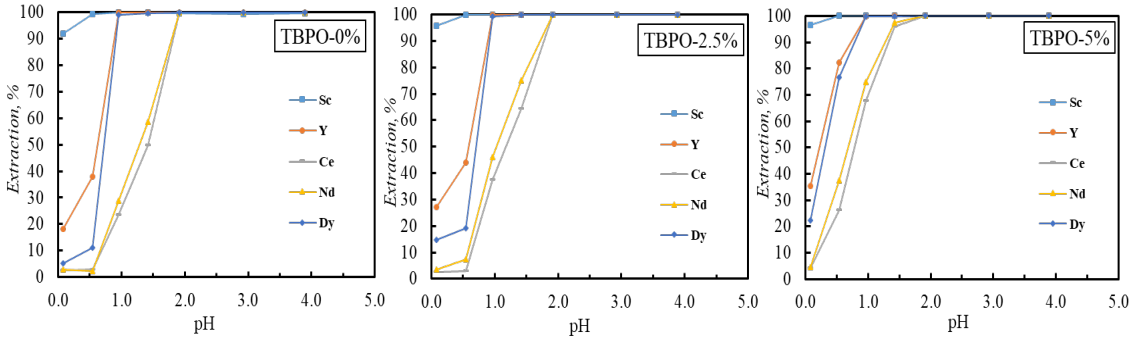

Figure 20. Effect of pH on the extraction efficiency of Sc(III), Ce(IV), Nd(III), Dy(III) and Y(III) at different TBPO concentrations. c(D2EHPA) = 0.2 M; V_0/V_A=1; T = 298 K; t = 10 min.

Figure 21 shows the effect of TBPO concentration on the extraction of five REEs. As shown, the presence of TBPO causes the extraction curves of Y(III), Nd(III), Dy(III) and Ce(IV) to shift towards lower pH values. In other words, the extraction efficiency of the four REEs increases with the increase of TBPO concentration at a given pH value. Although the extraction efficiency of Sc(III) is more than 90% in all cases, a slight increase can also be observed at pH 0.1 with the increase of TBPO concentration. The results confirm that the addition of TBPO improves the extraction of all five REEs.

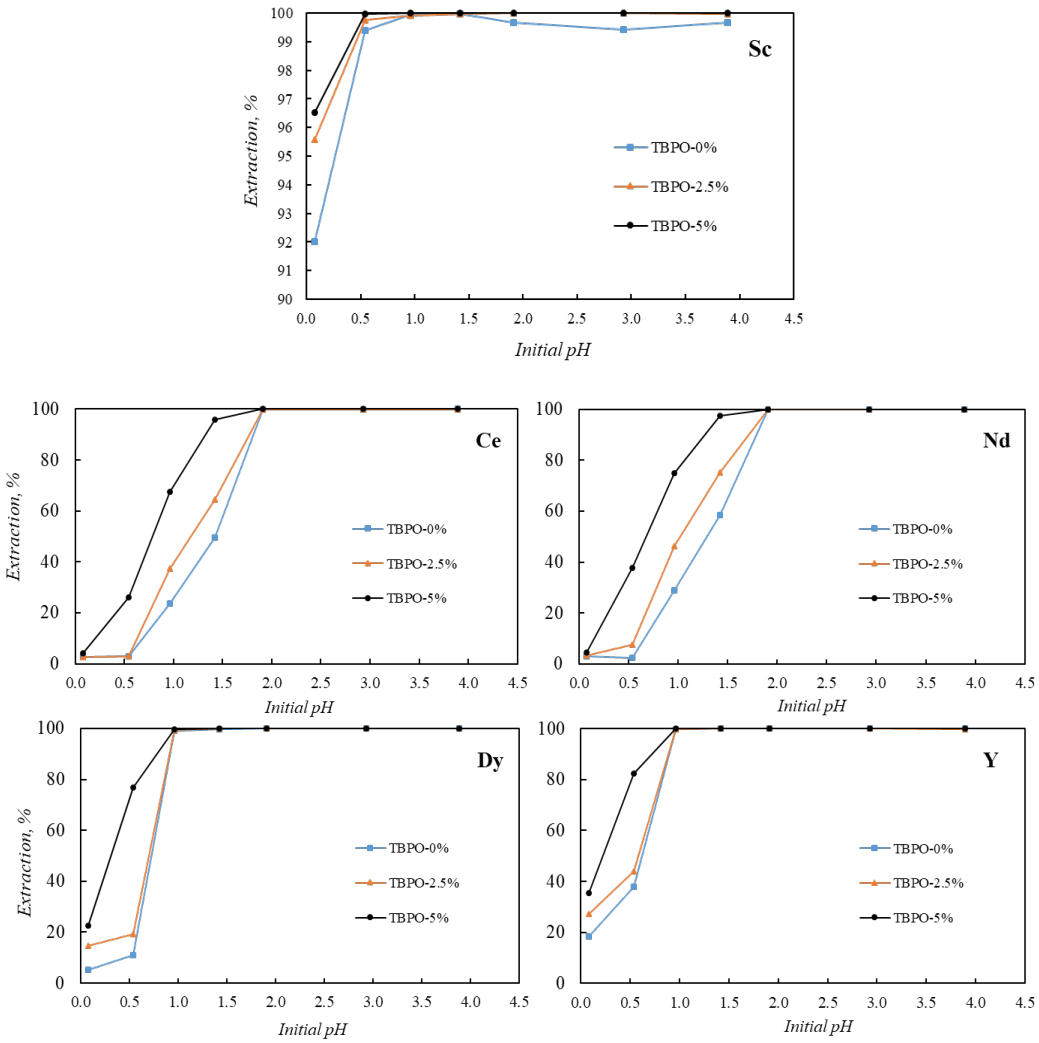

Figure 21. pH-extraction isotherms of Ce(IV), Nd(III), Dy(III), Y(III) and Sc(III) at different TBPO concentrations. c(D2EHPA) = 0.2 M; V_A/V_o=1; t = 10 min.

Conclusions

In this task, a parametric solvent extraction study was conducted to evaluate the selective extraction and stripping of five surrogate REEs. Tests were conducted to evaluate reaction time, feed concentration, D2EHPA concentration, aqueous pH, type of diluent, addition of modifier, the type and concentration of stripping reagent. Specific findings are listed below.

1. D2EHPA can be used to efficiently extract all REEs. The extraction of the five REEs with D2EHPA from nitrate media follows the order of $Ce(IV) < Nd(III) < Dy(III) < Y(III) < Sc(III)$ and the extraction efficiency increases with the increase of aqueous pH and D2EHPA concentration.
2. The Elixore range organics were proven a better choice of diluent than kerosene due to their high performance in the extraction of REEs as well as their improved health and safety features.
3. HCl and HNO_3 can be used to recover Ce(IV), Nd(III), Dy(III) and Y(III) from D2EHPA. Their stripping efficiency in both acids increases with the increase of acid concentration and HCl provides better recovery of REEs.
4. The use of NaOH provides a practical method to recover Sc(III) from D2EHPA by forming $Sc(OH)_3$ precipitate.

5. The addition of tri-n-butylphosphine will not only help the extraction of REEs but also the phase separation in stripping of Sc(III) with NaOH.

Based on the information above, the optimal chemical conditions were determined. Nearly 100% extraction efficiency of REEs can be obtained when solvent extraction experiments are conducted with 0.2 M D2EHPA + TBPO in Elixore 205 at pH 2. After extraction, 6 M HCl can be employed to recover REEs from organic and nearly 100% stripping efficiency can be obtained for Y(III), Nd(III), Dy(III) and Ce(IV). Moreover, 75.04% of Sc(III) can be precipitated from the organic by 2 M NaOH.

Subtask 4.3. Real System Evaluation, Batch Tests

Overview

Experimental work under this subtask used real feedstock samples to validate and improve the SX processing approach developed with synthetic solutions in Subtask 4.1 and 4.2. In work conducted under Task 2, REE pre-concentrate was generated using a pilot-scale mobile plant. This pre-concentrate assayed approximately 0.1% REE, which is notably lower than the values expected from laboratory testing but similar in distribution of gangue metals and REEs. These pre-concentrate materials were later delivered to university laboratory facilities and evaluated using batch SX tests. The objective of the work in this subtask was to assess the capability of the SX process to recover high-grade MREO, exceeding 90% purity, from the pre-concentrate generated from AMD.

Approach

After an optimal processing route is determined from the model system evaluation, validation tests were conducted using real product samples generated from Task 2.0 and 3.0. The specimens were first dissolved in an acid matrix (if applicable), and the resultant leachate was subjected to batch-wise, laboratory-scale testing in 500 to 1,000 mL separatory funnels. The optimal process route was followed, and additional stages of extraction, scrubbing, and stripping were used to successfully isolate the REE's. After SX separation, the resultant products were precipitated and roasted to produce an REE oxide product.

Results and Discussion

Materials – REE Pre-Concentrate

The REE pre-concentrate used as feedstock for the solvent extraction tests conducted under this subtask contained an average moisture content of 79.6% and a TREEs content of 0.13%. Table 20 shows the element composition of the dry concentrate.

Materials – Chemicals

In the present work, Di-(2-ethylhexyl) phosphoric acid (D2EHPA, 95%, Alfa Aesar, Haverhill, MA) and Tri-n-butylphosphine (95%, Alfa Aesar, Haverhill, MA) were used as the extractant and modifier without further purification, respectively. The two solvents were dissolved in Elixore 205 (supplied by Total Special Fluids, Inc. - Houston, TX).

Hydrochloric acid (HCl) was used as the reagent in the scrubbing and stripping tests and diluted using deionized water to obtain different concentrations. Hydroxylamine hydrochloride ($NH_3OH \cdot Cl$) was employed as the reductant and a precipitation reagent was used to selectively precipitate REEs, both of which were provided by Alfa Aesar (Haverhill, MA).

Table 20. Element composition of the dry REE concentrate.

REE	Concentration		Major Metal	Concentration	
Sc	101.8	mg/kg	Al	303.2	g/kg

Y	364.4	mg/kg	Ca	26.2	g/kg
La	71.6	mg/kg	Co	0.6	g/kg
Ce	253.4	mg/kg	Fe	21.8	g/kg
Pr	38.5	mg/kg	Mg	4.1	g/kg
Nd	180.4	mg/kg	Mn	3.0	g/kg
Sm	53.2	mg/kg	Na	1.2	g/kg
Eu	14.1	mg/kg	Si	102.8	g/kg
Gd	82.6	mg/kg	SO4	1.4	g/kg
Tb	15.1	mg/kg	Cl	0.0	g/kg
Dy	88.5	mg/kg	Total	464.4	g/kg
Ho	17.1	mg/kg			
Er	46.7	mg/kg			
Tm	6.4	mg/kg			
Yb	36.1	mg/kg			
Lu	5.5	mg/kg			
Total	1,375.4	mg/kg			

Experimental Procedure – Acid Leaching

Initially, 481.5 g of the REE pre-concentrate was mixed with 550 mL DI water in a beaker. Next, 150 ml concentrated nitric acid was added to the beaker in 30 incremental steps to ensure the leaching process was carried out at the appropriate pH. After 5 hours, the insoluble residue was filtered and a brown filtrate was obtained (Figure 22a). The metal content of filtrate was measured by ICP-MS. This filtrate is denoted as “pregnant leach solution (PLS)” in the following discussion.

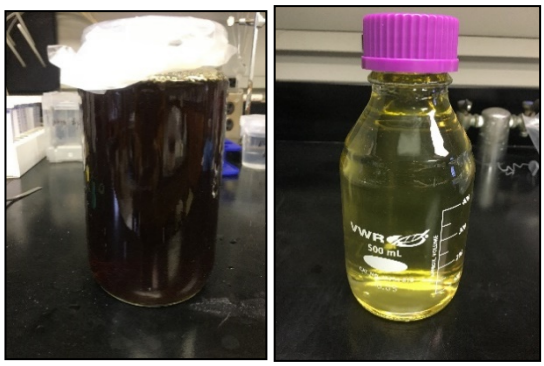

(a) (b)

Figure 22. Pregnant leach solution (a) and leachate (b).

Experimental Procedure – Iron Removal

In order to remove the residual iron that was present in the PLS, 1 M NaOH solution was slowly added to the PLS to bring the pH up, where the formation of $Fe(OH)_3$ was observed. The solution was stirred for 5 minutes, left to rest for half an hour, and subsequently filtered. The resulting filtrate was a light yellow color (Figure 22b) and its metal content was analyzed by ICP-MS. This filtrate is denoted as “leachate” in the following discussion.

Experimental Procedure – Solvent Extraction

Solvent extraction experiments were performed in a 1000 ml separatory funnel at room temperature, using a mechanical shaker (Yamato, SA320). After extraction, the aqueous phase was separated from the organic phase and diluted to rational multiples to analyze the concentrations of metals with ICP-MS. The organic phase was collected for the scrubbing tests.

As the organic phase could not be analyzed with ICP-MS directly, HNO_3 was used to digest the organics before analyzing. After digestion, the concentrations of metals in the loaded organic were determined with ICP-MS.

Scrubbing and stripping experiments were conducted in a 125 ml separatory funnel. In each test, the loaded organic was mixed with 0.1 M or 6 M HCl solution and agitated by a shaker for 10 min. After achieving equilibrium, the aqueous phase was separated from the organic phase and collected for the precipitation tests.

Experimental Procedure – REE Oxide Production

Precipitation experiments were conducted in a 100 ml beaker at room temperature. The mixed REEs were precipitated from the strip liquor. For each test, 2 g precipitation reagent was added in 100 ml strip liquor, followed by the addition of the 1 M NaOH solution. The mixture was stirred for half an hour and left to rest for 12 hours. Afterwards, the precipitated REE was filtered, washed with water, and dried at 60^{o} C. The precipitate was subsequently calcined in a muffle furnace at 800^{o}C for 5 h to convert it to an REE oxide product. The REE oxide was later washed with 2% nitric acid and dried at 60^{o} C. The purity of the final product was determined after subsequent dissolution in HCl and analysis of the solution with ICP-MS.

Results – Pregnant Leach Solution Concentration

Previous research has confirmed that nitric acid is the most suitable and reliable leaching reagent for acid mine drainage precipitates (AMDp). In addition, pilot-scale tests conducted in a separate DOE study (DE-FE0026927) have shown that the PLS tends to form a pernicious alumino-silicate gel when the leaching tests are carried out at pH < 1, As a result, nitric acid was employed as the reagent, and the leaching tests were conducted at pH = 1, which represents an optimal tradeoff between leaching efficiency and operability.

Table 21 shows the elemental composition of the PLS generated from this process. It can be seen that the concentration of REEs is 90.7 mg/L. Among them, Y, Ce and Nd are present at notable concentrations of 25.0 mg/L, 16.3 mg/L and 12.6 mg/L, respectively. Most of the other REEs are also present at concentrations ranging from around 1 mg/L to 5 mg/L.

The total concentration of major elements was 26,796.3 mg/L, among which Al accounts for more than 60% with a concentration of 16,271 mg/L. Other notable constituents included Ca, Fe and Si, each with a concentration of more than 1,000 mg/L. Minor constituents include Mg, Mn and Co each with concentrations less than 500 mg/L. The ratio of the major elements to REEs as well as the distribution of REEs in the real PLS is similar to that of the simulated leachate that was used in Subtask 4.1. This result suggests that the process knowledge and data generated from the simulated leachate testing has direct relevance to the real system evaluation.

Two notable exceptions, however, are that the concentration of Fe (1,307.1 mg/L) and Si (6,855.6 mg/L) are both higher than the values used in the simulated leachate. With regard to Fe, prior test work has shown that the Fe in the PLS must be reduced from Fe(III) to Fe(II) to prevent extraction into the organic phase (Fe(II) has a much lower extraction efficiency than Fe(III). Given the relatively high concentration of Fe in the real PLS, this approach was deemed infeasible, owing to the high reagent consumption and high cost needed to fully reduce all of the Fe. As an alternative approach, the Fe was instead removed from PLS by precipitating as iron hydroxide ($Fe(OH)_3$).

Table 21. Elemental composition of the PLS.

REE	Concentration		Major Metal	Concentration	
Sc	6.0	mg/L	Al	16271.0	mg/L
Y	25.0	mg/L	Ca	1825.5	mg/L
La	4.6	mg/L	Co	42.9	mg/L
Ce	16.3	mg/L	Fe	1307.1	mg/L
Pr	2.5	mg/L	Mg	251.6	mg/L
Nd	12.6	mg/L	Mn	140.4	mg/L
Sm	3.7	mg/L	Si	6855.6	mg/L
Eu	0.9	mg/L	Total	26796.3	mg/L
Gd	5.3	mg/L			
Tb	1.0	mg/L			
Dy	5.8	mg/L			
Ho	1.1	mg/L			
Er	3.1	mg/L			
Tm	0.4	mg/L			
Yb	2.4	mg/L			
Lu	0.3	mg/L			
Total	90.3	mg/L			

Results – Fe removal by Selectively Precipitation

The PLS was processed to remove Fe by selectively precipitation. Figure 23 shows the recovery of each element through this process (i.e. the amount that remained in solution after precipitation). The data shows that more than 90% of Fe and Si were removed, which was due to that the rapid hydrolysis of Fe(III) resulting in the precipitation of $Fe(OH)_3$. At the same time, $Fe(OH)_3$ provided a surface area for silicate absorption and thus a rapid Fe/Si co-precipitation (Dyer et al, 2010). However, most of the other major elements remained in solution during the precipitation process. Therefore, the recovery of total major elements is 78%.

For REEs, the total recovery is 91% which indicates a good separation efficiency between REEs and Fe/Si. The major loss of REEs is from Sc. As shown in Figure 23, 70% of Sc reported to the precipitate. Previous test work has shown that an additional stripping stage is necessary for the recovery of Sc as it cannot be stripped by acid with the other REEs. Prior work has also shown that Sc can be recovered from organic phase by the formation of $Sc(OH)_3$ precipitate. However, this method is time-consuming and involves a three-phase separation, which will make the recycle of solvent very difficult. Therefore, it will be more adequate for process development if all Sc can precipitate with Fe before solvent extraction

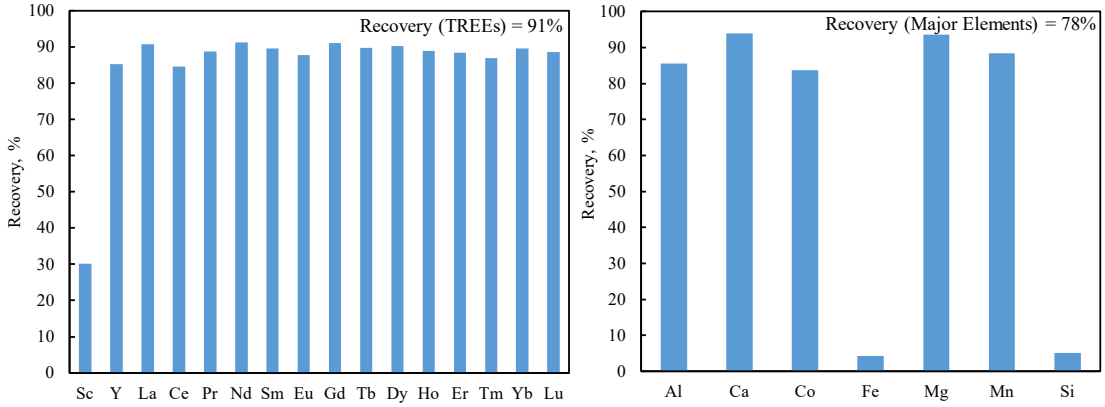

Figure 23. Recovery of REEs and gangue metals in selectively precipitation.

Table 22 shows the elemental composition of the leachate after Fe precipitation. Compared to the PLS, the leachate is more similar to the simulated leachate used in model system evaluation as the most of Fe and Si has been removed.

Table 22. Elemental composition of the leachate.

REE	Concentration		Major Metal	Concentration	
Sc	2.5	mg/L	Al	14094.6	mg/L
Y	23.3	mg/L	Ca	1721.3	mg/L
La	4.2	mg/L	Co	39.7	mg/L
Ce	14.7	mg/L	Fe	79.1	mg/L
Pr	2.2	mg/L	Mg	235.7	mg/L
Nd	11.5	mg/L	Mn	127.2	mg/L
Sm	3.4	mg/L	Si	118.9	mg/L
Eu	0.9	mg/L	Total	16416.5	mg/L
Gd	4.9	mg/L			
Tb	0.9	mg/L			
Dy	5.4	mg/L			
Ho	1.1	mg/L			
Er	2.8	mg/L			
Tm	0.4	mg/L			
Yb	2.2	mg/L			
Lu	0.3	mg/L			
Total	80.8	mg/L			

Results – Solvent Extraction

Preliminary tests on leachate showed insufficient extraction of LREEs with 0.2 M D2EHPA. To solve this problem, 0.5 M D2EHPA was used in the solvent extraction of the pre-concentrate. All the other conditions followed the optimal SX process described in earlier subtasks.

Figure 24 and Table 23 shows the concentrations of each element in the organic after extraction and scrubbing as well as the strip liquor obtained from the stripping. After extraction, the concentration of Al and Ca is reduced substantially; however, not all of the Co, Mg, Mn were extracted. Even though there is only a slight decrease in the concentration of Fe and even a slight increase in the concentration of Si, they will not lead to significant contamination as the majority of their mass was reomoved in the earlier stage by precipitation. The concentration of REEs is nearly doubled after solvent extraction, which

indicates good separation efficiency between REEs and major elements in solvent extraction.

The scrubbing stage does not lead to a signiciant change in concentration, but the process is needed to mitigae downstream formation of emulsion. Details on this result are presented in Subtask 6.1.

After stripping, REEs were further enriched from 161.9 mg/L in loaded organic to 466.8 mg/L in strip liquor. Likewise, most of the major gangue metals, i.e. Al and Ca, were removed. The concentration of Fe is notable, however, its concentration is lower than that of REEs.

Overall, the REEs are significantly concentrated through the SX process, and the total concentration increases from 80.8 mg/L to 466.8 mg/L. Al is still the primary contaminant in the strip liquor because of its high concentration in the original leachate. Fe is also major contaminant because of its high recovery in extraction and stripping stages; however, the low initial concentration (due to removal in the pre-concentration step) greatly improved the mitigation of crud in the SX extraction stage. In addition, the strip liquor also contains small amounts of Ca and Si. Furthermore, all of the Mg, Mn, and Co are removed by the process.

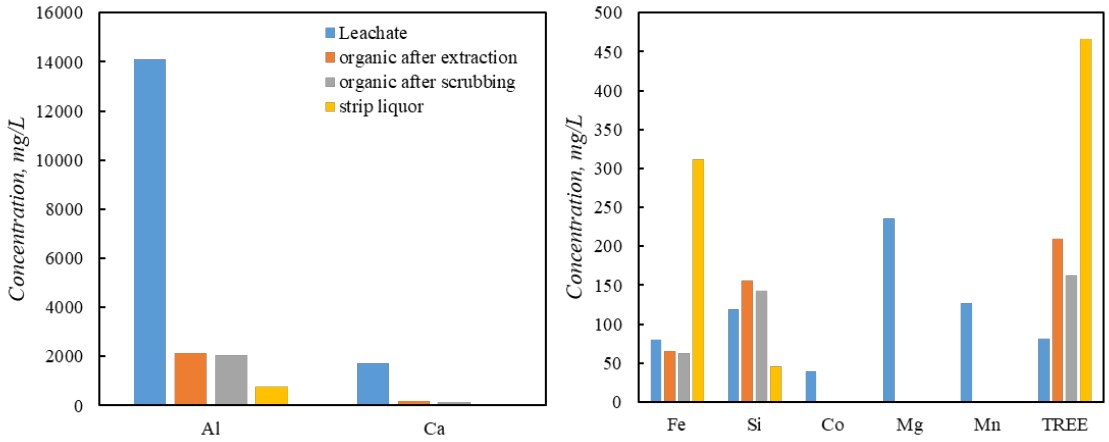

Figure 24. Concentration of the elements in the product of each stage in SX process.

Table 23. Elemental concentrations in the products of each stage in SX process.

REEs	Feed	Extraction	Scrubbing	Stripping	Gangue	Feed	Extraction	Scrubbing	Stripping
mg/L	Leachate	Loaded organic	Loaded organic	Strip Liquor	mg/L	Leachate	Loaded organic	Loaded organic	Strip Liquor
Sc	2.5	7.4	7.1	0.0	Al	14094.6	2120.8	2054.5	775.2
Y	23.3	72.9	70.0	107.4	Ca	1721.3	182.1	143.8	66.2
La	4.2	3.2	0.3	2.7	Co	39.7	0	0	0
Ce	14.7	25.7	6.3	42.4	Fe	79.1	65.8	62.7	311.5
Pr	2.2	4.7	1.6	10.3	Mg	235.7	0	0	0
Nd	11.5	26.0	11.0	68.0	Mn	127.2	0	0	0
Sm	3.4	9.5	8.5	46.0	Si	118.9	156.0	143.2	46.0
Eu	0.9	2.5	2.4	12.8	Total	16416.5	2524.8	2404.2	1207.1
Gd	4.9	14.6	13.6	73.6					
Tb	0.9	2.8	2.7	13.7					
Dy	5.4	17.8	17.4	65.7					
Ho	1.1	3.3	3.2	8.5					
Er	2.8	9.0	8.8	12.2					
Tm	0.4	1.2	1.2	0.7					
Yb	2.2	7.2	6.9	2.4					
Lu	0.3	1.0	1.0	0.3					
Total	80.8	208.9	161.9	466.8					

Results – REE Precipitate Recovery

The precipitation of REEs is widely used in industry for the selective recovery of rare earth metals (Xie et al., 2014). However, this method is usually applied to the leachate with enriched REEs (1-40 g/L) and limited impurities (Josso et al., 2018). The challenge for the current study lies in the low REEs concentration (0.5 g/L) and high concentration of impurities (1.2 g/L) in the strip liquor. The tests were conducted by the addition of excess precipitation reagent. Figure 25 shows the precipitation efficiency of each element. As shown in the plot, 88.5% of REEs were precipitated, while most of the major elements remained in solution. In addition, the precipitation efficiency of the LREE is higher than that of the HREE, due to the reduced affinity of LREE for the reagent ligand relative to HREE (Josso et al., 2018). Among the major elements, most of the Al, Fe, Si were removed, but more than 80% of Ca precipitated with REEs. Fortunately, Ca can be easily removed by acid washing in a subsequent processing step.

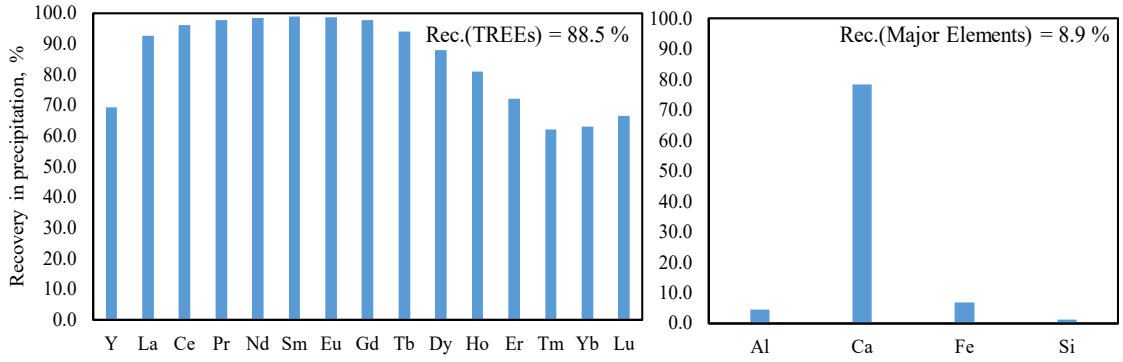

Figure 25. Recovery of REEs and major elements after precipitation.

Results – REE Oxide Production

The REE precipitate was calcined by heating at 800°C for 5 h to obtain REE oxide. The REE oxide was then washed by 2% nitric acid to remove the soluble impurities e.g. Ca and Na oxides. The distribution of the individual REE in the mixed oxide is given in Table 24 along with the mass fraction of each major element. As shown, the final product contains 90.5% TREO and 9.5% impurities. In addition, Y, Ce, Nd, Gd and Dy are enriched in the TREO with mass fractions over 10%.

Table 24. Compositions of REO product from pre-concentrate of AMD.

Oxides	Concentration		Oxides	Concentration	
Y	20.8	%	Al	4.0	%
La	0.4	%	Ca	1.8	%
Ce	14.9	%	Co	1.0	%
Pr	2.1	%	Fe	1.9	%
Nd	11.6	%	Mg	0.2	%
Sm	8.4	%	Mn	0.1	%
Eu	2.3	%	others	0.7	%
Gd	13.2	%	Total	9.5	%
Tb	2.7	%			
Dy	10.6	%			
Ho	1.3	%			
Er	1.7	%			
Tm	0.1	%			
Yb	0.3	%			
Lu	0.0	%			
Total	90.5	%			

Results – McCabe-Thiele Diagram Construction

The McCabe-Thiele diagram was constructed for the extraction step to identify the theoretical number of extraction stages and the extent of enrichment of TREEs in the loaded organic. Figure 26 shows that all REEs in the leachate can be extracted to organic phase in three counter-current extraction stages at a phase ratio (V_A:V_O) of 3:1 with 0.5 M D2EHPA + 2.5 vol.% TBPO. Under these conditions, the loaded organic phase will contain approximately 250 mg/L of TREEs.

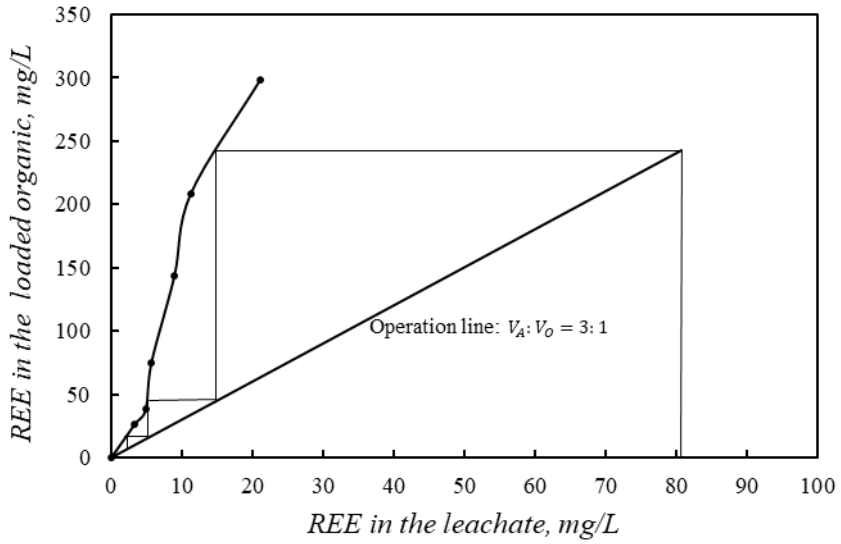

Figure 26. McCabe-Thiele diagram of extraction of TREE from leachate. c(D2EHPA) = 0.5 M; c(TBPO) = 2.5 vol. %, pH = 3.

The McCabe Thiele diagram was also constructed for the stripping stage. Figure 27 shows that all the REEs in the loaded organic can be recovered to the strip liquor in two counter current stripping stages at a phase ratio of (V_O:V_A) of 1:1 with 6 M HCl. The concentration of TREEs is anticipated to be approximately 160 mg/L.

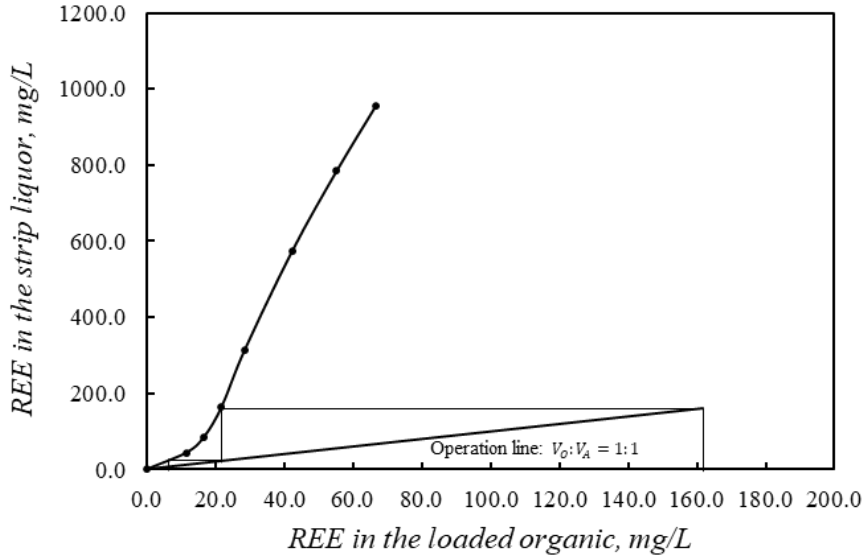

Figure 27. McCabe-Thiele diagram of stripping of TREE from loaded organic. c(HCl) = 6 M.

Results – Selective Stripping of Loaded Organic

Prior efforts in this task showed that a mixed REE oxide containing 90.5% REO can be obtained by solvent extraction and selective precipitation. However, this data also showed that only 29% of TREEs were recovered to strip liquor in the stripping stage. The major loss comes from the HREEs, which indicates that the parameters in stripping stage need to be reinvestigated in the real system. Further experiments were thus conducted to optimize the recovery of TREEs in the stripping stage. Moreover,

LREEs are more easily stripped than HREEs as D2EHPA has stronger affinity to HREEs than LREEs. Therefore, LREEs/HREEs separation was investigated by selective stripping.

The stripping experiments were conducted by using nitric acid (HNO_3) and hydrochloric acid (HCl) at different phase ratios. The loaded organic phase was obtained from the process described early in this subtask. The organic phase was digested with HNO_3 and diluted to analyze the concentrations of metals with ICP–MS. The results are listed in Table 25. The previous study has indicated that Sc(III) cannot be stripped from D2EHPA with acid under the tested conditions and the results of Sc(III) were not considered.

Table 25. The concentrations of elements in the organic feed for the stripping tests.

Con.	Al	Ca	Fe	Si	Total
mg/L	2185.0	49.1	90.4	29.5	2354.0

		LREE							HREE										
Con.	Sc	La	Ce	Pr	Nd	Sm	Eu	LREE	Y	Gd	Tb	Dy	Ho	Er	Tm	Yb	Lu	HREE	TREE
mg/L	7.4	2.1	17.1	3.4	18.7	9.2	2.7	67.6	72.8	14.5	3.1	17.8	3.5	9.5	1.3	7.5	1.1	116.5	191.6

Figure 28 shows the stripping behavior of gangue elements at different phase ratios. The stripping efficiency of four gangue elements increases with the increase of phase ratio (A:O). The stripping of Al, Ca and Si shows no significant difference between HCl and HNO_3, however, the stripping of Fe using HCl is much more efficient than that using HNO_3 under the same conditions. Specifically, the stripping efficiency of Fe increases from 29.6% to 78.4% when increasing the phase ratio (A:O) from 1:8 to 1:4 using HCl while the stripping efficiency of Fe remains less than 10% at all conditions using HNO_3. Therefore, the use of HNO_3 as the stripping reagent will provide some additional benefit in separating Fe from REEs.

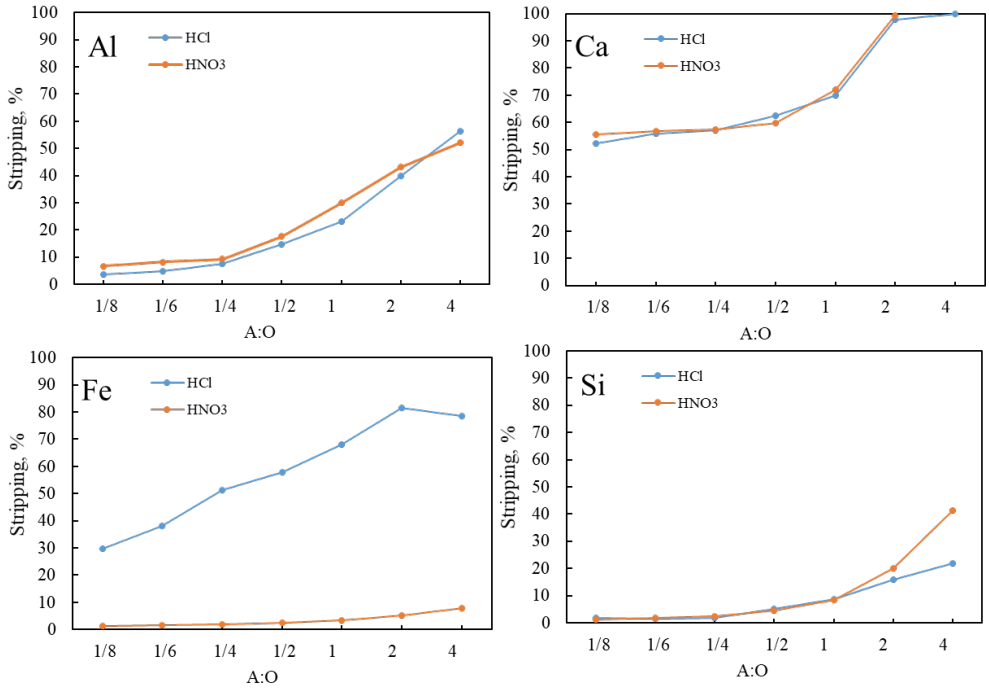

Figure 28. The effect of phase ratio (A:O) on the stripping efficiency of gangue elements. c(HCl) = 6 M, c(HNO3) = 6 M, T = 298 K; t = 10 min.

Figure 29 shows the stripping behavior of REEs using HCl and HNO_3 at different phase ratios. With an

increase in the phase ratio (A:O), the stripping efficiency of REEs increases in the order La > Ce > Pr > Nd > Sm > Eu > Gd > Tb > Dy > Ho > Y > Er > Tm > Yb > Lu, where Y is located between Ho and Er. This order is because REEs with smaller ionic radii form more stable complex with the extractant, suggesting that stripping of REEs increases with the increase of ionic radii of REEs.

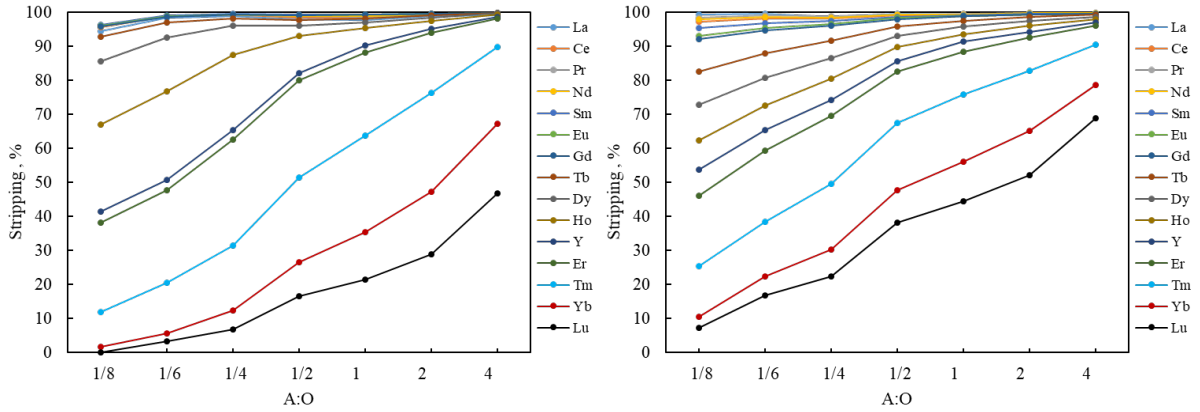

Figure 29. The effect of phase ratio (A:O) on the stripping efficiency of each REE. c(HCl) = 6 M, c(HNO_3) = 6 M, T = 298 K; t = 10 min.

Figure 30 shows the results analyzed by the groups of TREEs, LREEs, and HREEs. This data indicates that the stripping of LREE shows no significant difference between the two types of acid; however, LREEs are also easily stripped in general. Nearly 100% stripping efficiency of LREEs can be achieved at all conditions for both of HCl and HNO_3. Alternatively, HNO_3 is more efficient than HCl in the stripping of HREEs. The stripping efficiency of TREEs using HNO_3 is slightly higher than that using HCl at low phase ratios. When the phase ratio is higher than 1:1, the stripping efficiency of TREEs reaches more than 90% for both of HCl and HNO_3.

As a result, 6 M HNO_3 was selected as the stripping reagent because it represents the optimum for both the removal of Fe and the recovery of REEs. The optimal phase ratio (A:O) is set at 1:1.

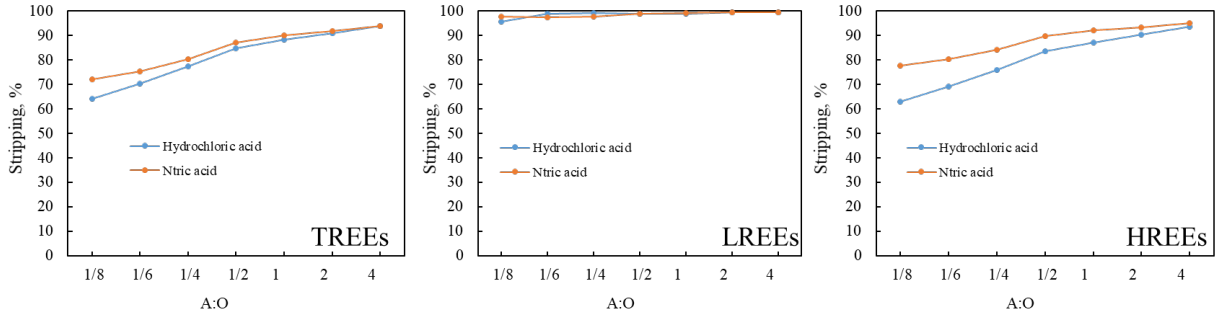

Figure 30. The effect of phase ratio (A:O) on the stripping efficiency of TREEs, LREEs and HREEs. c(HCl) = 6 M, c(HNO_3) = 6 M, T = 298 K; t = 10 min.

Using these results, the McCabe-Thiele diagram was constructed to find out the theoretical number of stripping stages and the extent of enrichment of TREEs in the strip liquor. Figure 31 shows that TREEs in the loaded organic are able to be recovered to the strip liquor in two counter current stripping stages at a phase ratio of (V_O:V_A) of 1:1 with 6 M HNO_3. At this condition, the concentration of TREEs reaches around 180 mg/L.

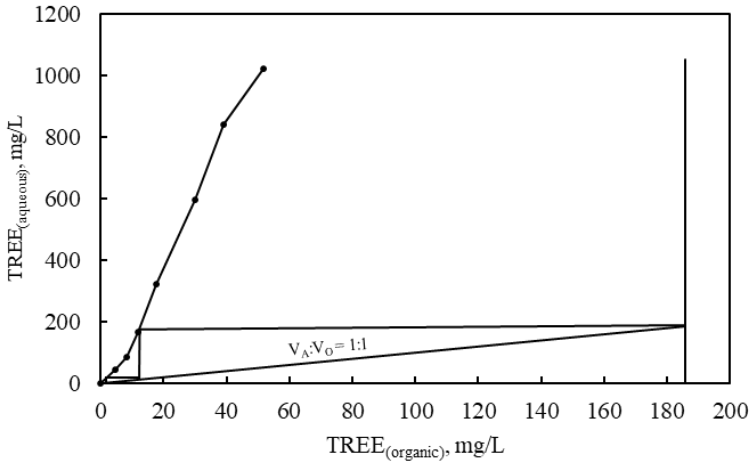

Figure 31. McCabe-Thiele diagram for the stripping of TREEs from loaded organic.

D2EHPA has stronger affinity to HREEs than LREEs. As a result, LREEs can be stripped selectively from the organic phase through the introduction of a selective stripping step. Figure 32 shows the effect of HNO_3 concentration on the stripping of HREEs, LREEs and gangue metals. The stripping efficiency increases with increasing acid concentrations, which is consistent with general expectations and previous studies. When increasing the acid concentration from 0 to 0.5 M, the stripping efficiency of LREEs increases significantly from 0% to 95.7%; however, the stripping efficiency of HREEs only increases from 0% to 13.7%. In addition, the stripping efficiency of gangue metals is 3.5% at 0.5 M. When the acid concentration exceeds 0.5 M, the stripping efficiency of LREEs remains the same and that of HREEs and gangue metals increase. More than 90% stripping efficiency can be obtained for HREEs when the acid concentration increases to 6 M and the stripping efficiency is 25% at 6 M for gangue metals.

Thus, a two-step stripping stage can be used to separate LREEs and HREEs. In the first stripping step, the LREEs are selectively recovered to the strip liquor by using 0.5 M HNO_3. Afterwards, the HREEs left in the organic phase are recovered by stripping with 6 M HNO_3.

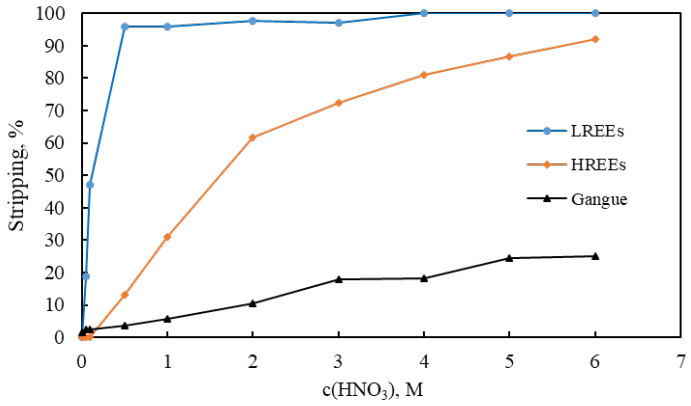

Figure 32. The effect of HNO3 concentrations on the stripping of HREEs, LREEs and Gangue metals. A:O = 1:1, T = 298 K; t = 10 min.

Conclusions

This task developed a process for REE recovery from AMD pre-concentrate of AMD based on the optimal solvent extraction process derived from simulated leachate. In this process, the AMD pre-concentrate is first dissolved in the nitric acid. The resultant PLS is precipitated for Fe removal and the optimal SX

process is then followed. After SX separation, the strip liquor is precipitated using a reagent and finally roasted to produce an REE oxide product. An oxide containing 90.5% REE was obtained from AMD pre-concentrate (0.1% REE) by this process.

The McCabe-Thiele diagrams were also constructed for the extraction and stripping stages. The diagrams show that theoretically the REEs in leachate can be operationally extracted in three counter-current extraction stages at a phase ratio (V_A:V_O) of 3:1 with 0.5 M D2EHPA + 2.5 vol.% TBPO and all the REEs in the loaded organic is able to be recovered to the strip liquor in two counter current stripping stages at a phase ratio of (V_O:V_A) of 1:1 with 6 M HCl.

Exploratory Testing on Precipitation of REEs from SX Stripping Solution

The first strip solution contained a high concentration of HCl (~3 M), a high concentration of Al (130 ppm), Fe (1700 ppm), Ca (40 ppm) and Mg (60 ppm), as well as a high concentration of REEs (80 ppm). Titration with base to selectively precipitate Fe and Al was judged to be impractical because of the formation of the very thick $Al(OH)_3$ floc. Selective precipitation of REEs with a precipitation reagent was chosen. Titrating the strip solution with NaOH solution and adding a precipitation solution did not result in a precipitate forming. Adding additional precipitation reagent (2.5 g/100 mLs) to the strip solution and then titrating with NaOH solution resulted in a precipitate that contained half of the initial amount of calcium and more than 90% of the REEs while most of the other metals remained in solution. Figure 33 shows the mass balances for the amount recovered and the amounts in the solution and precipitate. All of the rare earth elements were collected quantitatively. Titration results in only 10% of the Ca and greater than 90% of the REEs to be collected in the precipitate (Figure 34). Titration to lower pHs resulted in only partial precipitation of the REEs; an example of the titration is shown in Figure 35.

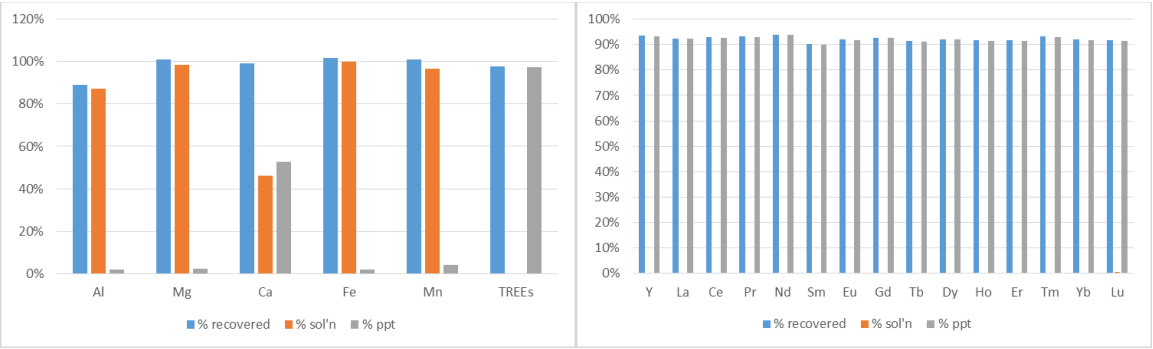

Figure 33. Mass balances for titration of first HCl strip solution. Left: mass balances of major metal cations and total REEs. Right: mass balances of the REEs.

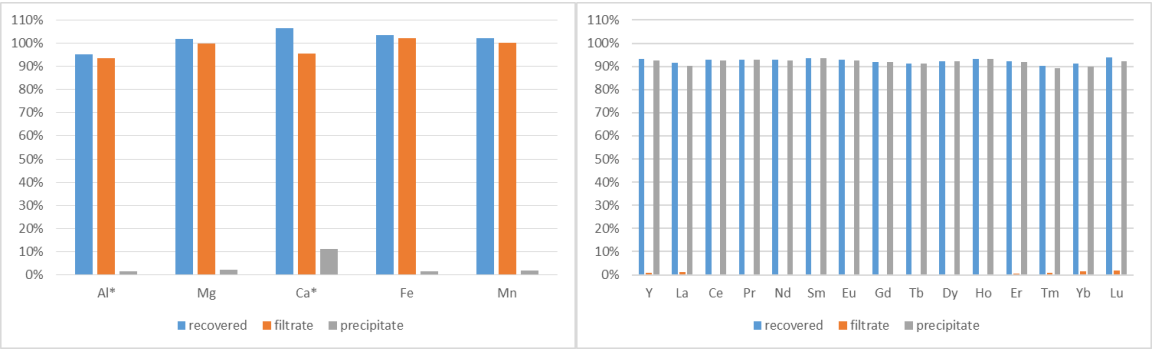

Figure 34. Mass balances for titration of second HCl strip solution. Left: mass balances of major metal cations. Right: mass balances of the REEs.

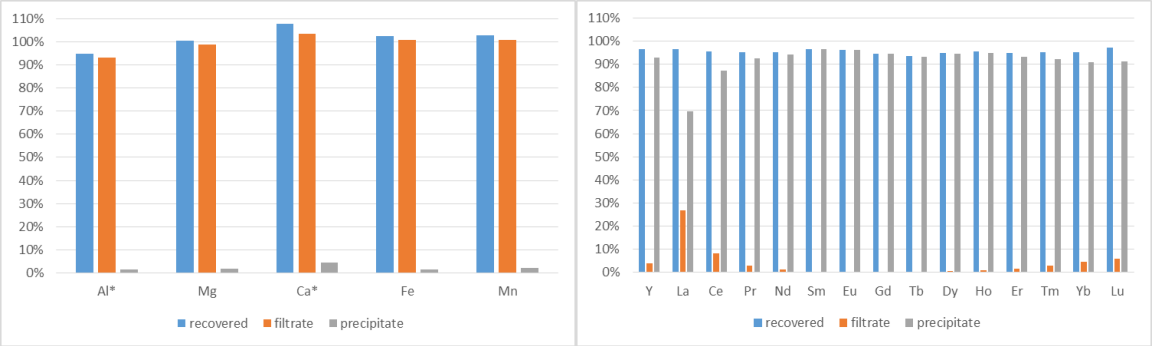

Figure 35. Mass balances for titration of third HCl strip solution. Left: mass balances of major metal cations. Right: mass balances of the REEs.

The second strip solution contained a high concentration of nitric acid (~2 M), Al (500 ppm), Fe (60 ppm) and especially Ca (1800 ppm) and REEs (370 ppm). As a consequence, titration with NaOH after adding precipitation reagent resulted in substantial precipitation of calcium with near quantitative (>90%) collection of REEs in the precipitate. The precipitation reagent concentration could be reduced from 2.5 g/100 mLs to 1.0 g/100 mL with quantitative collection of REEs after titrating (Figure 36), but also with near quantitative collection of the Ca. In both cases, most of the Al, Fe and Mg were retained in the filtrate. Concentrated ammonia was used in place of sodium hydroxide again with quantitative collection of REEs in the calcium oxalate (Figure 37). The advantages of using ammonia instead of sodium hydroxide include less heat generation during neutralization of the nitric acid and reduction of sodium concentrations in the collected precipitate.

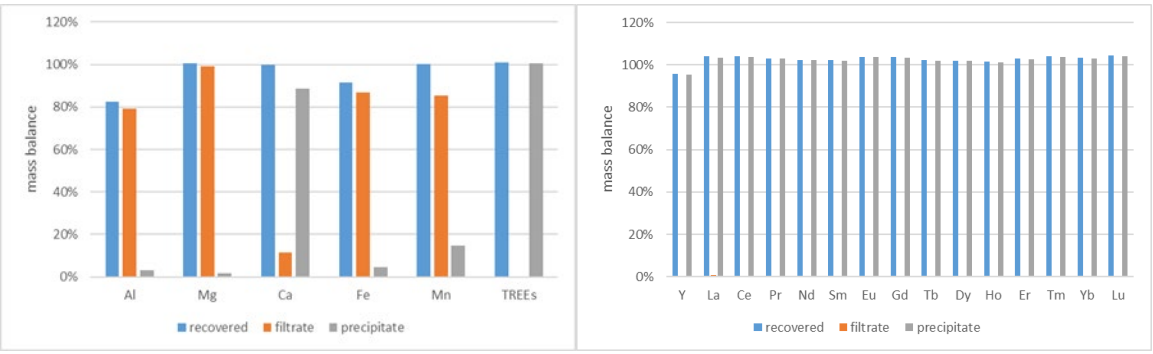

Figure 36. Mass balances for titration of HNO_3 strip solution. Left: mass balances of major metal cations. Right: mass balances of the REEs.

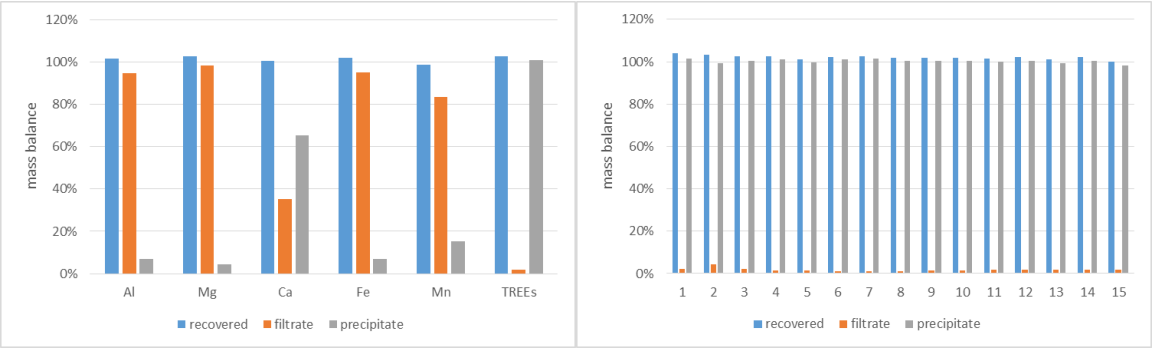

Figure 37. Mass balances for titration of HNO_3 strip solution with NH_4OH. Left: mass balances of major metal cations. Right: mass balances of the REEs.

The collected precipitate contained mainly calcium oxalate, zinc oxalate and REE oxalate salts. Thermogravimetric analysis (linear temperature vs time from 25 to 1000°C) shows loss of unbound water (100°C), waters of crystallization (240°C), decomposition of the REE precipitate to REE oxides and decomposition of Ca to $CaCO_3$ (320 – 500°C), and then decomposition of $CaCO_3$ to CaO (above 730°C) (Figure 38). Based on the weight loss between 700 and 1000°C, the amount of CaO in the calcined solid was estimated (67%). Chemical analysis of the calcined solid yielded a similar value for CaO (64%). The REE oxide content was 26%. XRD spectrum confirmed the presence crystalline CaO and REE oxides (Figure 39).

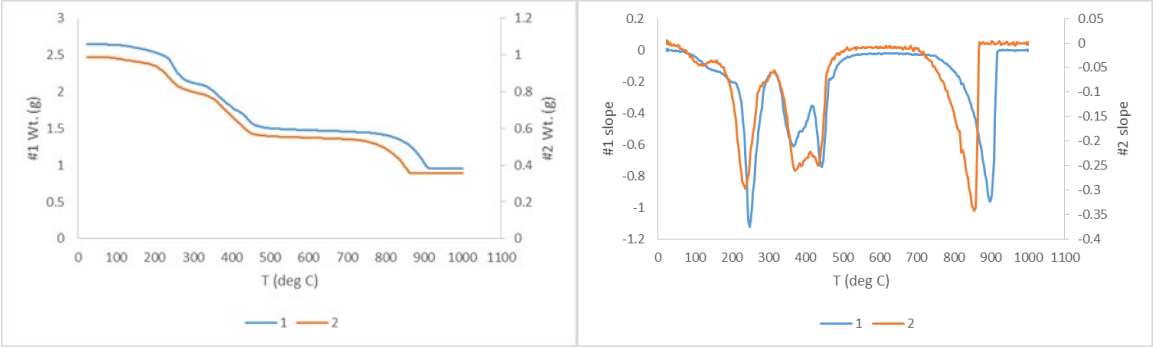

Figure 38. TGA analysis of dried precipitates collected by ammonium hydroxide titration. Left: Weight vs temperature. Right: slope (dw/dt) vs temperature. Two separate samples from the same precipitate were analyzed.

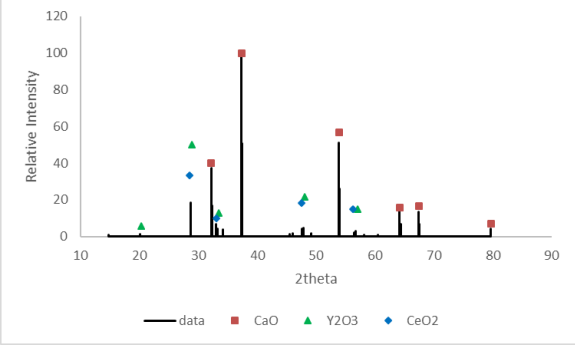

Figure 39. Line representation of x-ray diffraction peaks of the calcined solid.

The calcined precipitates were treated with dilute nitric acid in an attempt to dissolve the CaO selectively and retain the REE oxides. The crushed solids were suspended in 1% or 6% nitric acid solutions with stirring, separated from the solution, dried and analyzed. In Figure 40, the mass% of major metals and TREEs in the calcined and washed solids are compared. The 1% HNO_3 wash lowered the Ca content from 45% to 31 %, resulting in only a slight increase in the TREE content (23% to 26%). The 6% HNO_3 was successful in reducing the Ca content to 5% and raising the TREE content to 50%. This mass% is lower than the value expected for a pure sample of REE oxides (~85%). Incomplete drying may be the reason. However, analysis of the 6% HNO_3 wash solution showed that roughly one-third of the REEs were dissolved in the solution. The distribution of dissolved REEs is uneven, with La content high (62%), Ce content low (7%), and most other elements near 40%.

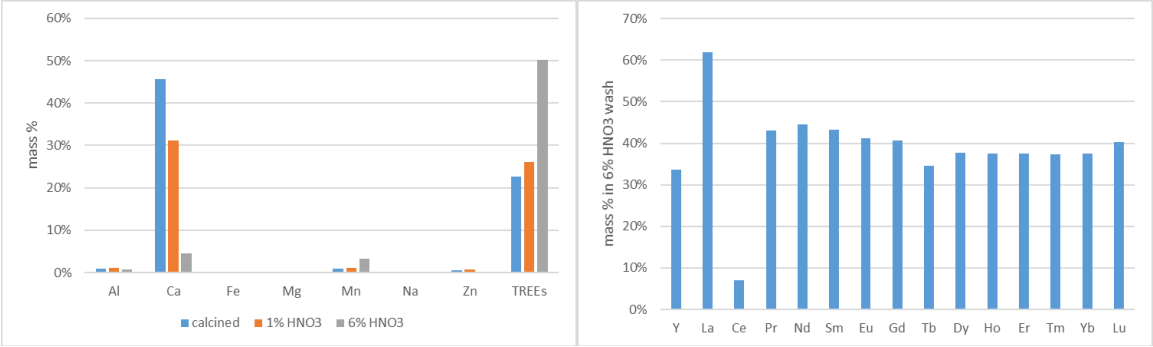

Figure 40. Results of washing the calcined solid. Left: mass% of major metals and total REEs in the respective solids. Right: mass% of the individual rare earth elements dissolved in the 6% HNO_3 wash.

Subtask 4.4. End-to-End System Evaluation, Pilot Tests

Overview

The final product generated through the Task 2.0 procedure was processed through the WVU REE-ALSX bench-scale plant. The plant was operated for seventy-one hours and the final product was separated into two different aliquots. These two aliquots resulted in 4.82 and 4.36 grams (after sampling and analytical losses) of a MREO product that assayed at 85% and 72% TREE on a metal basis. This evaluation was successful at demonstrating the technology and indicated that further testing is required to increase overall process efficiency.

Approach

The final solvent extraction test series will be conducted in the REE-ALSX bench-scale facility located in the NRCCE High Bay at West Virginia University. This test will include a long production run (20 - 40 operating hours) using the optimal flowsheet and feedstock selected from the prior tasks. This production run will be designed to produce several grams of high purity REE oxide, thus validating the technical approach and substantially raising the TRL of the end-to-end technology. Any technical or logistical concerns that arise during testing will be noted and described in the final technology development report.

Results and Discussion

In all, the ALSX plant was operated for over seventy-one hours to generate a concentrated MREO product. This continuous testing was split into two different runs in an attempt to create a product more concentrated in HREEs. This was accomplished; however, the overall grade of the product was lower than 90% on an oxide basis.

Acid Leaching

In all, 15.85 kg (dwb) of the MPP was processed in the acid leaching circuit of the ALSX plant. The results from this leaching process is shown in Table 26. These results indicate there is a significant reduction of Fe transferred from the MPP to the PLS. Similar reductions in Fe were previously observed in the leaching circuit when using certain AMDp feedstocks. This rejection of Fe is essential to successful processing in the solvent extraction circuit as past experimental data has shown that Fe contributes to third phase formation in the SX circuit.

Table 26. Leaching circuit mass balance.

Sample ID	191010 OM SUPER SL		191010 OM PLS Super			191010 OM SUPER FC		
Leaching Mass Balance:								
	Sludge Assay	**Sludge Mass**	**PLS Assay**	**PLS Mass**	**Unit PLS Recovery**	**Filter Cake Assay**	**Filter Cake Mass**	***Mass Balance***
Major Ions	(mg/kg)	(g)	(mg/L)	(g)	(%)	(mg/kg)	(g)	*(g)*
Al	120,742.38	1,913.39	5,305.80	853.70	45%	46,399.34	570.0	***489.69***
Ca	28,897.76	457.94	1,541.87	248.09	54%	5,687.95	69.9	***139.98***
Co	991.73	15.72	50.10	8.06	51%	195.32	2.4	***5.25***
Fe	37,434.89	593.23	23.82	3.83	1%	63,624.99	781.6	***-192.21***
Mg	5,490.40	87.01	292.70	47.10	54%	1,031.00	12.7	***27.24***
Mn	3,334.25	52.84	132.61	21.34	40%	1,112.81	13.7	***17.83***
Si	73,965.97	1,172.13	81.83	13.17	1%	1,278.78	15.7	***1,143.26***
Cl	14.08	0.22	13.53	2.18	976%	6.85	0.1	***-2.04***
TMM	**270,857.38**	**4,292.25**	**7,428.74**	**1,195.28**	**28%**	**119,330.19**	**1,465.93**	***1,631.04***
Rare Earth Elements	(mg/kg)	(g)	(µg/L)	(g)	(%)	(mg/kg)	(g)	*(g)*
Sc	44.22	0.70	1,009.45	0.16	23%	50.74	0.62	***-0.09***
Y	475.14	7.53	27,865.24	4.48	60%	82.14	1.01	***2.04***
La	109.61	1.74	6,479.72	1.04	60%	19.46	0.24	***0.46***
Ce	316.42	5.01	17,588.00	2.83	56%	61.80	0.76	***1.43***
Pr	46.54	0.74	2,824.91	0.45	62%	8.40	0.10	***0.18***
Nd	224.21	3.55	13,765.13	2.21	62%	40.21	0.49	***0.84***
Sm	59.29	0.94	3,653.41	0.59	63%	10.87	0.13	***0.22***
Eu	15.43	0.24	1,004.99	0.16	66%	2.87	0.04	***0.05***
Gd	97.81	1.55	6,168.75	0.99	64%	17.83	0.22	***0.34***
Tb	17.88	0.28	1,060.87	0.17	60%	3.07	0.04	***0.07***
Dy	99.26	1.57	6,213.82	1.00	64%	17.76	0.22	***0.35***
Ho	20.61	0.33	1,248.07	0.20	61%	3.58	0.04	***0.08***
Er	52.23	0.83	3,284.11	0.53	64%	9.42	0.12	***0.18***
Tm	7.00	0.11	432.57	0.07	63%	1.21	0.01	***0.03***
Yb	36.66	0.58	2,274.61	0.37	63%	6.72	0.08	***0.13***
Lu	5.61	0.09	349.50	0.06	63%	1.00	0.01	***0.02***
TREE	**1,627.91**	**25.80**	**95,223.16**	**15.32**	**59%**	**337.1**	**4.14**	***6.33***
HREE	856.42	13.57	49,906.99	8.03	59%	193.5	2.38	***3.16***
LREE	771.49	12.23	45,316.16	7.29	60%	143.6	1.76	***3.17***

Leaching recovery for the REEs in the leaching circuit exceeded sixty percent. As with other projects, these calculations can only be considered estimates as the mass balance is difficult to obtain when using solid samples. It was shown that small variations in moisture calculations can have a significant impact on the overall recovery of the leaching circuit.

Figure 41 shows the individual distributions elemental if the MPP feedstock, PLS, and filter cake resulting from the acid leaching process. This figure highlights the significant rejection of Fe during the leaching process. Additionally, the REEs transferred into the aqueous phase in a manner consistent with the distribution in the MPP, with the exception of Sc. Again, this behavior is consistent with research using other AMD precipitates.

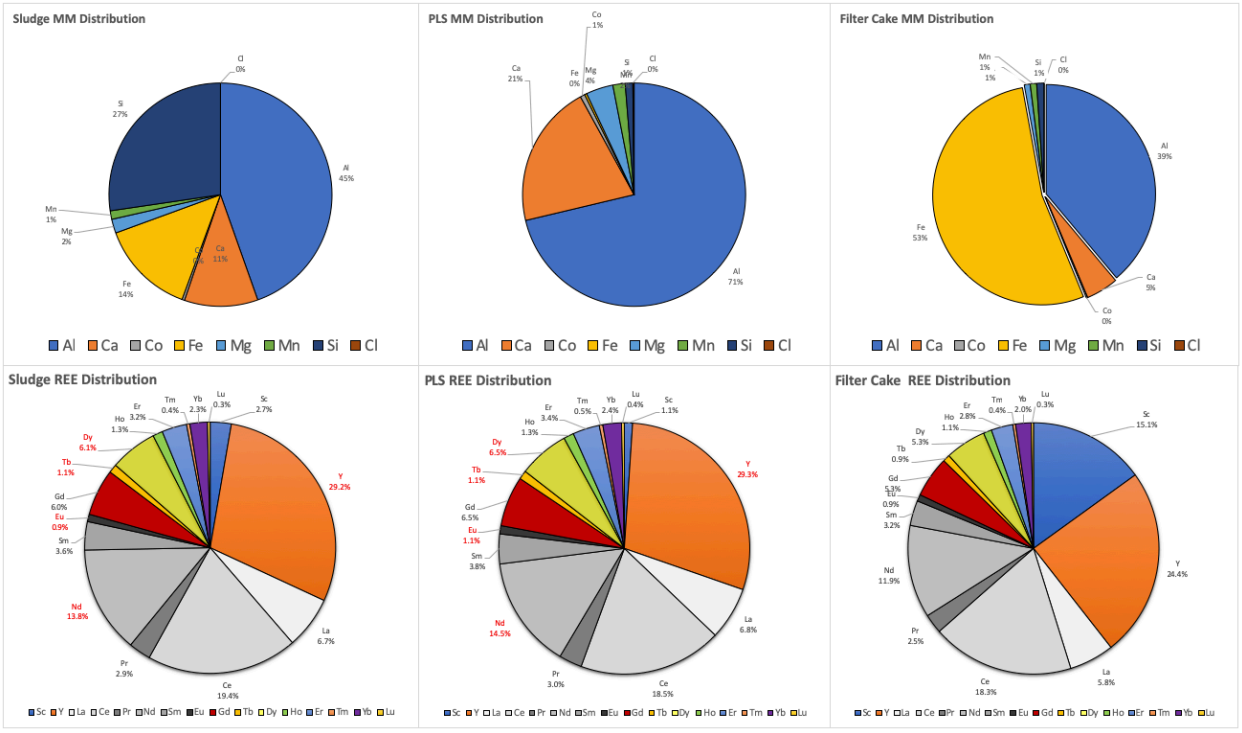

Figure 41. Individual elemental distributions for the sludge, PLS, and filter cake.

SX Results

Overall, results from the SX testing demonstrated the technology was capable of producing a high grade REE product. Table 27 shows the grade of the two products after processing in the ALSX system. The two products vary greatly in regard to the distribution of REEs. As shown, Sample 2972 contains a much higher distribution of LREEs verses Sample 2879. This difference demonstrates the ability of solvent extraction to target groups of or even elemental REEs.

Table 27. Comparison of REE products generated with the ALSX plant.

Sample 2972						Sample 2879					
Analyte	Acid-Wash Product Assay	Acid-Wash Product Mass	Oxide Ratio	Oxide Based Assay	Oxide Product Mass	Analyte	Acid-Wash Product Assay	Acid-Wash Product Mass	Oxide Ratio	Oxide Based Assay	Oxide Product Mass
Mass (g)	4.82					**Mass (g)**	4.36				
Major Ions	(mg/kg)	(g)		(mg/kg)	(g)	**Major Ion**	(mg/kg)	(g)		(mg/kg)	(g)
Al	9,585.16	0.05	0.53	18,105.30	0.09	**Al**	12,818.98	0.06	0.53	24,213.63	0.11
Ca	8,152.81	0.04	0.71	11,413.94	0.06	**Ca**	3,874.37	0.02	0.71	5,424.11	0.02
Co	1.27	0.00	0.79	1.62	0.00	**Co**	0.00	0.00	0.79	0.00	0.00
Fe	947.43	0.00	0.70	1,353.47	0.01	**Fe**	130.82	0.00	0.70	186.88	0.00
Mg	0.00	0.00	0.60	0.00	0.00	**Mg**	0.03	0.00	0.60	0.05	0.00
Mn	128.01	0.00	0.77	165.25	0.00	**Mn**	78.59	0.00	0.77	101.45	0.00
Ni	137.40	0.00	0.79	174.85	0.00	**Ni**	83.68	0.00	0.79	106.49	0.00
Si	2,823.84	0.01	0.47	6,051.09	0.03	**Si**	807.94	0.00	0.47	1,731.30	0.01
S	330.16	0.00	0.33	990.48	0.00	**S**	424.87	0.00	0.33	1,274.61	0.01
Zn	238.30	0.00	0.80	296.61	0.00	**Zn**	119.17	0.00	0.80	148.33	0.00
REEs	(mg/kg)	(g)			(g)	**REEs**	(mg/kg)	(g)			(g)
Sc	-	-	0.65	-	-	**Sc**	0.02	0.00	0.65	0.02	0.00
Y	127,249.23	0.61	0.87	145,508.12	0.70	**Y**	158,919.03	0.69	0.87	181,722.19	0.79
La	55,370.66	0.27	0.85	64,937.26	0.31	**La**	36,874.63	0.16	0.85	43,245.60	0.19
Ce	331,431.78	1.60	0.81	407,122.73	1.96	**Ce**	163,498.58	0.71	0.81	200,837.67	0.88
Pr	32,713.81	0.16	0.83	39,523.86	0.19	**Pr**	28,512.66	0.12	0.83	34,448.15	0.15
Nd	145,846.80	0.70	0.86	170,114.16	0.82	**Nd**	138,937.19	0.61	0.86	162,054.86	0.71
Sm	38,603.60	0.19	0.86	44,765.39	0.22	**Sm**	43,212.33	0.19	0.86	50,109.74	0.22
Eu	9,311.95	0.04	0.86	10,782.45	0.05	**Eu**	10,842.54	0.05	0.86	12,554.74	0.05
Gd	55,236.40	0.27	0.87	63,666.75	0.31	**Gd**	66,384.19	0.29	0.87	76,515.96	0.33
Tb	6,529.31	0.03	0.85	7,679.63	0.04	**Tb**	8,424.56	0.04	0.85	9,908.78	0.04
Dy	28,392.87	0.14	0.87	32,586.28	0.16	**Dy**	37,848.77	0.17	0.87	43,438.74	0.19
Ho	4,757.76	0.02	0.87	5,450.09	0.03	**Ho**	6,517.59	0.03	0.87	7,466.00	0.03
Er	10,749.79	0.05	0.87	12,292.27	0.06	**Er**	14,533.24	0.06	0.87	16,618.60	0.07
Tm	1,087.80	0.01	0.88	1,242.34	0.01	**Tm**	1,483.12	0.01	0.88	1,693.83	0.01
Yb	4,774.08	0.02	0.88	5,436.23	0.03	**Yb**	5,960.65	0.03	0.88	6,787.37	0.03
Lu	563.71	0.00	0.88	641.03	0.00	**Lu**	700.78	0.00	0.88	796.91	0.00
Actinides	(mg/kg)	(g)			(g)	**Actinides**	(mg/kg)	(g)			(g)
Th	53.45	0.00	0.94	57.13	0.00	**Th**	53.45	0.00	0.94	57.13	0.00
U	39.80	0.00	0.91	43.81	0.00	**U**	39.80	0.00	0.91	43.81	0.00
Summary	mg/kg	(%)		mg/kg	(%)	**Summary**	mg/kg	(%)		mg/kg	(%)
TMM	22,344	2%		38,553	4%	TMM	18,338	2%		33,187	3%
TREE	852,620	85%		1,011,749	101%	TREE	722,650	72%		848,199	85%
TACT	93	0%		101	0%	TACT	93	0%		101	0%
Total Ions	**875,057**	**88%**		**1,050,402**	**105%**	**Total Ions**	**741,082**	**74%**		**881,487**	**88%**
REE Distibution						**REE Distibution**					
TREE	852,620	85%		1,011,749	101%	TREE	722,650	72%		848,199	85%
LREE	613,279	72%		737,246	73%	LREE	421,878	58%		503,251	59%
HREE	239,341	28%		274,503	27%	HREE	300,772	42%		344,948	41%
CREE	317,330	37%		366,671	36%	CREE	354,972	49%		409,679	48%
Residual						**Residual**					
Unaccounted Ions	**124,943**	**12%**		**(50,402)**	**-5%**	**Unaccount**	**258,918**	**26%**		**118,513**	**12%**

Sample 2972 meets the overall project objective of producing a MREO product exceeding 90% purity. While Sample 2879 falls short of the 90% goal (88%) is does contain a considerably higher distribution of CREE and HREEs. Additionally, gangue elements between the two sample vary considerably. Sample 2972 is predominantly contaminated with Al and Ca, while Sample 2879 contains predominantly Al. These differences in both major metal and REE distributions demonstrates the critical need for additional and larger scale research on elemental separations.

One primary concern resulting from this research is the ability to separate individual REEs. Currently, no market exists for MREO products and elemental separations are essential to advancing this technology in order to produce a salable product. Currently, the objective of creating a MREO product is profound and has successfully demonstrated that AMD is a viable resource for REEs; however, relatively few markets exist for this material.

Furthermore, the lack of downstream processing facilities located in the United States for processing a MREO is nonexistent. The only REE mine located in the United States, Mountain Pass, currently transports concentrate to China for beneficiation. This demonstrates the need for further research and development of REE technologies in order to obtain a reliable and domestic supply of these critical elements.

Task Completion Status

100% complete.

Task 5.0 – Feedstock Suitability and Availability: Untreated AMD versus. Treated AMD Sludge

Overview

AMD is a significant water quality impairment observed in the Appalachian region and is typically the result of coal mining in the region. This research seeks to validate the use of AMD as a potential resource for REEs. During the research, both acidic and net alkaline AMD flows were evaluated. The results from this work showed that the net alkaline AMD was not a viable feedstock and therefore it was not able to produce an enriched REE product due to low concentrations of REEs coupled with the use of liquid supported membranes. Alternatively, the acidic AMD flows were viable and resulted in the production of a MREO product that exceeds 90% purity.

Approach

Evaluate the results of Tasks 2, 3, and 4 to determine the effect of feedstock AMD chemistry on results from the Case A, Case B extraction strategies and then the effect on performance in the ALSX facility. This effort will form the nexus of results from Tasks 2, 3, and 4 and monthly meetings will be held to evaluate results. This will facilitate:

a) Standardization of the Case A extraction strategy;
b) Standardization of the Case B extraction strategy;
c) Optimization of operating conditions in the ALSX facility; and
d) Determination of input parameters for Task 6.0, the Techno-economic analysis.

Results and Discussion

In the Appalachian Coal Basin, AMD constitutes one of the most significant and widespread water quality challenges. AMD occurs when pyrite-bearing mine spoil oxidizes after mining. It consists of acidity, a varied suite of metals such as iron, aluminum, and manganese as well as the dominant anion, sulfate. Mining exposes these sulfide minerals to weathering, and the increased mineral surface area then leads to elevated oxidation and leaching, resulting in AMD formation.

Each coal mine has unique geochemical features even among those that are in relatively close geographic proximity and coal seam. Furthermore, the elevation of the mine works, whether above or below drainage, also has a clear effect on the quantity of REEs in the aqueous AMD discharging from the mine.

The feedstock for Task A is net-acidic AMD which typically originates in surface mines, above-drainage underground mines, and refuse piles. The water chemistry of these AMD outflows differs significantly from below-drainage mines. Typically, the pH of AMD discharged from these mines is lower since the oxidizing conditions that produce acidic AMD are present. Table 28 shows the ICP-MS and ICP-OES results for five different feedstocks evaluated using the Case A process.

Table 28. ICP-MS & ICP-OES results for five AMD feedstocks

Site	AQ-2	AQ-8	AQ-50	AQ-51-5	AQ-3
Major Ions (mg/L)					
Al	68.57	72.23	36.74	28.58	27.17
Ca	90.17	208.59	128.64	53.73	160.82
Cd	0.01	0.01	0.02	0.00	0.00
Co	0.25	0.89	1.09	0.25	0.13
Cr	0.04	0.01	0.01	0.00	0.01
Cu	0.31	0.04	0.11	0.01	0.13
Fe	95.53	34.54	260.93	2.71	27.08
Mg	29.98	129.80	76.56	40.80	33.86
Mn	1.17	44.47	36.23	15.06	1.25
Ni	0.57	1.06	0.96	0.33	0.25
Zn	1.73	3.48	3.10	0.70	0.69
REEs (ug/L)					
Sc	37.64	6.64	4.30	4.32	3.61
Y	75.54	388.44	355.00	96.37	36.03
La	1.60	91.94	136.42	29.40	8.46
Ce	43.28	260.80	293.07	77.69	27.52
Pr	7.10	40.60	36.51	10.81	4.66
Nd	35.60	204.55	158.70	49.82	23.86
Sm	10.87	61.38	37.35	14.48	6.96
Eu	2.78	17.35	10.50	4.05	1.73
Gd	16.29	96.27	58.63	21.45	9.24
Tb	2.80	14.64	9.62	3.29	1.41
Dy	18.07	80.38	57.24	18.39	8.11
Ho	3.38	14.56	11.53	3.42	1.52
Er	9.76	38.24	31.33	9.23	4.07
Tm	1.29	4.98	4.06	1.22	0.55
Yb	7.47	28.67	23.74	7.24	3.12
Lu	1.08	4.29	3.39	1.02	0.44
Totals					
pH	**2.68**	**3.10**	**2.80**	**3.10**	**2.80**
TREE	274.52	1,353.72	1,231.40	352.18	141.29
HREE	173.31	677.10	558.84	165.93	68.09
LREE	101.22	676.62	672.56	186.25	73.20
CREE	148.28	786.99	640.08	190.07	78.97

The TREE concentration of the acidic AMD is typically higher (by one to two orders of magnitude) than net-alkaline AMD. Additionally, the different feedstocks used in this case possess varying qualities as shown in Figure 42. For example, AQ-8 and AQ-50 have a considerably higher TREE value than the other AMD sites. Likewise, AQ-51-5 has a much lower Fe content than the other feedstocks, while AQ-8 has a significantly higher Mg content. Because of this variation, the Case A procedure allowed for the testing of the overall robustness of the method, despite the incoming AMD quality.

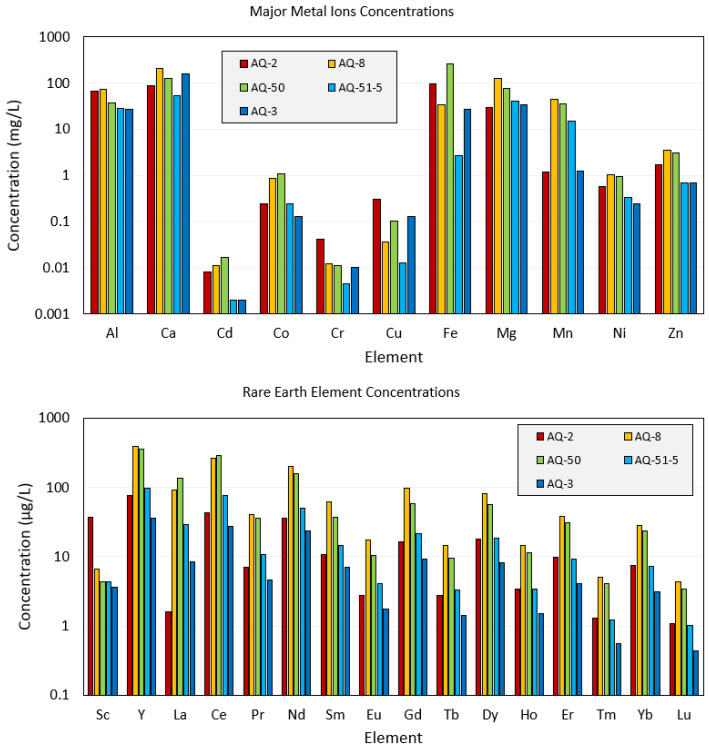

Figure 42. Concentration profiles of five different AMD feedstocks.

Estimates of Resource

The results from previous sampling campaigns are analogous to an initial prospecting survey and may be used to approximate the overall regional production at a high level. Unfortunately, comprehensive AMD flowrate datasets are practically nonexistent due to the complexity of flow interactions, large seasonal variations, and the temporal nature of the effluent constituents. As a result, multiple AMD outfall datasets were compiled to estimate the regional AMD flow rate estimate by the researchers. These data are comprised of projects completed by the West Virginia Water Research Institute (WVWRI), Pennsylvania Department of Environmental Protection Abandoned Mine Land Department, West Virginia Department of Environmental Protection (WVDEP), and various studies from others [1–3].

In all, this regional estimate compasses over 1,100 unique AMD outlets, predominately in the Northern Appalachia (NAPP) region, and indicated that the regional AMD flow rate is approximately 94,700 L/sec. Consequently, this estimate may be considered conservative in relation to the actual flow rate. Previously, Stewart et al provided a regional flow estimate of 417,448 L/sec [4]. By comparison, the methods used by Stewart could lead to overestimation of the true quantity of AMD due to the incorrect assumption that all coal mining leads to the generation of AMD and neglecting the spatial reduction of multi-seam extraction, which is common in Central Appalachia (CAPP).

Given these complexities, an accurate and precise determination of AMD flowrate for the Appalachian basin would require a more extensive study well beyond the scope of this research. Nevertheless, for the current study, both Stewart's methodology and the authors' methodology were used to estimate the high and low AMD flow rate values, respectively. In addition, the REE content of this AMD was assumed to be the average for the NAPP values shown in Table 29. Given these inputs, the estimated REE production from AMD was determined to be between 771 to 3,400 tonnes of REEs per year. The high variance in the two estimated production rates indicates that further exploration of the resource is required to identify an economically feasible process to extract REEs from AMD.

Table 29. Estimate of REE resources in Central and Northern Appalachian coal basins.

Regional AMD Flow Estimate	Units	Low[1]	High[2]
PA	(L/s)	51,401	-
WV	(L/s)	24,095	-
OH	(L/s)	18,900	-
MD	(L/s)	317	-
TOTAL	(L/s)	**94,712**	**417,448**
TREE Concentration (mg/L)	(mg/L)	0.258	0.258
TREE Load	(tonne/yr)	771	3,400

1 Regional flow estimates based on proprietary AMD studies

2 Regional flow estimate by Stewart et.al. [17]

Laboratory Testing Results

Traditional AMD treatment consists of alkaline addition to force precipitation of metals ions from the affected water. As the pH is raised, the AMD precipitate (AMDp) is either collected in storage ponds (for later disposal) or injected into old underground mine works. Currently, AMD treatment methods are not selective, with the sole objective of removing the deleterious metals to meet a predefined set of effluent limits. The Case A strategy seeks to isolate certain gangue elements as well as the REEs within this process by implementing multiple pH setpoints.

Under these circumstances, AMD waters were collected and subjected to a series of incremental pH adjustments. Initial testing indicated that pH setpoints at values of 4, 5 and 8 isolated the Fe, Al, and REEs respectively. Next, a three-step precipitation procedure was developed that would isolate the solid and liquid components at each pH setpoint.

Selective precipitation was performed on 75 liters of AMD from each feedstock during each experiment. The pH was raised using $Ca(OH)_2$ to the predefined setpoint. Once equilibrium was obtained at the pH value, the precipitate was separated from the aqueous phase by vacuum filtration. The supernatant was then adjusted to the next pH setpoint. Table 30 shows the results of the AMDp acquired at the last stage of the precipitation testing for all five feedstocks.

Table 30. Analysis of pH 8 precipitate for each feedstock

Analyte	Units	AQ-2	AQ-8	AQ-50	AQ-51-5	AQ-3
Sc	*(mg/kg)*	176	7	8	20	23
Y	*(mg/kg)*	5,981	7,836	5,511	2,972	4,634
La	*(mg/kg)*	321	1,852	1,923	1,051	1,014
Ce	*(mg/kg)*	2,026	5,005	4,507	2,394	4,173
Pr	*(mg/kg)*	412	892	581	362	701
Nd	*(mg/kg)*	2,220	4,298	2,530	1,687	3,354
Sm	*(mg/kg)*	881	1,289	566	454	953
Eu	*(mg/kg)*	240	362	163	142	233
Gd	*(mg/kg)*	1,363	2,004	937	663	1,253
Tb	*(mg/kg)*	258	293	147	111	181
Dy	*(mg/kg)*	1,663	1,519	854	547	969
Ho	*(mg/kg)*	310	269	166	114	185
Er	*(mg/kg)*	897	667	439	267	469
Tm	*(mg/kg)*	122	81	53	39	53
Yb	*(mg/kg)*	685	419	283	218	275
Lu	*(mg/kg)*	101	62	42	33	40
TREE	*(mg/kg)*	17,656	26,855	18,709	11,075	18,512
Grade	*(%)*	1.77%	2.69%	1.87%	1.11%	1.85%

All feedstocks produced an enriched AMDp product that contains significantly higher REE concentration than the AMDp generated through traditional AMD treatment, typically by two orders of magnitude. Additionally, the grade of the AMDp collected in this experiment was independent of the initial AMD REE concentration. For example, AQ-3 had the lowest aqueous REE concentration (141 µg/L); however, the grade of the AMDp was comparable to that of aqueous feedstocks with higher REE concentrations. This indicates that the process may be applied to AMD outflows with both high and low REE concentrations while achieving similar grades of product.

Moreover, the distribution of REEs in the AMDp product is also relatively consistent among the feedstocks. One variation is in the AQ-2 product that was slightly elevated in the HREEs. This variation may be attributed to the higher percentage (63%) of HREEs in the AQ-2 raw water when compared to HREE percentage of the other feedstocks (~50%). The distribution of REEs in each feedstock is shown in Figure 43.

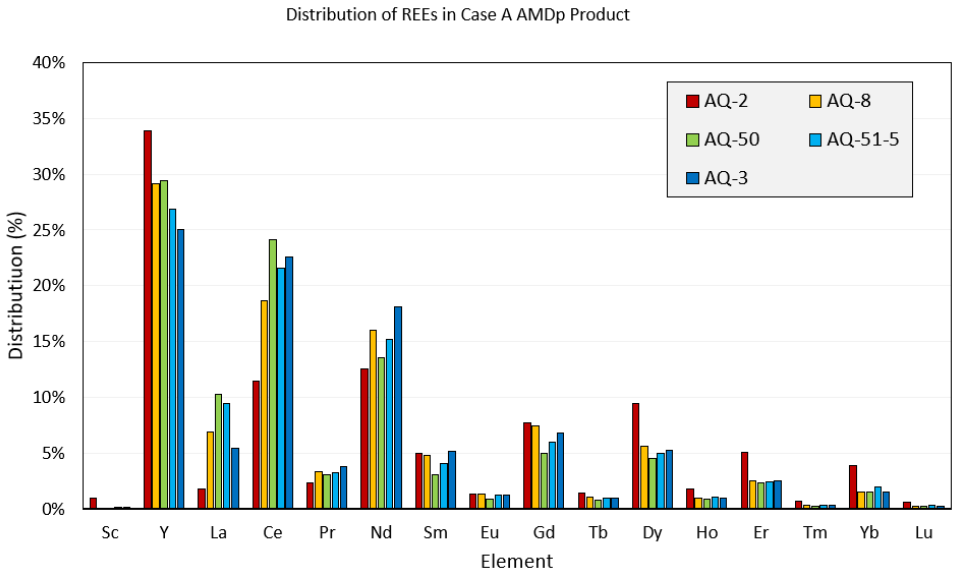

Figure 43. Distribution of REE in AMDp products after staged precipitation.

Generation of these 1 – 2% precipitates is significant, as this product will provide a higher-grade feed with less gangue metals that can be upgraded using solvent extraction. Unfortunately, very large quantities of raw AMD are required to generate a quantity of AMDp that is sufficient to process through an SX system.

Overall, efforts by the members of the research teams showed that a solid pre-concentrate, nominally 0.1 to 2% REE, can be readily produced from AMD; however, that pre-concentration process cannot provide the further enrichment needed to generate high purity oxides suitable for downstream markets. To meet these objectives, solvent extraction was investigated as a secondary process used to further enrich the low-grade pre-concentrate to a purity exceeding 90%. Initially, laboratory-scale batch solvent extraction tests were performed on synthetic REE solutions to determine the influence of various process parameters (e.g. pH, extractant dosage, diluent type, and feedstock concentration). Next, the separation of REEs from major AMD gangue elements was investigated using synthetic leachate solutions with concentrations similar to those expected from the pre-concentrate samples. This process showed that the grade targets could easily be met when combining optimal parameters from each step. From this work with synthetic solutions, an optimal SX process was developed and validated using a real leachate generated from a pre-concentrate sample. By integrating leachate preparation, solvent extraction, scrubbing, stripping, and precipitation, an oxide containing 90.5% rare earth oxides was generated.

Finally, to validate these results, the solid AMD pre-concentrate generated using the two-step precipitation process was fed into a bench-scale solvent extraction plant. Results of this testing demonstrated that a high purity MREO product exceeding 90% was obtainable. Furthermore, operation of the plant previously indicated that acid consumption is a primary driver in achieving a favorable economic outcome. Therefore, this factor was established as a key parameter for developing the techno-economic analysis. Also, a previous TEA from DE-FE0026444 indicated that haulage cost of low-grade and high moisture content AMD precipitates was also a key driver in the economic success of a ALSX facility that relied on a hub-and-spoke operating principle. The results from Task 2.0 show that a higher-grade AMD precipitate can be obtained. When coupled with other novel dewatering solutions, the potential exists to greatly reduce costs shown in the previous TEA.

Task Completion Status
100% complete.

Task 6.0 – Techno-Economic Analysis: Untreated AMD versus Treated AMD Sludge

Overview
In this task, a techno-economic analysis was used to compare two potential REE production scenarios: one which utilizes raw sludge produced using traditional AMD treatment methods and a second which utilizes REE pre-concentrate produced using the technology developed in this project. The methodology utilized in this study incorporated power law scaling function for capital cost estimation and itemized operating costs estimates for consumables, power, and labor. Other overhead and miscellaneous costs were estimated using standard chemical engineering costing criteria. The economic model was constrained by numerous financial and operational assumption as prescribed in the NETL document *Guidance for Development of Techno-Economic Analyses for DOE/NETL's Feasibility of Recovering Rare Earth Elements Program*[2]. Results from this analysis include comparative economic indicators for both processing methods as well as sensitivity analyses for the pre-concentrate approach developed in this project. Overall, this assessment largely confirms the economic and financial benefit of pre-concentration. The results show that this approach is the enabling technology for a distributed REE production network that has notable logistic, social, and environmental benefits.

Approach
Experimental results from the various testing campaigns were integrated into a techno-economic analysis (TEA). The analysis reports costs and performance at the existing scale and project those costs to the next design scale and/or a commercial implementation using standard scaling factors and itemized costs as appropriate. All analyses use guidelines and assumptions provided by NETL. As indicated, this analysis includes: a clear statement of the assumptions; cash forecasts on an annual basis; a discussion of potential NPV and IRR; a summary of the tax structure imposed; and a sensitivity analysis with respect to grade, price, and other significant input factors.

Results from this analysis are compared to similar TEA modeling conducted for treated AMD sludge under other DOE projects. The results are compiled to generate an optimal global REE supply chain that potentially includes both AMD and sludge-based resources.

Results and Discussion
The REE resource at individual AMD treatment sites and individual AMD sludge ponds tends to quite limited. Results from a prior regional survey (DE-FE0026444; Vass et al., 2019a, 2019b) showed that the REE flux from an average AMD outfall is only 400 kg/year, while the average sludge pond contains less than 10,000 kg REE in total. Neither of these values are large enough to justify a commercial-scale REE concentration and refining plant at a single AMD treatment site. However, one alternative option is to integrate a disperse network of on-site handling operations that feed a centralized acid leaching-solvent extraction (ALSX) system. The economic viability of this approach has been repeatedly demonstrated in our prior DOE projects. For example, a feasibility study, conducted as a part of DE-FE0026927, showed that a 2,100 TPD ALSX facility processing raw AMD sludge has the potential to produce an IRR of 37 % and a net present value of $80 million over a 20-year operating period. The total capital cost for this plant is $46 million and the operating cost is $141/kg.

While this result is promising, a detailed techno-economic analysis showed that these favorable results are very sensitive to the sludge acid consumption and the sludge feed moisture. For example, Figure 44a

[2] Available: < https://netl.doe.gov/sites/default/files/netl-file/Rare-Earth-Element-TEA-Guidance.pdf >

shows the maximum possible acid dose required to keep the total acid cost below an economic threshold of $100/kg as a function of REE feed grade and leaching recovery. As shown, raw sludge (~0.6% REE, ~75% recovery) can only be processed in a cost-effective manner if the maximum acid dose is on the order of 100 to 150 kg/t. Figure 44b shows a similar analysis whereby the maximum haulage distance needed to keep the total shipping cost below 5% of the feedstock contained value (CV) has been determined as a function of feed grade and feed moisture. For raw sludge (0.6% REE, 50-80% moisture), the maximum haulage distance is nearly negligible—less than 10-15 miles.

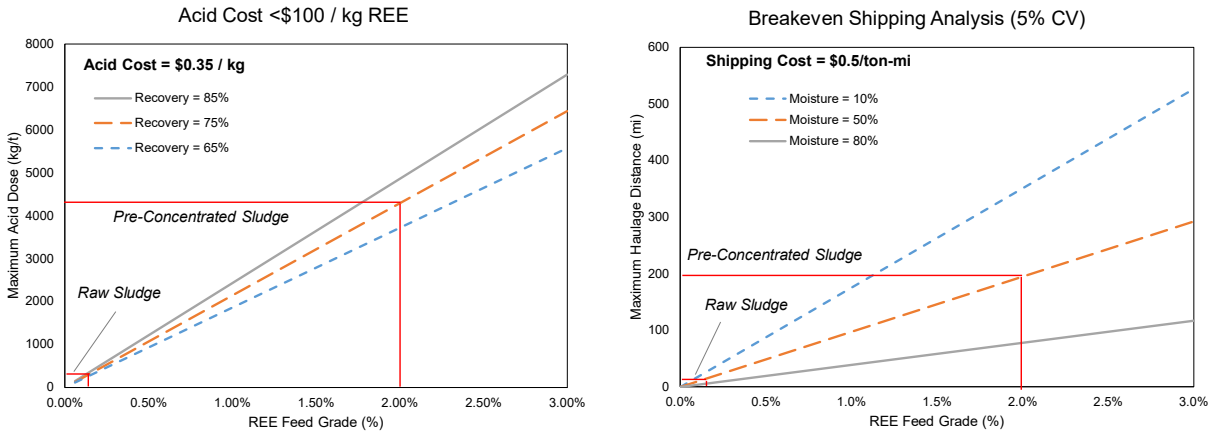

Figure 44. Sensitivity analyses showing maximum acid dose as a function of sludge feed grade and leaching recovery (left, a) and breakeven shipping distance as a function of feed grade and moisture (right, b).

Unfortunately, traditional compliance-based treatment of AMD tends to push both the sludge acid consumption and the sludge moisture to unfavorable values. Many AMD treatment operators tend to overdose lime addition to avoid non-compliant discharges. This practice leaves large quantities of unreacted lime in the final precipitate, and this base must be fully consumed during the acid leaching step of our process at a significant cost to the REE producer. Moreover, traditional sludge drying cells are ineffective at reducing sludge moisture, and many of the sludge samples evaluated in our prior studies have values exceeding 80-90%. Both of these issues are problematic for commercialization as they reduce the number of viable sludge sites that meet thresholds for economic viability. Sludge samples that do not meet the economic thresholds are considered *stranded resources* and are not considered relevant to a regional production scenario. When taken together these results indicate that the hypothetical 2,100 TPD ALSX plant described above may have difficulty identifying a sufficient quantity of raw sludge feedstock that meet these criteria. A reduction in total plant throughout will inevitably lead to a proportional reduction in economic outcomes.

The upstream concentration process developed in this project offers a comprehensive solution to both issues. Most significantly, the upstream concentrator will increase the grade of the ALSX feed by rejecting iron and aluminum during the standard water treatment process. Figure 44a and Figure 44b show the drastic influence that the increased feedstock grade will have on maximum acid dose (>4,000 kg/t) and maximum haulage distance (increased to >200 miles). In addition to the simple grade increase, the upstream concentrator will provide better pH control technology to mitigate the acid consumption issues associated with overdosed lime addition; moreover, the use of geotubes or other advanced passive dewatering technologies will assist in reducing product moisture. All of these factors will substantially reduce processing costs, while simultaneously increasing the quantity of feedstock meeting the economic thresholds. If widely implemented across the Appalachian region, the pre-concentration

plants will ensure consistent and reliable supply of feedstock for ALSX operations.

To investigate the economic viability of processing pre-concentrates of the upstream concentration through ALSX, a techno-economic analysis (TEA) spreadsheet models was produced and utilized in this project. The TEA has used standard economic guidelines provided by NETL and incorporates the most recent process knowledge developed in this project. Since the upstream concentrator can be easily integrated into existing AMD treatment technologies, the capital and operating cost for this process are assumed to be external to the REE producing entity and are not included in the analysis; however, an additional $50/t feedstock acquisition cost is included to account for any additional reagent addition, capitalization expenses, or handling needed to deliver the pre-concentrate to the ALSX plant. The results of this analysis are shown in Table 31 for a nominal 175 TPD plant.

The results confirm the economic gains inherent to the upstream concentration prior to ALSX. Compared to the prior scenario, which treated raw sludge, the current model output shows that a similar NPV ($80 million) can be achieved at a much smaller overall plant size (175 TPD vs. 2,100 TPD). The smaller plant also entails a much lower capital cost and a lower operating cost, $20 million and $54/kg REE respectively. While both scenarios have been shown to be economically favorable, the pre-concentrated route is much more viable from a commercial perspective, owing to the smaller feedstock requirement and reduced capital cost. Both of these items reduce overall project risk and are thus more favorable for investment. In addition, Figure 45 shows a sensitivity analysis of operating cost with respect to both feed grade and plant size. As shown, for most plant sizes, the largest incremental reduction in operating cost is achieved.

Table 31. Economic Indicators for Commercial ALSX System

Economic Parameter	Value
Plant Feed Rate/Grade	175 TPD @ 2% REE
Product Rate/Grade	2 TPD @ 90% MREO
Operating Period	20 years; 10% discount rate
REE Basket Price	$147 /kg
REE Recovery	59%
Plant CAPEX	$20 Million
Plant OPEX	$54 / kg
NPV	$80 Million
IRR	61%
Payback period	1.5 operating years

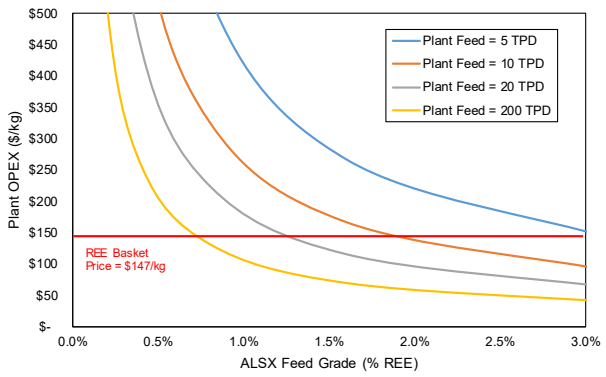

Figure 45. Sensitivity analysis showing ALSX operating cost as a function of plant size and feed grade.

Other matters pertaining to commercialization include permitting and regulatory factors, downstream refining capacity, and REE pricing factors. With regard to permitting, the proposed approach is preferred to greenfield REE production scenarios, as the initial pre-concentration and the ALSX will take place on permitted sites. Wastes from these processes can be easily integrated into the existing infrastructure without the need for new permits. This outcome is also desirable for commercialization, as it will minimize the startup time needed to initiate new projects. With regard to refining capacity, the US currently has no domestic facilities that can produced refined REE products from mixed REOs. Nevertheless, data collected under Task 4 of this study has shown a potential pathway to producing individual target REEs using selective stripping in SX. With regard to pricing, all of the economic results in Table 31 have been determined using a price discount of 50% relative to the standard oxide prices provided by NETL. This price discount accounts for charges from downstream refining and also indicates that the process can still be profitable despite price volatility.

Task Completion Status

100% complete.

References

1. Armarego, Wilfred LF. *Purification of Laboratory Chemicals*. Butterworth-Heinemann, 2017.
2. Chiou, M.-S., & Li, H.-Y. (2002). Equilibrium and kinetic modeling of adsorption of reactive dye on cross-linked chitosan beads. *Journal of Hazardous Materials*, 93(2), 233-248.
3. Dyer, L., Fawell, P. D., Newman, O. M. G., & Richmond, W. R. (2010). Synthesis and characterisation of ferrihydrite/silica co-precipitates. *Journal of Colloid and Interface Science*, 348(1), 65-70.
4. Huang, X.-Y., Bin, J.-P., Bu, H.-T., Jiang, G.-B., & Zeng, M.-H. (2011). Removal of anionic dye eosin Y from aqueous solution using ethylenediamine modified chitosan. *Carbohydrate Polymers*, 84(4), 1350-1356.
5. Ismail, N. A., Aziz, M. A. A., Yunus, M. Y. M., & Hisyam. (2019). A. Selection of Extractant in Rare Earth Solvent Extraction System: A Review. *International Journal of Recent Technology and Engineering* 8(1), 728-743.
6. Josso, P., Roberts, S., Teagle, D. A., Pourret, O., Herrington, R., & de Leon Albarran, C. P. (2018). Extraction and separation of rare earth elements from hydrothermal metalliferous sediments. *Minerals Engineering*, 118, 106-121.
7. Krishnamurthy, N., & Gupta, C. K. (2004). *Extractive Metallurgy of Rare Earths*. CRC Press.
8. Li, X., Wei, C., Deng, Z., Li, M., Li, C., & Fan, G. (2011). Selective solvent extraction of vanadium over iron from a stone coal/black shale acid leach solution by D2EHPA/TBP. *Hydrometallurgy*, 105(3-4), 359-363.
9. Parhi, P., Park, K., Nam, C., & Park, J. (2015). Liquid-liquid extraction and separation of total rare earth (RE) metals from polymetallic manganese nodule leaching solution. *Journal of Rare Earths*, 33(2), 207-213.
10. Sun, H., Zhao, F., Zhang, M., & Li, J. (2012). Behavior of rare earth elements in acid coal mine drainage in Shanxi Province, China. *Environmental Earth Sciences*, 67(1), 205-213.
11. Wang, W., Pranolo, Y., & Cheng, C. Y. (2013). Recovery of scandium from synthetic red mud leach solutions by solvent extraction with D2EHPA. *Separation and Purification Technology*, 108, 96-102.
12. Wilson, A. M., Bailey, P. J., Tasker, P. A., Turkington, J. R., Grant, R. A., & Love, J. B. (2014). Solvent extraction: the coordination chemistry behind extractive metallurgy. *Chemical Society Reviews*, 43(1), 123-134.
13. Vass, C. R., Noble, A., & Ziemkiewicz, P. F. (2019). The Occurrence and Concentration of Rare Earth Elements in Acid Mine Drainage and Treatment By-products: Part 1—Initial Survey of the Northern Appalachian Coal Basin. *Mining, Metallurgy & Exploration*, 36(5), 903-916.
14. Vass, C. R., Noble, A., & Ziemkiewicz, P. F. (2019). The Occurrence and Concentration of Rare Earth Elements in Acid Mine Drainage and Treatment Byproducts. Part 2: Regional Survey of Northern and Central Appalachian Coal Basins. *Mining, Metallurgy & Exploration*, 36(5), 917-929.
15. Xie, F., Zhang, T. A., Dreisinger, D., & Doyle, F. (2014). A critical review on solvent extraction of rare earths from aqueous solutions. *Minerals Engineering*, 56, 10-28.
16. Zhang, J., Zhao, B., & Schreiner, B. (2016). *Separation Hydrometallurgy of Rare Earth Elements*.

Springer.

17. Stewart BW, Capo RC, Hedin BC, Hedin RS. Rare earth element resources in coal mine drainage and treatment precipitates in the Appalachian Basin, USA. Int J Coal Geol 2016;169:28–39. doi:10.1016/j.coal.2016.11.002.

Products

1. Liu, Shushu. (2019). Production of High-Grade Mixed Rare Earth Oxides from Acid Mine Drainage via Solvent Extraction: Laboratory Scale Process Development. M.S. Thesis. Virginia Tech. December 4, 2019.
2. Liu, Shushu and Aaron Noble. (2019). "Parametric Study on Solvent Extraction of Rare Earth Elements form AMD-Based Feedstock." Mineral Processing Division – Student Poster Session: 2019 SME Annual Meeting & Exhibit. Denver, CO. February 27, 2019.
3. Ziemkiewicz, Paul, Chris Vass, Aaron Noble. (2019). "AOI 3: At-source Recovery of Rare Earth Elements from Coal Mine Drainage." 2019 Crosscutting Research & Rare Earth Elements Portfolios Review Meeting. Department of Energy. Pittsburgh, PA. April 9 – 11, 2019.
4. Ziemkiewicz, Paul, Lian-Shin Lin, Harry Finklea, and Aaron Noble. (2018). "At-source Recovery of Rare Earth Elements from Coal Mine Drainage," Poster Presentation, Project Review Meeting for Rare Earth Elements (REE) Program, Pittsburgh, PA, April 10, 2018.

Changes/Problems

N/A

Budgetary Information

SF-425 Federal Financial Report will be submitted by WVU's Sponsored Research Accounting (SRA) Office. All financial reports and official numbers are submitted through this office and will cover federal costs and recipient cost share incurred. Our Cost Plan/Status table can be found below in Table 32. Amounts contained within reflect internal adjustments currently making their way through WVU's financial systems.

Table 32. Cost Plan/Status Table.

Baseline Reporting Quarter	Budget Period 1															
	Q1		Q2		Q3		Q4		Q5		Q6		Q7		Q8	
	1/1/18 - 3/31/18		4/1/18 - 6/30/18		7/1/18 - 9/30/18		10/1/18 -12/31/18		1/1/19 - 3/31/19		4/1/19 - 6/30/19		7/1/19 - 10/31/19		11/1/19 - 11/15/19	
	Q1	Cumulative Total	Q2	Cumulative Total	Q3	Cumulative Total	Q4	Cumulative Total	Q5	Cumulative Total	Q6	Cumulative Total	Q7	Cumulative Total	Q8	Cumulative Total
Baseline Cost Plan																
Federal Share	$64,406	$64,406	$128,812	$193,218	$128,812	$322,030	$128,812	$450,842	$128,812	$579,654	$64,406	$644,060	N/A	$644,060	N/A	$644,060
Non-Federal Share	$0	$0	$0	$0	$0	$0	$0	$0	$205,606	$205,606	$0	$205,606	N/A	$205,606	N/A	$205,606
Total Planned	$64,406	$64,406	$128,812	$193,218	$128,812	$322,030	$128,812	$450,842	$334,418	$785,260	$64,406	$849,666	N/A	$849,666	N/A	$849,666
Actual Incurred Cost																
Federal Share*	$5,011	$5,011	$51,052	$56,064	$88,270	$144,334	$80,372	$224,706	$73,789	$298,495	$102,303	$400,798	$106,301	$507,099	$135,192	$642,291
Non-Federal Share**	$0	$0	$0	$0	$0	$0	$0	$0	$146,585	$146,585	$34,071	$180,656	$300	$180,956	$24,636	$205,591
Total Incurred Costs	$5,011	$5,011	$51,052	$56,064	$88,270	$144,334	$80,372	$224,706	$220,374	$445,080	$136,374	$581,454	$106,600	$688,054	$159,828	$847,883
Variance																
Federal Share	$59,395	$59,395	$77,760	$137,155	$40,542	$177,696	$48,440	$226,136	$55,023	$281,159	-$37,897	$243,262	N/A	$136,961	N/A	$1,769
Non-Federal Share	$0	$0	$0	$0	$0	$0	$0	$0	$59,021	$59,021	-$34,071	$24,950	N/A	$24,650	N/A	$15
Total Variance	$59,395	$59,395	$77,760	$137,155	$40,542	$177,696	$48,440	$226,136	$114,044	$340,180	-$71,968	$268,212	N/A	$161,612	N/A	$1,783

Milestone Status Report

Our Milestone Status Report is contained in Table 33 below.

Table 33. Milestone Status Report Table.

Milestone Title/Description	Verification Method	Planned Completion Date	Actual Completion Date	Percent Completed To date	Comments
Low pH Mine Drainage Extraction Strategy: Net Acid Cost-Effectiveness Assessment	Net-positive economic viability of low pH extraction technology	10/31/18	N/A	100%	Complete.
Net Alkaline Mine Drainage Extraction Strategy: Net Alkaline Cost- Effectiveness Assessment	Net-positive economic viability of alkaline extraction technology	10/31/18	N/A	100%	Complete.
Solvent Extraction of Precipitates: Solvent Extraction, Gangue Removal	Successful gangue removal and REE enrichment precipitate	8/31/19	N/A	100%	Complete.
Solvent Extraction of Precipitates: Real System Evaluation	Production of feedstock for pilot testing	9/30/19	N/A	100%	Complete.
Solvent Extraction of Precipitates: Pilot Tests - End-to-End System Evaluation	Production of high purity REE oxide	10/31/19	N/A	100%	Complete.
Suitability & Feedstock: Untreated AMD vs. Treated AMD Sludge: Input Parameters for TEA	Standardization of Cases A & B and optimized system operating conditions	11/15/19	N/A	100%	Complete.